2004

Tribological studies of polyphenylene sulfide composites filled with micro/nano particles and reinforced with short fibers or carbon nano-tubes/carbon nano-fibers

Minhaeng Cho
Iowa State University

Tribological studies of polyphenylene sulfide composites filled with micro/nano particles and reinforced with short fibers or carbon nano-tubes/carbon nano-fibers

by

Minhaeng Cho

A dissertation submitted to the graduate faculty

in partial fulfillment of the requirements for the degree of

DOCTOR OF PHILOSOPHY

Major: Mechanical Engineering

Program of Study Committee:
Shyam Bahadur, Major Professor
Abhijit Chandra
Scott Chumbley
Vinay Dayal
Sundararajan Sriram

Iowa State University
Ames, Iowa
2004

Graduate College
Iowa State University

This is to certify that the doctoral dissertation of

Minhaeng Cho

has met the dissertation requirements of Iowa State University

Signature was redacted for privacy.

Committee Member

Signature was redacted for privacy.

Committee Member

Signature was redacted for privacy.

Committee Member

Signature was redacted for privacy.

Committee Member

Signature was redacted for privacy.

Major Professor

Signature was redacted for privacy.

For the Major Program

TABLE OF CONTENTS

CHAPTER 1. GENERAL INTRODUCTION 1

1.1 Introduction 1

1.2 Thesis organization 2

CHAPTER 2. A STUDY OF THE SYNERGIAM EFFECTS IN THE TRIBOLOGICAL BEHAVIOR OF NANOSIZE CuO-FILLED AND FIBER-REINFORCED POLYPHENYLENE SULFIDE COMPOSITES 3

2.1 Abstract 3

2.2 Introduction 4

2.3 Experimental details 6

2.3.1 Materials 6

2.3.2 Sample preparation 7

2.3.3 Sliding tests 8

2.4 Results and discussion 9

2.4.1 Effect of filler and fiber reinforcement on wear and friction 9

2.4.2 Transfer film studies 11

2.4.2.1 By Atomic Force Microscopy 12

2.4.2.2 By Optical Microscopy 13

2.4.2.3 By Scanning Electron Microscopy 14

2.4.3 Examination of worn surfaces 15

2.5 Discussion 16

2.6 Conclusions 18

2.7 References 19

CHAPTER 3. OBSERVAIONS ON THE EFFECTIVENESS OF SOME SURFACE TREATMENTS OF MINERAL PARTICLES AND INORGANIC COMPOUNDS

FROM ARMENIA AS THE FILLERS IN POLYPHENYLENE SULFIDE FOR TRIBOLOGICAL PERFORMANCE 30

3.1 Abstract 30

3.2 Introduction 31

3.3 Experimental details 32

3.3.1 Materials 32

3.3.2 Surface treatments 33

3.3.3 Pin-on-disk sliding wear tests 35

3.3.4 Abrasivity tests 36

3.4 Results and discussion 37

3.4.1 Effect of mineral deposits on wear and friction 37

3.4.2 Abrasiveness of minerals 41

3.4.3 Transfer film studies 41

3.5 Conclusions 43

3.6 References 45

CHAPTER 4. FRICTION AND WEAR STUDIES USING TAGUCHI METHOD ON POLYPHENYLENE SULFIDE FILLED WITH A COMPLEX MIXTURE OF MoS_2, Al_2O_3, AND OTHER COMPOUNDS 57

4.1 Abstract 57

4.2 Introduction 58

4.3 Experimental Details 60

4.3.1 Materials 60

4.3.2 Specimen preparation 61

4.3.3 Sliding tests 62

4.3.4 Design of experiment by Taguchi analysis 63

4.4 Results and discussions 64

4.4.1 Effect of fillers on friction and wear 64

4.4.2 Taguchi analysis of wear rate and friction 65

4.4.3 Transfer film studies 67

4.4.4 XPS analysis of transfer film 69

4.5 Conclusions 71

4.6 References 72

CHAPTER 5. DESIGN OF EXPERIMENTS APPROACH TO THE STUDY OF TRIBOLOGICAL PERFORMANCE OF Cu-CONCENTRATE-FILLED PPS COMPOSITES 88

5.1 Abstract 88

5.2 Introduction 89

5.3 Experimental details 90

5.3.1 Materials 90

5.3.2 Sample Preparation 91

5.3.3 Pin-on-disk sliding tests 91

5.3.4 Design of experiments 92

5.4 Results 92

5.4.1 Effect of fillers on wear and friction 92

5.4.2 Taguchi analysis of wear and friction 94

5.4.3 Wear particle, transfer film, and worn surface studies 95

5.4.4 XPS studies of transfer films 97

5.5 Discussion 98

5.6 Conclusions 99

5.7 References 100

CHAPTER 6. A STUDY OF THE THERMAL, MECHANICAL AND TRIBOLOGICAL PROPERTIES OF POLYPHENYLENE SULFIDE COMPOSITES REINFORCED WITH CARBON NANOTUBES AND CARBON NANOFIBERS 118

6.1 Abstract 118

6.2 Introduction 119

6.3 Experimental details 120

6.3.1 Materials 121

6.3.2 Sample preparation 121

6.3.3 DSC and DMTA studies 122

6.3.4 Flexural test 122

6.3.5 Pin-on-disk sliding tests 123

6.4 Results and discussion 123

6.4.1 Differential scanning calorimetry 123

6.4.2 Dynamic mechanical thermal analysis 125

6.4.3 Flexural behavior 125

6.4.4 Friction and wear studies 126

6.4.5 Transfer film and worn surface studies 128

6.5 Conclusions 129

6.6 References 130

CHAPTER 7. GENERAL CONCLUSIONS 143

ACKNOWLEDGMENTS 147

CHAPTER 1
GENERAL INTRODUCTION

1.1 Introduction

Polymer and its composites have replaced a great number of metal products in industry and are still in a rapid growth in many areas due to their attractive properties such as low density, high specific strength and specific stiffness, corrosion resistance, and manufacturability. The properties of polymers have been considerably improved by the incorporation of fillers and fiber reinforcement. The mechanical and tribological studies on polyphenylene sulfide (PPS) and its composites have not been hitherto carried out extensively and are deserving of attention in view of their potential for being used in a wide variety of applications.

PPS has a great potential in high speed sliding applications owing to its high temperature capability. However, its wide application as a promising matrix material in tribology is still at infancy and so there is a need of the comprehensive study of its mechanical and tribological behaviors. In this dissertation, the effect of fillers and fibers as reinforcements in PPS was performed with respect to the tribological and mechanical properties. A number of fillers based on the minerals abundantly available in Armenia were used in this study along with other inorganic compound fillers and short micro fibers as reinforcement. The fillers used were both in micro and nano sizes. Finally, the effect of carbon nanotubes and carbon nanofibers as the reinforcements in PPS has also been studied in terms of their thermal, mechanical and tribological properties.

1.2 Thesis organization

The thesis is presented in the form of five papers. Each paper consists of abstract, introduction, experimental details, results and discussion, and conclusions followed by the references, tables, and figures. General conclusions are given in the final chapter followed by acknowledgement. The first part is on the study of synergistic effects by incorporation of nanosize inorganic filler and short fiber reinforcement. The second part is a general study on the effectiveness of mineral deposits from Armenia as filler materials in PPS in terms of the tribological behavior. The third part examines the effect of Mo-concentrate and the fourth part that of Cu-concentrate as the fillers in PPS in improving the friction and wear behavior. In these two parts, the design of experiments approach was applied. The fifth part deals with the study of thermal, mechanical, dynamic and tribological behavior of PPS reinforced with carbon nanotubes and carbon nanofibers.

CHAPTER 2
A STUDY OF THE SYNERGIAM EFFECTS IN THE TRIBOLOGICAL BEHAVIOR OF NANOSIZE CuO-FILLED AND FIBER-REINFORCED POLYPHENYLENE SULFIDE COMPOSITES

A paper published in *Wear*

Minhaeng Cho and Shyam Bahadur

2.1 Abstract

Nanosize CuO-filled and fiber-reinforced polyphenylene sulfide (PPS) composites were prepared by compression molding. The tribological behaviors of these materials and the synergism as a result of the incorporation of both the nanoparticles and the fibers were investigated. The reinforcement materials were short carbon fibers (CF) and aramid (Kevlar) fibers. The proportions of the filler material varied from 1 to 4 vol.% and of the reinforcement material from 5 to 15 vol.%. For the measurement of wear volume and the coefficient of friction, a pin-on-disk sliding configuration was used. The counterface was made of tool steel hardened to 55-60 HRC and finished to 0.09-0.11 μm Ra. Wear tests were run at a sliding speed of 1 m/s and over a duration of 6 hours, which provided the wear data for steady state sliding. In case of the filler only, the lowest steady state wear rate was observed for PPS+2%CuO composite and of the fiber reinforcement only for PPS+10%Kevlar composite. The particulate filler did not affect much the coefficient of friction while the latter was reduced to half of that in the case of CF reinforcement. The lowest steady state wear rates that were obtained with hybrid composites made with nanosize CuO particles and fiber reinforcement both could not be obtained with the composites made with either the filler or the fiber reinforcement only. With Kevlar fiber reinforcement alone,

the coefficient of friction did not change much. With reinforcement of the CuO-filled polymer with Kevlar fibers, the coefficient of friction increased, but with reinforcement with carbon fibers it either decreased or remained unaffected. The transfer films were studied by optical microscopy and the topographical changes of transfer films by atomic force microscopy (AFM). Worn surfaces and transfer films on the counterface were also studied by scanning electron microscopy.

2.2 Introduction

Polymeric composites filled with inorganic fillers or reinforced with fibers are the most common engineering materials today. Incorporating fillers and/or fibers to a base polymer material provides substantial improvement in terms of the mechanical properties [1-2]. Attempts to understand the modifications in the tribological behavior of the polymers with the addition of fillers or fibers reinforcements have been made by many researchers [3-4]. PPS (polyphenylene sulfide) is an attractive engineering thermoplastic that is widely used in practice due to its excellent properties such as chemical resistance, electrical properties, and low coefficient of friction [5]. The enhancement in tribological properties of this polymer has been reported with the addition of nanoscale inorganic fillers [6] and fibers [7].

Polymers filled with micro inorganic particulates have been extensively studied in terms of their tribological behavior. Bahadur and coworkers [8-9] reported that the fillers such as CuS, CuF_2, CaS, and CaO reduced the wear rate of polyamide but many other fillers such as CuAc and CaF_2 fillers increased the wear rate. They also showed that wear rate decreased with the addition of CuS and CuF_2 fillers to PEEK [10]. Tribological studies showed that the addition of micro fillers such as CuO and Pb_3O_4 to high-density polyethylene resulted in

considerable reduction of the wear rate of the polymer [11]. As for the PPS polymer, the micro fillers such as Ag_2S, CuO, and TiO_2 have been reported to reduce the wear rate of the polymer, but the wear rate increased when PbTe, SiC, and ZnO were used as the fillers [6, 12].

It is known that the angularity of particles is increased with the increase in size. The higher angularity of filler particles increases the possibility of abrasion during sliding which is detrimental to wear resistance. Nanoscale particulates seemingly are better in this respect. Furthermore, as the particulate size becomes smaller, the surface area-to-volume ratio becomes larger. This increases the possibility of enhanced bonding between the filler and the surrounding polymer, which would produce a stronger transfer film. A few tribological studies have been reported for nano-particle filled polymer composites as well. For example, Wang and coworkers [13-14] reported that the wear rate of PEEK was reduced when filled with 7.5 wt.% 10 nm ZrO_2 particles and increased when filled with 86 nm particles. They also reported that nanometer SiO_2 filler reduced both the wear rate and the coefficient of friction of PEEK. Shi *et al.* [15] showed that both wear rate and the coefficient of friction were reduced when epoxy was filled with nanometer Si_3N_4 particles. Schwartz and Bahadur [16] reported that the wear rate of PPS was reduced when filled with 1-2 vol.% nanoscale alumina particles. They demonstrated that the reduction in wear rate was related to the increase in bond strength between the transfer film and the counterface. It has also been reported that PPS filled with nanoscale CuO and TiO_2 had increased wear resistance but reduced wear resistance when filled with nanoscale SiC and ZnO fillers [6].

The role of fiber reinforcement in reducing the wear rate of polymers has been widely reported [17]. The credit for the reduction in wear rate has mostly been given to the increase in mechanical strength with fiber reinforcement. In this respect, continuous fibers are more

effective than short fibers. The advantage of the polymer composites made with short fibers is that they can be prepared by normal production methods. The wear reduction for composites with short fiber reinforcement is less than that with continuous fiber reinforcement [1].

The incorporation of a polymer with nanosize inorganic particles and fibers both could provide a synergism in terms of the improved wear resistance - a possibility that has not been adequately addressed so far. Bahadur *et al.* [18] reported some results for polyamide filled with microsize CuS filler and reinforced with carbon fiber. They found that the wear rate of polyamide was reduced with 35 vol. % microsize CuO filler and 5 vol.% carbon fiber to a level not achievable with either the fiber or the filler alone. They also found that glass fiber reinforcement instead of the carbon fiber reinforcement along with CuO filler did not result in the reduction of wear rate of polyamide. Wang *et al.* [4] reported a synergistic action in the tribological behavior of polyamide composites made with carbon fiber and microsize MoS_2 filler. It is thus obvious that a further study in this respect is needed in particular with nanosize filler particles both in view of the scientific understanding and commercial importance. It is a novel approach and is decidedly worthy of investigation.

2.3 Experimental details

2.3.1 Materials

PPS was used as the matrix material because of its commercial importance in view of its high strength and high temperature capability. The latter is important because high sliding speeds as used in this investigation contribute to significantly high temperature at the sliding interface. The polymeric material in the form of powder was supplied by Phillips Chemical

Company. It was sieved to a size less than 45 μm for use in this work.

Nanoscale CuO particles from Nanophase Technologies Corporation were used for the filler material. The reason for their use was because they have shown their effectiveness as the filler in PPS in both the micro [6] and nano sizes [6]. The average size of CuO particles was 16 – 32 nm.

The common fiber reinforcement materials used with polymers are carbon, polyaramid (Kevlar), and glass. In this investigation, carbon and Kevlar fibers were used. It was decided not to use glass fibers because they are abrasive and so could be detrimental for wear resistance. Chopped carbon fibers, 7 μm diameter and 6.0 mm long, were supplied by the Union Carbide Corporation. Kevlar-29 fibers, 20 μm diameter and 6 mm long, were supplied by the Du Pont Company.

2.3.2 Sample preparation

For making PPS-CuO composites, PPS and nanosize CuO particles were dried at 125°C for 5 hours. They were then weighed and mixed in required proportions. The mixture was put in an ultrasonic bath of acetone and agitated mechanically. After acetone evaporated, the mixture was dried again at 125°C for 1 hour. The dried mixture was compacted in a mold of the size 36 mm x 27 mm which was heated to 310°C, and a maximum pressure of 36 MPa was maintained for one minute in order to expel entrapped air out of the mold. The pressure was then lowered to 18 MPa and maintained there for 20 minutes until PPS melted. Afterwards, the heat was turned off and the mold was left under pressure to cool for 30 minutes in the press. Later the mold was removed from the press and left to cool in normal atmosphere.

For PPS-CuO-fiber-reinforced composites, carbon or Kevlar fibers, which were bundled together, were put in deionized water and separated by a mechanical agitator for 30 minutes. After the fibers were well separated, they were dried at 125°C for 1 hour. PPS, CuO, and fibers were then weighed and mixed in different proportions. The mixture with sufficient amount of acetone was agitated in an ultrasonic bath in order to allow the PPS and CuO particles to cover fiber surfaces well. After agitation for 30 minutes, the mixture was dried at 125°C for 1 hour. Since PPS and CuO could settle down to the bottom of container, the dried mixture was agitated mechanically again. The mixture was later compression molded as stated above.

Quenched and hardened tool steel (composition: 0.9% C and 1.6% Mn) disks were used for the counterface which had a hardness of 55-60 HRC. The disk was 76.5 mm in diameter and 5 mm thick. The disks were finished by grinding followed by abrasion to a surface roughness of 0.09-0.11 μm Ra. They were cleaned ultrasonically in a bath of acetone, dried, and stored in a desiccator.

2.3.3 Sliding tests

Sliding tests were performed in the pin-on-disk wear test machine. Here, the polymer pin with a nominal contact area of 5 mm x 6 mm rested on the flat surface of the counterface disk and provided a wear track diameter of 63 mm. The maximum contact between the pin and the disk was achieved by finishing the pin with 240-grade SiC abrasive paper mounted on another rotating disk. The linear sliding speed during the test was 1 m/s and the nominal contact pressure was 0.65 MPa. The tests were run under ambient condition and the counterface roughness of 0.09-0.11 μm Ra was kept the same for all tests. The wear tests

were interrupted at the intervals of ½ hour, ½ hour, and thereafter every hour for gravitational measurements of the wear loss to an accuracy of 10 μg. By plotting the wear loss vs. sliding distance, it was ensured that the wear test was run long enough for the system to be in the steady state condition. For comparison of the wear rates of different composites, it was found necessary to convert the mass loss data into wear volume data using the density values. Friction data was obtained from the output of strain gages mounted on the loading arm. For each condition, two to three tests were run and the data plotted is the mean of the measured values. The maximum variation of wear from one test to another for the same condition was about 20 % and the same also for friction.

2.4 Results and discussion

2.4.1 Effect of filler and fiber reinforcement on wear and friction

Wear volume and the coefficient of friction plots as a function of sliding distance for unfilled PPS, PPS filled with nanosize CuO particles, and PPS reinforced with carbon and Kevlar fibers are shown in Figs. 2.1-2.5. From the wear volume and sliding distance plots, steady state wear rates were calculated by the regression method and these are listed in Table 2.1. It is seen from Fig. 2.1 that the wear of PPS initially increases rapidly with sliding distance up to about 5 km and thereafter it increases moderately at a steady rate. Thus, for the unfilled polymer, transient and steady states of wear are distinctly observed. With the addition of nanosize CuO filler, the transient state is practically obscured. Steady state wear rates of the composites filled with 1 and 2 vol.% CuO particles are close and lower by a factor of about 5 compared to the wear rate of unfilled PPS (Table 2.1). With the increase in CuO vol.% to 4, wear rate increases considerably but is still lower than that of the unfilled

PPS. The lowest steady state wear rate of 0.047 mm^3/km is obtained for PPS+2%CuO composite. The coefficient of friction in the steady state of sliding was not largely affected by the addition of CuO particles, the variation being from 0.45 to 0.55. For the filled composites, the coefficient of friction tends to decrease as the filler proportion increases. This is probably due to partial smoothing of the counterface by ultra fine CuO particles.

Figure 2.2 gives wear and the coefficient of friction plots for PPS reinforced with carbon fibers. It shows that steady state wear rate decreases as the proportion of fibers increases (Table 2.1). The transient wear state for the composites is much milder than for the unreinforced polymer. The lowest wear rate of 0.054 mm^3/km was obtained in the case of PPS+15%CF composite. The reduction in wear rate with reinforcement is a widely reported phenomenon [17]. It should, however, be noted that reduction in the steady state wear rate of PPS was greater with 2 vol.% nanosize CuO filler than with 15 vol.% CF. The steady state coefficient of friction for all PPS+CF composites was reduced to about half of that of the unreinforced polymer. This reduction in the coefficient of friction has been attributed to the lubricating effect of carbon fibers.

Next, the coefficient of friction and wear behaviors of PPS composites made with both the filler and the fiber were studied. The results are shown in Fig. 2.3. In this case, CuO proportion was fixed at 2 vol. % because it provided the lowest wear rate in the case of PPS+CuO composites. The fiber was added in addition to CuO in the proportions of 5, 10, and 15 vol.%. As may be seen from Table 2.1, the lowest steady state wear rate of 0.020 mm^3/km was observed for PPS+5%CF+2%CuO composite. It should be noted that wear of these hybrid composites is lower than for any of the filled or reinforced composite. As for the coefficient of friction, it was about 0.5 for all the composites except 2%CuO+15%CF in

which case the coefficient of friction was reduced to 0.25. The coefficient of friction values for the other composites became higher than those of the CF-reinforced composites and were about the same as for the CuO-filled composites. It could thus be said that 5-10 vol.% carbon fiber was not effective in lowering the coefficient of friction of PPS in the presence of filler.

The plots of wear and the coefficient of friction with sliding distance for PPS reinforced with Kevlar fibers are shown in Fig. 2.4. It was found that reinforcement with Kevlar fibers was more effective than that with carbon fibers in reducing the wear rate. No transient wear behavior was seen in the case of these composites. The steady state wear rate was lower for 10 and 15 vol.% Kevlar fiber reinforcement than for 5 vol.% reinforcement. The coefficient of friction for all the reinforced composites was about the same being within the normal scatter range.

As done earlier, next the hybrid composites made with nanosize CuO filler and Kevlar fiber were studied for their friction and wear behaviors. The plots for these materials are shown in Fig. 2.5. With the exception of 5 vol.% Kevlar fiber reinforcement, the wear rates for all the hybrid composites were lower than those for the CuO-filled or Kevlar fiber-reinforced composites. Thus, the synergism effect between filler and fiber in terms of wear reduction is clearly seen. The lowest wear rate in case of hybrid composites was observed for PPS+15%Kevlar+2%CuO composite. The transient wear state observed for all hybrid composites was very mild. The coefficients of friction for these hybrid composites were about the same but higher than those for all the composites discussed above.

2.4.2 Transfer film studies

2.4.2.1 By Atomic Force Microscopy

The transfer films formed on metal counterfaces during some sliding wear tests were examined by Atomic Force Microscopy (AFM). Figures 2.6(a-d) show three-dimensional views of typical compositions studied in this paper. On the right side of each view are also presented the top view and the phase contrast for the corresponding composition. The three-dimensional and the top views are both presented so as to develop an understanding of the three-dimensional nature of the transfer film from the top views alone presented later. It was concluded from the phase contrasts that mixing of the composite ingredients in the transfer film was thorough to the extent that these could not be recognized individually. In the case of unfilled PPS (Fig. 2.6(a)), deep and wide plowing features consisting of the peaks and valleys are clearly seen. The existence of deep and straight furrows indicates that the effect of counterface topography obtained as a result of finishing operation is still predominant. In other words, the polymer transfer is too thin to produce smoothening effect on the metal counterface. A topography like this is conducive to abrasion of the soft polymer material and so the wear rate would be high. The deep grooves as seen here were not observed in the case of PPS+2%CuO composite transfer film, as seen in Fig. 2.6(b). Instead, there is an appearance of accumulated layers of fine wear particles formed during sliding. Since wear particles have filled in the valleys, the surface is smoother and the transfer film is thick especially in the valleys. As the likelihood of abrasion in this case decreased markedly, wear was also reduced compared to that of the unfilled PPS. In other words, changes in the topographical features accounted for the wear reduction mechanism. Furthermore, one could expect enhancement in the adhesion of transfer film to the counterface by interlocking of nanosize CuO particles into the metal crevices.

The transfer film was more uniform and coherent in the case of PPS+5%CF+2%CuO composite, as seen in Fig. 2.6(c), and so the wear rate was further lowered. The three-dimensional view showed that transfer film was comprised of a multitude of spikes rising from the surface. These spikes appear in the form of fine dots in the planar top view. The smoothest and the most coherent transfer film in this study was observed for the case of PPS+10%Kevlar+2%CuO composite. The top view shows that the film was fully compacted and the sliding tracks are barely seen. The wear rate in this case was the lowest of all the PPS compositions with filled CuO or CuO+CF.

Figures 2.7(a-c) show the transfer film of unfilled PPS at higher magnification taken from a minute area of Fig. 2.6(a), which is indicated by the arrow. It shows how the tiny wear fragments formed during sliding are deposited in the peak and valley locations. The extent of deposition is greater on the peaks than in the valleys. The phase contrast (Fig. 2.6(c)) shows that wear fragment boundaries do not blend well as they can be seen distinctly. The repeated sliding action on this surface will thus be able to pull some of these fragments apart which would contribute to wear loss.

2.4.2.2 By Optical Microscopy

Figures 2.8(a-f) show the transfer films observed by optical microscopy during the steady state sliding of PPS and its composites. As may be seen, the transfer film is formed in case of all the compositions. The fact that abrasion marks from finishing operation on the counterface can be seen in all the cases indicates that the films are very thin. The deposition of material in the transfer film is not uniform and seems to depend upon the angle between sliding direction and abrasion grooves on the counterface. This factor does not matter for

wear because all possible angles are encountered by the polymer pin in contact with the rotating metal disk. The transferred film appeared to be the thickest in the case of PPS+5%CF. The steady state wear rate for this composite was also the highest of all the compositions shown in Fig. 2.8. The next lower wear rate for the compositions shown in Fig. 2.8 was for PPS+15%CF composite and the transfer film for this was also thinner than for PPS+5%CF composite. The wear rates for other composites were lower and the transfer films in these cases were also thinner. Thus, it is obvious that a thin transfer film is one of the prerequisites for low wear.

2.4.2.3 By Scanning Electron Microscopy

Scanning electron microscopy of the transfer films for three compositions was performed in order to get an insight into the texture and makeup of transfer films. Figure 2.9(a) for PPS+2%CuO shows that wear particles were compacted under heavy pressure and presumably at high temperature at the interface so that they were flattened and deposited on the counterface surface layer by layer. The boundaries of adjacent flattened wear particles tended to blend but not completely. Because of multilayer formation, the surface appears to have a stepped structure. In the case of PPS+5%CF+2%CuO composite, transfer film became more uniform because patches formed by the deposition of large wear particles are not seen. This was so because wear particles formed in this case were finer than in the earlier case. The white dotted appearance is because of the peak structure observed by AFM (Fig. 2.6(c)) in the presence of CF. In case of PPS+10%Kevlar+2%CuO, the transfer film became smoother than in the previous two cases, as seen in Fig. 2.9(c). In case of the fiber-reinforced composites studied here, transfer films formed were thin as some abrasion marks on the

metal counterface are barely seen. The surface in Fig. 2.9(c) also shows some wear particles not yet fully compacted. The size of these wear particles is much smaller than that of the non-reinforced composite (Fig. 2.9(a)). Though the transfer films formed are thin, they seem to cover the metal counterface well so that the probability of direct contact between the hard counterface asperities and the soft polymer pin is eliminated.

2.4.3 Examination of worn surfaces

The worn surfaces for three typical compositions were examined by scanning electron microscopy for possible wear mechanism and are shown in Fig. 2.10. On the surface of PPS+2%CuO specimen, sliding tracks and an abundance of white spots are seen (Figure 2.10(a)). The analysis of a white dot by EDXA revealed that the oxygen content in it was larger compared to that on the unworn surface. This indicates tribochemical reaction which was promoted by high temperature generated at the sliding interface. Other than superficial plowing, there was no damage seen on the worn surface even at higher magnification (Fig. 2.10(b)). So, wear presumably occurred by fatigue and the depletion of transfer film. Figure 2.10(c) for the worn surface of PPS+5%CF+2%CuO composite shows compact wear debris adhering to the worn surface. The plowing action in this case is more distinct because of the presence of fibers, and the disintegration of material at fiber ends because of high stress concentration may be seen. The higher magnification view in Fig. 2.10(d) shows microcracking of polymer material along the length of the fiber. The cracks are oriented at 45° to the sliding direction thereby indicating shear failure. The disintegration of material in the process of fiber debonding is seen in Fig. 2.10(e) for PPS+10%Kevlar+2%CuO composite.

2.5 Discussion

It has been shown in this work that nanosize CuO particles and carbon or Kevlar fibers used together in PPS modify the tribological behavior and reduce wear rate to an extent not achievable by the filler or the fiber alone. The reduction of steady state wear rate and the coefficient of friction has been attributed to the filler and fiber materials modifying the transfer film formation and wear reduction mechanisms. Specifically speaking, the composites filled with 1 to 4 vol.% nanosize CuO particles had lower steady state wear rates than that of the unfilled PPS. The filler particles promoted the formation of transfer film which was more uniform and coherent than that formed in the case of unfilled PPS. In the presence of such film, the pin surface was not subjected to damage by the exposed hard asperities on the metal counterface and so the wear rate was lower. The filler needed for optimum wear reduction was 2 vol.% because larger quantities of filler tend to make the specimen fragile.

Reinforcement with both carbon and Kevlar fibers reduced the wear rate of PPS. In the case of carbon fibers, the reduction in wear rate was of the same order as with nanosize CuO particles, but the Kevlar fibers were more effective. This could be because the modulus of elasticity of Kevlar is much lower than that of carbon so that the former provided a more uniform stress distribution around the fiber because of greater flexibility. The coefficients of friction of carbon fiber-reinforced composites were lower than those of Kevlar fiber-reinforced composites by a factor of 2 because of the lubricating action of carbon.

The reduction in steady state wear rates was much greater when both nanosize CuO particles and fibers were used together. The lowest steady state wear rate was obtained for PPS+15%Kevlar+2%CuO composite. The steady state coefficients of friction were 0.45-0.60

in all cases except when carbon fibers were used for reinforcement. In the presence of 2 vol.% nanosize CuO filler, only a high 15 vol.% carbon fibber was effective in reducing the coefficient of friction.

It is known that wear rate and the coefficient of friction are closely related to the formation of transfer film on counterface. The generation of a thin and uniform transfer film during sliding is believed to be responsible for reducing wear rate. Close examination of the transfer films by AFM provided the likelihood of wear reduction mechanism using topographical interpretation. In general, it was seen that more compact, uniform, and cohesive transfer films were conducive to the reduction of wear rate. Optical micrographs of the transfer films showed that the appearance of films could look different at different locations depending upon the angle between sliding direction and abrasion marks. Thus, for wear reduction, the thickness of transfer film was more important than the superficial appearance of the texture as seen in an optical micrograph. The examination at higher magnification by SEM revealed a stepped structure on the surface of the transfer film, which contributed to larger size wear particles and also higher wear rate. On the other hand, a low wear rate was obtained when the transfer film was thin and uniform and presumably bonded well to the counterface.

The examination of worn pin surfaces showed multiple phenomena such as plowing action, microcracking at fiber tips, and fiber debonding. These events along with the depletion of transfer film under repetitive sliding action contributed to wear. Friction was mainly because of adhesive action between the asperities on contacting surfaces and also the lubricating action of graphite when carbon fibers were present.

2.6 Conclusions

1. With the addition of nanosize CuO filler, the wear of PPS decreased considerably. The lowest steady state wear rate of 0.047 mm^3/km was obtained in the case of PPS+2 vol.% CuO.
2. Wear rate of PPS was reduced when reinforced with carbon or Kevlar fibers. In the case of carbon fibers, the lowest wear rate of 0.054 mm^3/km was obtained for PPS+15% CF, and for Kevlar fibers the lowest wear rate of 0.028 mm^3/km was for PPS+10% Kevlar.
3. The reduction in steady state wear rates was much greater when both nanosize CuO particles and fiber were added to PPS. In this study, the lowest wear rate of 0.014 mm^3/km was found for PPS+15%Kevlar+2%CuO composite. This steady state wear rate was reduced to one twentieth of that of the unfilled PPS.
4. The lowest steady state coefficient of friction of 0.20-0.23 was observed for PPS+15%CF and PPS+15%CF+2%CuO composites. For all other composites, the coefficient of friction was about 0.45 and higher. The effect of the lubricating action of graphite was thus obvious in this study.
5. Examination of the topographical characteristics of transfer films by AFM for typical composites revealed that smooth and compact transfer films were associated with low wear rate.
6. The analysis of transfer film by optical and scanning electron microscopy indicated that uniform, thin, and coherent transfer films were prerequisites for the reduction of steady state wear rates.
7. There was no obvious damage on the worn pin surfaces of nanosize CuO-filled PPS composites and so wear was concluded to occur mainly by fatigue. In the case of fiber-

reinforced composites, microcracking at fiber tips and debonding of fiber surface along with the disintegration of polymer material were observed and so these phenomena also contributed to wear.

2.7 References

1. K. Friedrich, Wear of reinforced polymers by different abrasive counterparts, Vol.1. Friction and Wear of Polymer Composites, K. Friedrich (Ed.), (1986) 233-287.
2. G.C. Richardson, J.A. Sauer, Effect of reinforcement on the mechanical properties of polypropylene composites, Polymer Engineering and Science, 1976, Vol.16 (4) 252-256.
3. J. Bijwe, C. M. Logani, U. S. Tewari, Influence of fillers and fiber reinforcement on abrasive wear resistance of some polymeric composites, Wear 138 (1990) 77-92.
4. Junxiang Wang, Mingyuan Gu, Bai Songhao, Shirong Ge, Investigation of the influence of MoS_2 filler on the tribological properties of carbon fiber reinforced nylon 1010 composites, Wear 255 (2003) 774-779.
5. J. Bucher, Polyphenylene sulfide, Plastics World 55 (1997) 53.
6. C. Sunkara, The role of particulate inorganic fillers on the tribological behavior of polyphenylene sulfide, MS thesis, Iowa State University, Ames, 2000.
7. Zeng Hanmin, He Guoren, Yang Guicheng, Friction and wear of poly (phenylene sulfide) and its carbon fiber composites: I Unlubricated, Wear 116 (1987) 59-68.
8. S. Bahadur, D. Gong, J.W. Anderegg, Tribochemical studies by XPS analysis of transfer films of nylon 11 and its composites containing copper compounds, Wear 165 (1993) 205-212.

9. S. Bahadur, D. Gong, J.W. Anderegg, Investigation of the influence of CaS, CaO, and CaF_2 fillers on the transfer and wear of nylon by microscopy and XPS analysis, Wear 197 (1996) 271-279.

10. S. Bahadur, D. Gong, The investigation of the action of fillers by XPS studies of the transfer films of PEEK and its composites containing CuS and CuF_2, Wear 160 (1993) 131-138.

11. B.J. Briscoe, A.K. Pogosian, D. Tabor, The friction and wear of high density polythene: the action of lead oxide and copper oxide fillers, Wear 27 (1974) 19-34.

12. Q. Zhao, S. Bahadur, A study of the modification of the friction and wear behavior of polyphenylene sulfide by particulate Ag_2S and PbTe fillers, Wear 217 (1998) 62-72.

13. Qihua Wang, Qunji Xue, Huiwen Liu, Weichang Shen, Jinfen Xu, The effect of particles size of nanometer ZrO_2 on the tribological behavior of PEEK, Wear 198 (1996) 216-219.

14. Q. Wang, Q. Xue, W. Shen, The friction and wear properties of nanometer SiO_2 filled polyetheretherketone, Tribology International Vol. 30, No. 3, pp. 193-197, 1997.

15. Guang Shi, Ming Qiu Zhang, Min Zhi Rong, Bernd Wetzel, Klaus Friedrich, Friction and wear of low nanometer Si_3N_4 filled epoxy composites, Wear 254 (2003) 784-796.

16. C. J. Schwartz, S. Bahadur, Studies on the tribological behavior and transfer film-counterface bond strength for polyphenylene sulfide filled with nanoscale alumina particles, Wear 237 (2000) 261-273.

17. S. Bahadur, Mechanical and tribological behavior of polyester reinforced with short fibers of carbon and aramid, Lubrication Engineering, Vol. 47, No.8, pp. 661-667, 1990.

18. S. Bahadur, Q. Fu, D. Gong, The effect of reinforcement and the synergism between CuS and carbon fiber on the wear of nylon, Wear 178 (1994) 123-130.

Table 2.1 Steady state wear rate for unfilled PPS and its composites

Sample	Nano filler	Reinforcement, vol. %		Density[1]	Steady state wear rate[2]
	CuO, vol. %	Carbon fiber	Kevlar	g/cc	mm^3/km
PPS	-	-	-	1.360	0.291
PPS+CuO	1			1.409	0.061
PPS+CuO	2	-	-	1.459	0.047
PPS+CuO	4			1.558	0.161
PPS+CF		5		1.382	0.148
PPS+CF	-	10	-	1.404	0.093
PPS+CF		15		1.426	0.054
PPS+CuO+CF		5		1.481	0.020
PPS+CuO+CF	2	10	-	1.503	0.039
PPS+CuO+CF		15		1.525	0.042
PPS+Kevlar			5	1.364	0.052
PPS+Kevlar	-	-	10	1.368	0.028
PPS+Kevlar			15	1.372	0.033
PPS+CuO+Kevlar			5	1.463	0.031
PPS+CuO+Kevlar	2	-	10	1.467	0.023
PPS+CuO+Kevlar			15	1.471	0.014

[1]: The densities of PPS, CuO, CF, and Kevlar fiber are 1.36, 6.30, 1.80, and 1.44 g/cc, respectively.

[2]: The correlation coefficient (R^2) value is over 0.9 for all the cases.

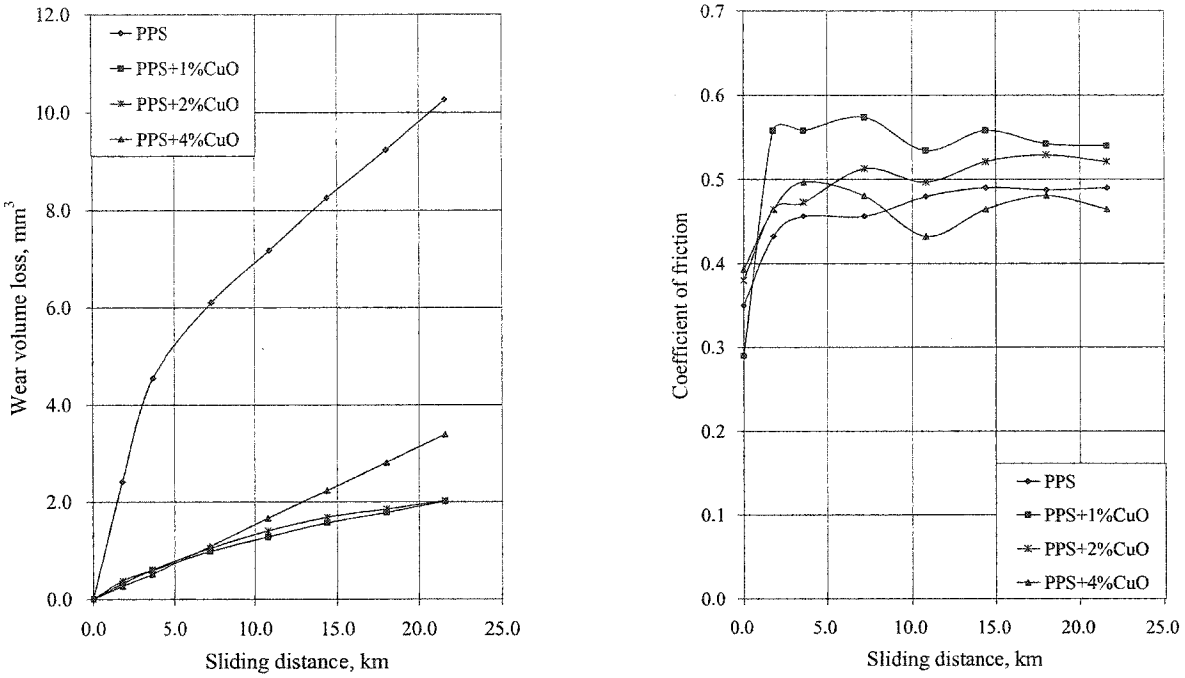

Figure 2.1 Variation of wear and coefficient of friction with sliding distance for PPS filled with nanosize CuO particles. Test conditions: Sliding speed 1.0 m/s, contact pressure 0.65 MPa, and counterface roughness 0.09-0.11 μm Ra

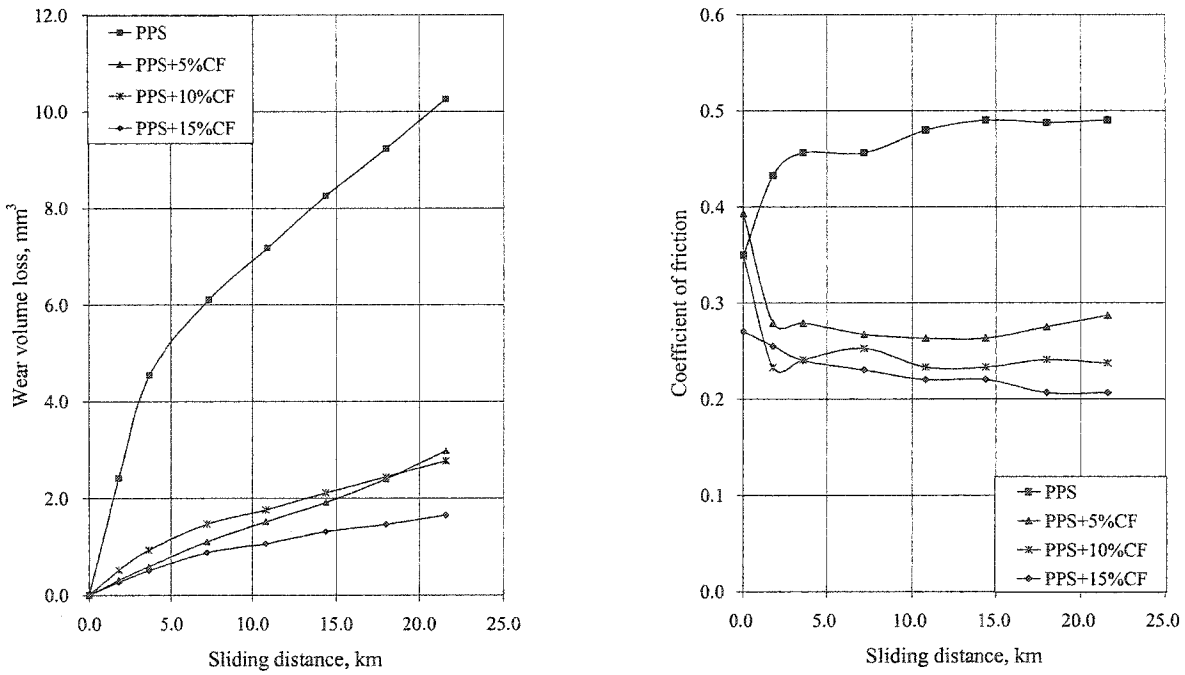

Figure 2.2 Variation of wear and coefficient of friction with sliding distance for PPS reinforced with carbon fibers. Test conditions same as in Fig. 2.1.

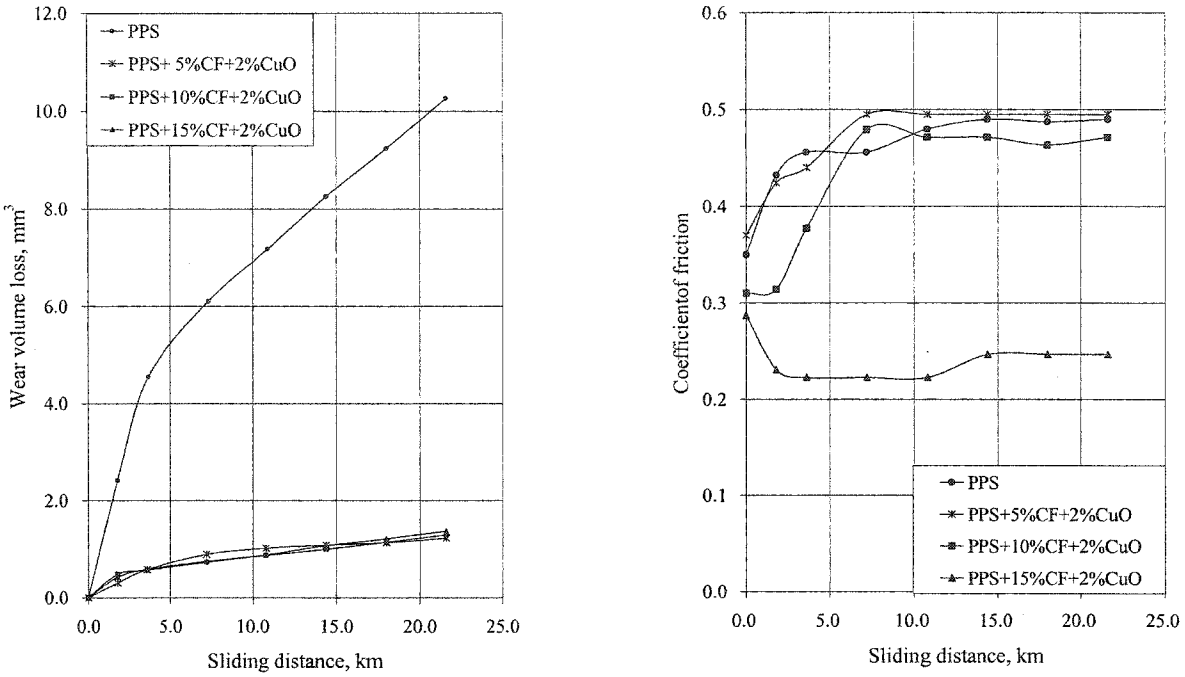

Figure 2.3 Variation of wear and coefficient of friction with sliding distance for PPS filled with nanosize CuO and reinforced with carbon fibers. Test conditions same as in Fig. 2.1.

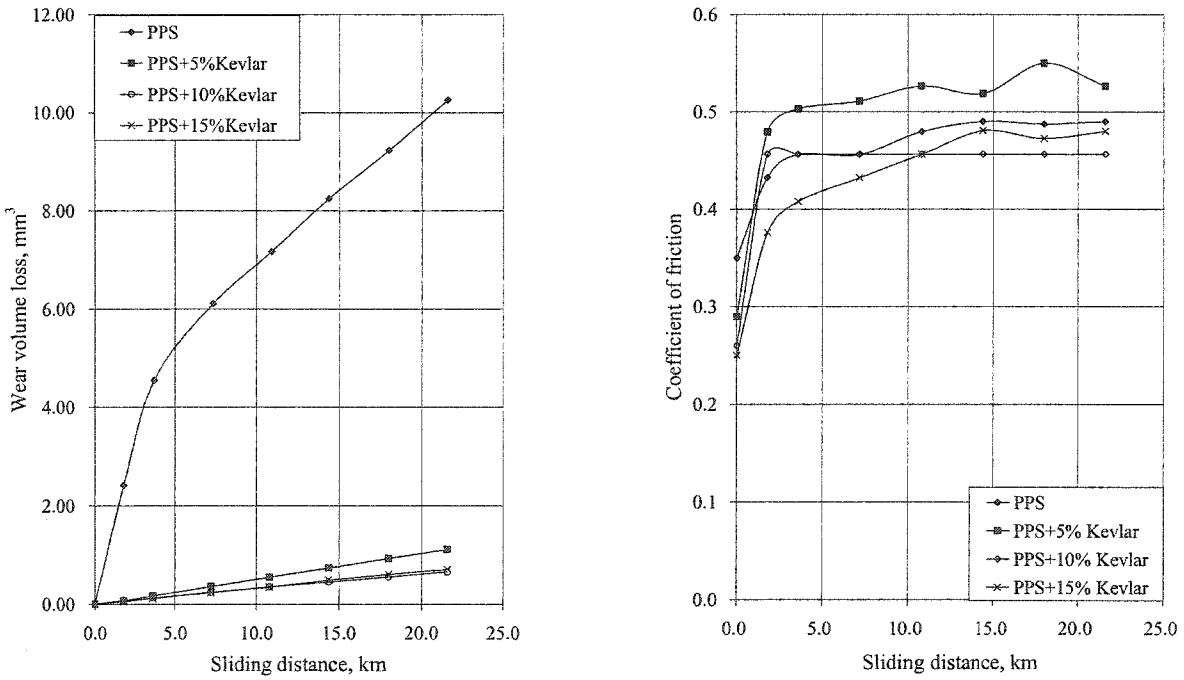

Figure 2.4 Variation of wear and coefficient of friction with sliding distance for PPS reinforced with Kevlar fibers. Test conditions same as in Fig. 2.1.

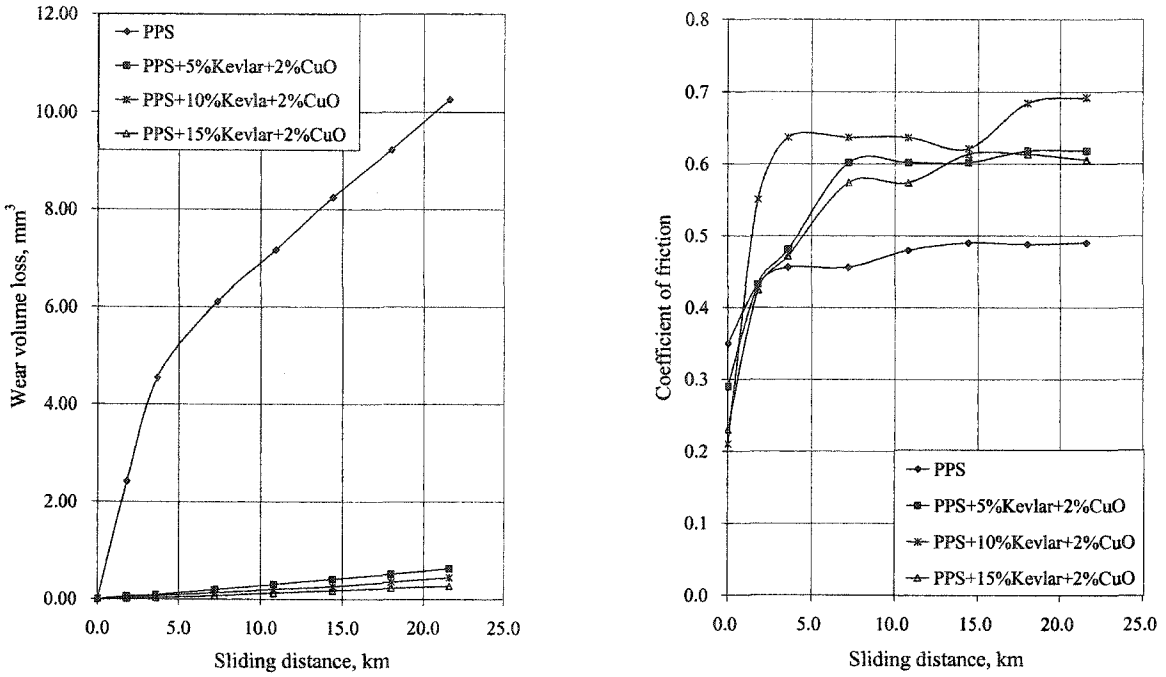

Figure 2.5 Variation of wear and coefficient of friction with sliding distance for PPS filled with nanosize CuO and reinforced with Kevlar fibers. Test conditions same as in Fig. 2.1.

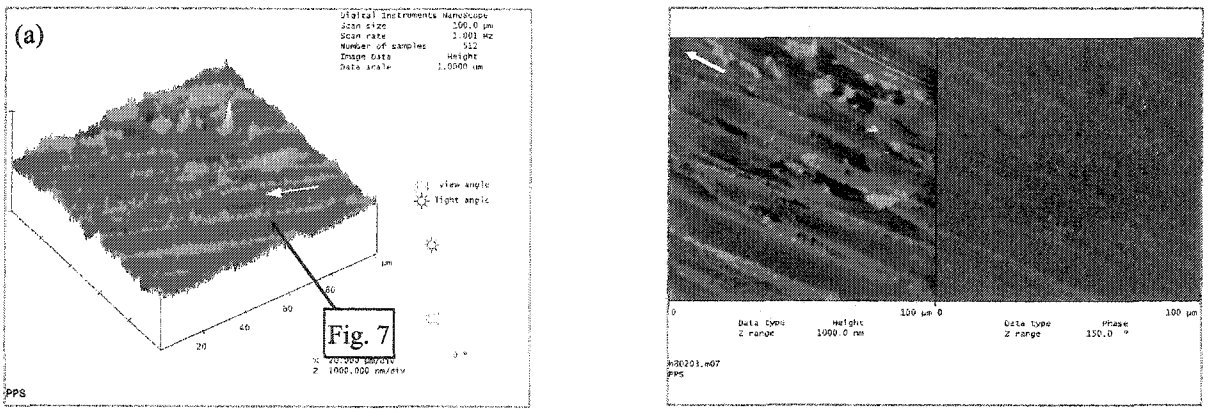

Figure 2.6 AFM micrographs of transfer films; (a) PPS, (b) PPS+2%CuO, (c) PPS+5%CF+2%CuO, and (d) PPS+10%Kevlar+2%CuO. Arrow indicates sliding direction. Test conditions same as in Fig. 2.1.

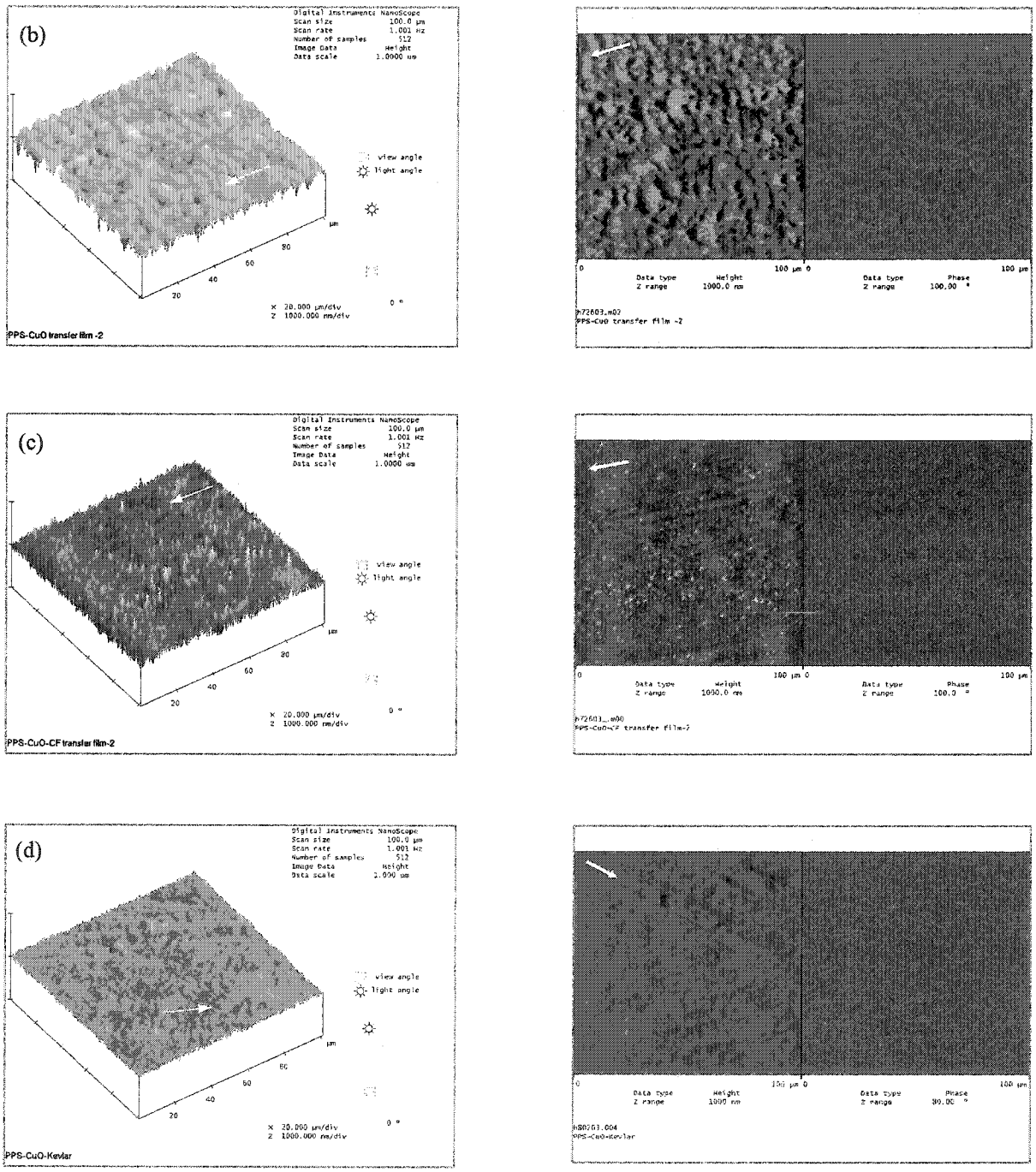

Figure 2.6 continued. AFM micrographs of transfer films; (b) PPS+2%CuO, (c) PPS+5%CF+2%CuO, and (d) PPS+10%Kevlar+2%CuO. Arrow indicates sliding direction. Test conditions same as in Fig. 2.1.

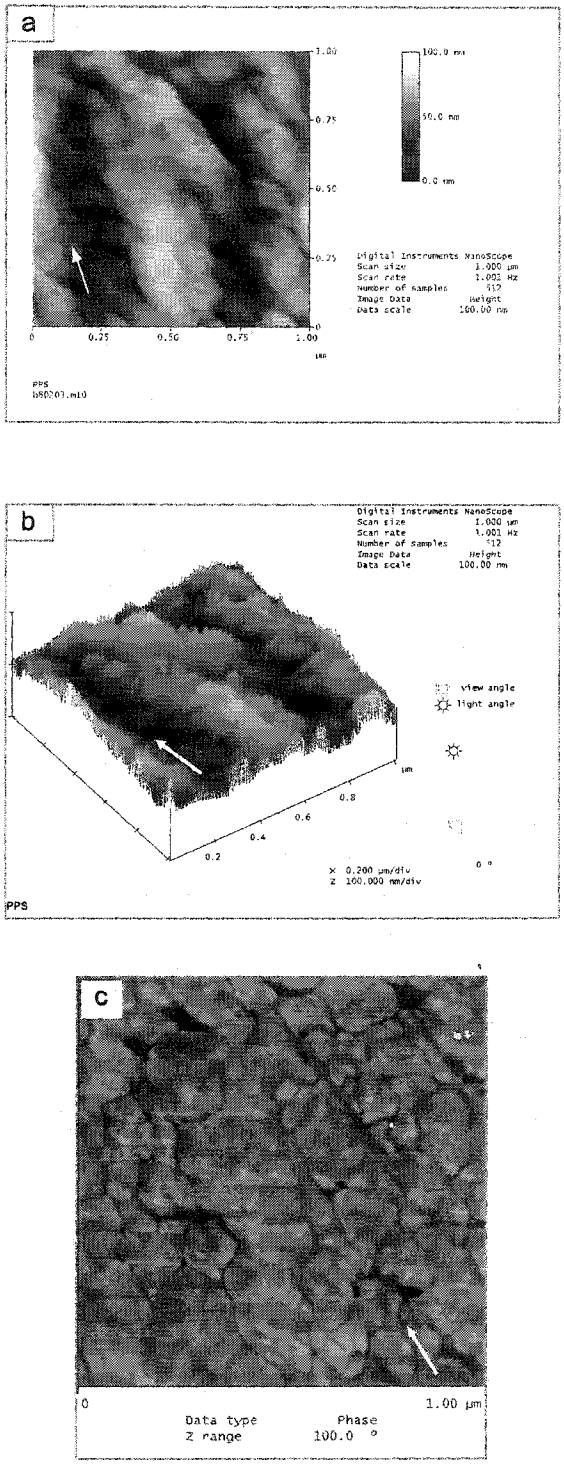

Figure 2.7 AFM micrographs of unfilled PPS transfer film; (a) Planar view, (b) 3-dimensional view, and (c) phase contrast. Arrow indicates sliding direction. Test conditions same as in Fig. 2.1.

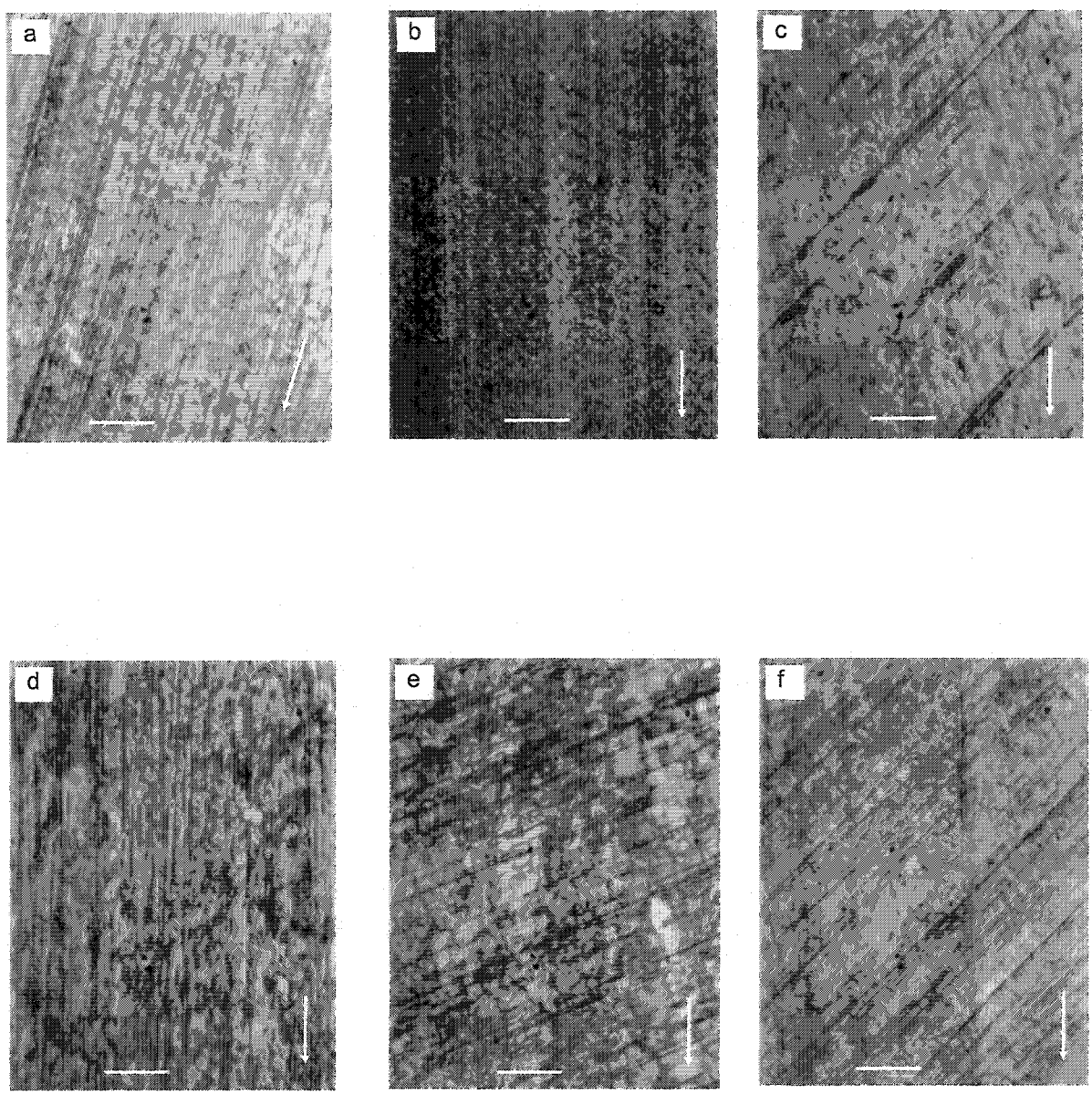

Figure 2.8 Optical micrographs of transfer films in steady state sliding wear; (a) PPS+2%CuO, (b) PPS+5%CF, (c) PPS+15%CF, (d) PPS+5%CF+2%CuO, (e) PPS+15%Kevlar, and (f) PPS+10%Kevlar+2%CuO. Arrow indicates sliding directions. Bar length is 50 μm. Test conditions same as in Fig. 2.1.

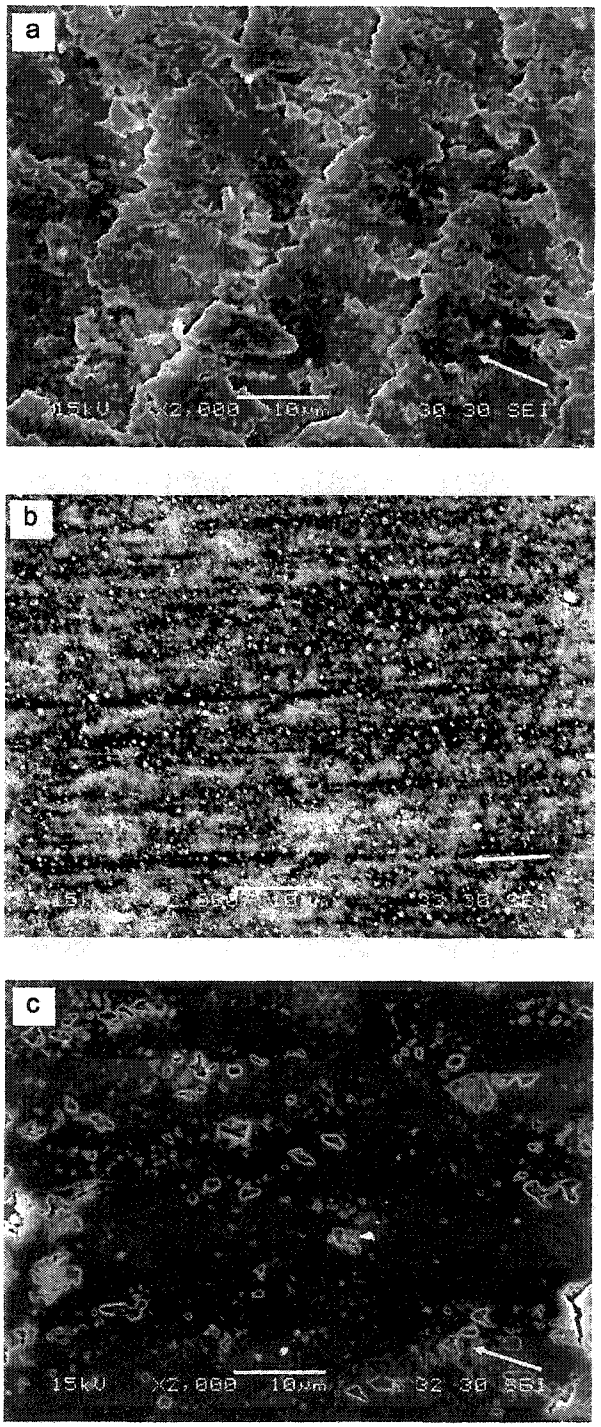

Figure 2.9 SEM micrographs of transfer films; (a)PPS+2%CuO, (b)PPS+5%CF+2%CuO, and (c) PPS+10% Kevlar+2%CuO composite. Arrow indicates sliding direction. Test conditions same as in Fig. 2.1.

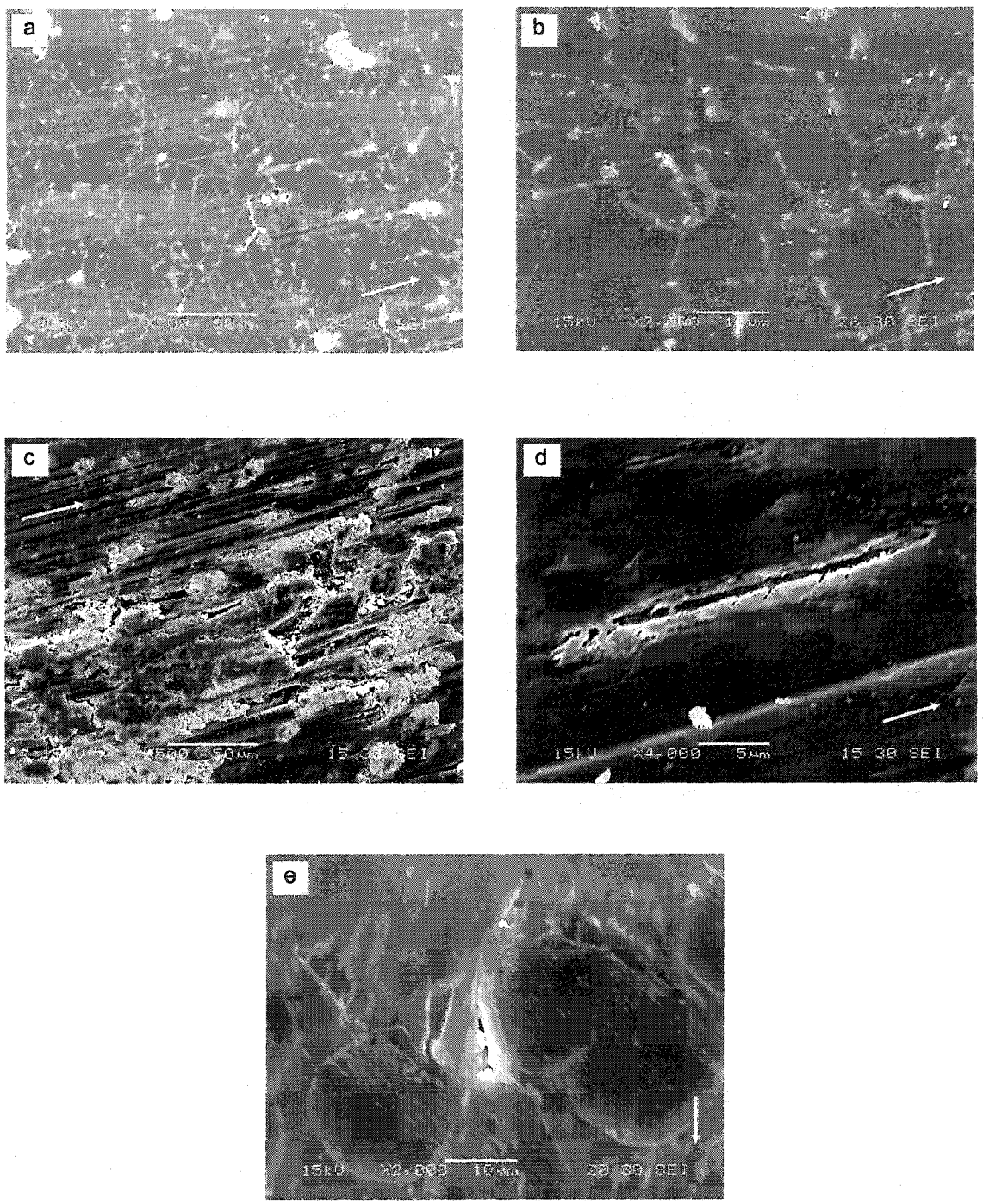

Figure 2.10 SEM micrographs of worn pin surfaces; (a-b) PPS+2%CuO, (c-d) PPS+5%CF+2%CuO, and (e) PPS+10%Kevlar+2%CuO composite. Arrow indicates sliding direction. Test conditions same as in Fig. 2.1.

CHAPTER 3
OBSERVAIONS ON THE EFFECTIVENESS OF SOME SURFACE TREATMENTS OF MINERAL PARTICLES AND INORGANIC COMPOUNDS FROM ARMENIA AS THE FILLERS IN POLYPHENYLENE SULFIDE FOR TRIBOLOGICAL PERFORMANCE

A paper submitted to *Tribology International*

Minhaeng Cho and Shyam Bahadur

3.1 Abstract

This is a general study in which a number of minerals and inorganic compounds from Armenia were investigated for their effectiveness as the fillers in polyphenylene sulfide (PPS) for tribological performance. The minerals studied were tuff, bentonite, and travertine, and inorganic compounds MoO_3 and MoO_2. The filled polymer specimens were prepared by compression molding and tested for tribological behavior in the pin-on-disk sliding configuration. The particulate fillers included many variations in terms of the size (micro and nano) and surface treatment. Friction and wear test results revealed that MoO_2 and nano size bentonite particles were effective in improving the wear resistance. The lowest steady state wear rate in this study was observed for PPS+7%MoO_2 (50nm)+5%PTFE composite, and MoO_2-filled composites had generally lower coefficients of friction than that of the unfilled PPS. From the wear plots, filler abrasiveness, and transfer film studies, it was concluded that the abrasion by filler was mostly responsible for the detrimental wear behavior. The wear behavior has been discussed in terms of the abrasion by filler and transfer film uniformity, texture, thickness, and coverage. The effects of particulate size and surface treatment are also included in the discussion. In view of the results reported for these fillers

in formaldehyde and dioxolane copolymer (CFD) and the observations in this study, it is felt that the fillers from Armenia with the exception of tuff and MoO_3 have considerable appeal for further investigation using other innovative surface treatments for fillers.

3.2 Introduction

This study was done under a CRDF[1] project whose objective was to explore the effectiveness of mineral deposits in Armenia as the fillers in polymer for wear resistance. Since Armenia is very rich in mineral deposits, there is a great potential for the improvement of economy of the country by utilization of these deposits for industrial usage. The minerals are complex mixtures of inorganic compounds and the tribological behavior of such mixtures has not been studied from a fundamental perspective. The study reported herein is general in nature intended to screen a number of mineral deposits for their effectiveness as the fillers in polymers. Whereas this study uses polyphenylene sulfide (PPS) as the base polymer, a parallel study was done at the State Engineering University of Armenia with the copolymer of formaldehyde with dioxolane (CFD-acetal resin). With this as the base study, follow-up studies with select minerals as the fillers will be reported. These will examine the behavior of these minerals on a more fundamental level. Attempts were made to understand the tribological behaviors of PPS composites with five fillers and the results are presented in this study.

Many studies on polymer composites have been done using inorganic compounds as a single filler material. Mineral deposits differ from these compounds because they are a mixture of many compounds usually with one or two of these in large proportions. Since

---

[1] US Civilian Research & Development Foundation for the Independent States of the Former Soviet Union

polymer composites filled with single compounds such as CuO, TiO_2, Ag_2S, SiC, Si_3N_4, and Cr_3C_2 have shown increased wear resistance while others filled with compounds such as ZnO, SiC, PbTe, and Al_2O_3 decreased wear resistance [1, 2-3], a study with mineral deposits as the fillers is expected to be much more complex.

The tribological behavior of polymer composites filled with minerals would essentially depend upon the constituents in the mineral. The minerals examined in this study are tuff, bentonite, and travertine. The constituents in these minerals are SiO_2, Al_2O_3, $CaCO_3$, MoO_3, MoO_2, MgO, Na_2O, K_2O, etc. A limited number of tribological studies with these compounds as the individual fillers have been reported. For example, Wang *et al.* [4] reported that the coefficient of friction and wear rate of PEEK were lowered with the addition of nanometer SiO_2 particles. Yang and Hlavacek [5] found that the wear resistance of PVC improved with the addition of Al_2O_3 but decreased with the addition of $CaCO_3$ and SiO_2. The wear resistance of PPS was reported to decrease with the addition of microscale Al_2O_3 particles [3]. With Al_2O_3 particles reduced to nanosize, Schwartz and Bahadur [6] reported that the wear resistance of PPS increased. This indicated that apart from the composition of a filler, its size also affects the tribological behavior. With more than one compound present in the filler material, there could as well be counteracting effects in terms of the wear resistance. This makes the study a lot more challenging.

3.3 Experimental details

3.3.1 Materials

PPS was used as the base polymer because of its high temperature capability that was considered necessary for the sliding conditions used in this study. It had been supplied by the

Phillips Chemical Company in powder form.

The chemical compositions of the mineral deposits are listed in Table 3.1 and their properties are given in Table 3.2. The mineral tuff is a complex mixture of large percentages of SiO_2 and Al_2O_3, both of which are abrasive materials. It has relatively low density, moderate compressive strength, high thermal stability, low thermal conductivity, and high hardness. It has a large porosity and high moisture absorption characteristic. It is known to consist of volcanic glass fragments and its structure is shown in Fig. 3.1.

Similar to tuff, bentonite also contains high percentages of SiO_2 and Al_2O_3 along with Fe_2O_3 (Table 3.1). Its hardness is lower than that of tuff and the material is fairly hygroscopic. It is a soft clay mineral composed mainly of montmorillonite ($Al_2O_3 \cdot 4SiO_2 \cdot H_2O$), which is hydrous aluminum silicate.

Travertine is basically mineral calcite ($CaCO_3$) and it contains very small fractions of the compounds such as MgO, SiO_2, Fe_2O_3, etc as well (Table 3.1). It has high compressive strength and its moisture absorption is much lower than that of tuff.

In addition to the above minerals, the inorganic compounds MoO_2 and MoO_3 from Armenia were also studied.

3.3.2 Surface treatments

The mineral particles were treated as follows in order to modify the particle surface for enhanced bonding with the polymer. The particulate hygroscopic tuff material was dried overnight in an electric oven at 125°C in order to get rid of the absorbed moisture. The particulates of 80 μm size tuff were treated in the aqueous solution of Q9-6300 vinyltrimethoxysilane coupling agent (CH_2=$CHSi(OCH_3)_3$) to provide silanol groups for

bonding with the polymer. This is the recommended coupling agent for siliceous materials such as SiO_2 which was the major constituent in tuff. The particles of 45 μm tuff were encapsulated in a shell of high-density polyethylene (HDPE). For this purpose, HDPE was dissolved in toluene at 120°C and the particulate material was immersed in this solution. The encapsulated particles were then mechanically separated by agitation in a blender. This treatment was also applied to 80 nm size tuff particles. The tuff particles were also treated with acetic acid to enhance surface energy. Microscale CuO and Ag_2S particles were used as the filler without any surface treatment.

Bentonite particles of the size 5-50 μm were treated by three methods. Firstly, they were treated with acetic acid which enhanced their surface energy. Secondly, the particles were wetted with an aqueous solution of Katamin AB-18, which is the surfactant alkyldimethylbenzylammonium chloride, $C_{12}H_{25}N(CH_3)_2$-C_7H_7Cl. The treated particles were dried at 105°C for 1 hour. Thirdly, bentonite particles were treated with Z-6032 silane coupling agent, which is vinylbenzylaminoethylaminopropyltrimethoxysilane chloride with the formula $H_2NCH_2CH_2NH(CH_2)_3Si(OCH_3)_3$. This coupling agent is recommended for improved chemical bonding between the inorganic and polymer materials.

Finer size bentonite particles were separated from the powder by decantation process. For this purpose, bentonite powder was suspended in deionized water and the top part of the mixture was separated. The mixture was filtered thereby giving about 5 μm size particles. The bentonite particles of about 100 nm size were also used in this study.

Travertine particles were treated in the following ways. Firstly, the same silane coupling agent, as used for bentonite particles, was applied to travertine particles in the form of an aqueous solution. Secondly, the particles were modified thermally by heating to 350 °C and

treated with fluoroalcane. Thirdly, the particles were treated with Katamin AB-18 as done for bentonite particles.

The samples of filled polymer composites were prepared by compression molding. For this purpose, the polymer powder and the filler particles were weighed in required proportions. The mixture was then blended mechanically in an ultrasonic bath for 30 minutes. It was dried in an electric oven at 125°C for 1 hour and then loaded in a cylindrical die of 6.35 mm diameter and compacted by applying a maximum pressure of 36 MPa. When the die heated, the pressure was lowered to 18 MPa and maintained at that level for 10 minutes. It was further lowered to 9 MPa and maintained there for 5 minutes. The mold was then cooled to room temperature in the machine. The molding temperature used was 310°C. The test samples in the form of pins 6.2 mm diameter and 10 mm long were prepared by machining.

3.3.3 Pin-on-disk sliding wear tests

Sliding experiments were carried out in a pin-on-disk configuration. The counterface disk, 5 mm thick and 76 mm diameter, was made of tool steel hardened to 55–60 HRC. It was finished by abrasion against 320 grit SiC paper to a roughness of 0.09-0.11 μm Ra. The test surface of polymer specimen was finished by abrasion against 320 grit SiC paper. The specimen was washed in water and acetone, dried, and stored in a dessicator overnight prior to testing.

In sliding tests, the pins rested on the counterface and produced a wear track of 63 mm diameter. The sliding conditions consisted of a sliding speed of 1 m/s, contact pressure of 0.65 MPa, and test duration of 6 hours. Mass loss was measured every 30 minutes for the first hour and every hour thereafter with an accuracy of 10 μg. It was converted into volume

loss by using the density values. A minimum of two tests in cases where the data were close were run for each condition. In other cases, three to four tests were run in order to get reliable results.

3.3.4 Abrasivity tests

An improvised abrasion test method was devised to test the relative abrasivity of mineral filler particles. It was structured on the principle used in the sand/rubber wheel apparatus. Here, a wheel of 228.6 mm diameter mounted with rubber, as recommended in the ASTM G65 standard, contacted a flat surface under a load of 0.25 N. The surface speed of the rubber wheel was 0.8 m/s. Tests were performed for 2.5 minutes in the case of 80 μm size particles and for 6 minutes in the case of 45 μm size particles.

The mineral particles such as tuff, bentonite, and travertine were suspended in a liquid and the mixture was admitted into the contact zone between the rubber wheel and the flat surface. The suspension of particles in liquid was considered necessary in order to prevent particle agglomeration, control flow rate, and provide cooling. The mixture was prepared with 5 g of particles suspended in 30 ml alcohol and 70 ml deionized water. It was mechanically agitated in an ultrasonic bath for 10 minutes. The counterface material was a highly polished low carbon steel foil 0.0508 mm thick. It was cleaned with acetone for 5 minutes and then securely mounted on a hard substrate with scotch tape. The suspension was released from a pipette at a controlled rate of about 40 ml/min in the case of 80 μm particles and 17 ml/min for 45 μm particles. After the abrasion test, the foil was removed from its substrate and cleaned in an ultrasonic bath of acetone. Abrasive wear loss of the metal foil was measured gravimetrically with an accuracy of 10 μg.

3.4 Results and discussion

3.4.1 Effect of mineral deposits on wear and friction

Figure 3.2 shows wear and the coefficient of friction plots for PPS filled with 80 μm untreated microscale tuff particles in the proportions of 3 to 15 vol.%. For comparison, it also shows the plot for a composition where tuff particles had been treated with a coupling agent. It may be seen that in all cases wear loss increased linearly with sliding distance. This kind of variation is attributed to the abrasive behavior of the constituents such as SiO_2 and Al_2O_3 in the mineral tuff. Abrasive wear is further supported by the fact that the higher the proportion of tuff, the greater was the wear rate. It is obvious that the coupling agent was not effective in enhancing the wear resistance of filled PPS. The coefficient of friction for PPS+3%tuff was about the same as that of PPS. With the proportion of tuff increased to 9%, the coefficient of friction decreased by about $1/3^{rd}$ because of considerable moisture absorption in the tuff particles, as indicated in Table 3.2.

In view of the above tribological behavior dominated by the abrasive nature of tuff, it was decided to test the effectiveness of tuff as filler by reducing its size. It was so because the angularity of particles decreases with the decrease in particle size. As such 45 μm and 80 nm size particles were tried as the fillers. They were also cleaned with acetic acid to enhance their surface energy and alternately encapsulated with HDPE to reduce their angularity. The wear and friction plots for PPS filled with 45 μm tuff particles are given in Fig. 3.3. Neither smaller particle size nor HDPE encapsulation helped in increasing the wear resistance of PPS. The coefficient of friction of PPS filled with 2% tuff (45 μm) was similar to that of unfilled PPS, but it decreased when the filler proportion increased to 10%, as seen in Fig. 3.3, for the

same reason as given above.

Figure 3.4 shows the wear and friction plots for PPS filled with 80 nm tuff particles, both in the untreated and treated conditions. There is still no improvement in wear resistance. The change in the coefficients of friction in steady state sliding was also not markedly significant.

It was now decided to use tuff along with CuO or Ag_2S as the fillers in PPS. The additional fillers were used because they have been reported to enhance the wear resistance of PPS significantly [5-6]. Figure 3.5 shows the wear and friction behaviors of the composites made with the mixture of tuff and CuO or Ag_2S. Though the wear results for some cases are somewhat better compared to those in Figs. 3.2 to 3.4, they are still of no practical significance. The light reduction in the coefficient of friction presumably occurred again because of a significant proportion of the hygroscopic tuff material.

Figure 3.6 shows the variation of wear and the coefficient of friction for PPS filled with microscale (5 – 45 μm) bentonite particles. It may be seen that the wear rate of PPS increased with the filler. The straight line plots of wear volume vs. sliding distance indicate the possibility of abrasion during the sliding process. This is not unexpected because bentonite like tuff has also large proportions of abrasive SiO_2 and Al_2O_3. The surfactant treatment of bentonite with Katamin AB-18 was not effective in lowering the coefficient of friction of filled PPS whereas friction was lowered with untreated bentonite particles. This is possibly because of the hygroscopic character of untreated surface of bentonite particles. The reduction in the coefficient of friction was larger as the proportion of bentonite filler increased. In view of the reported observation [7] that bentonite treated with fluoroalcane was effective in increasing the wear resistance of formaldehyde and dioxolane copolymer, new treatments for improving the wear resistance of PPS are called for.

It was next decided to use nanosize bentonite as the filler in PPS. The latter was also treated in different ways, as indicated in Fig. 3.7, and the wear and friction behaviors are shown in this figure. With the reduction in size of bentonite to 100 nm, the wear rate decreased and for 5% 100 nm bentonite, the wear rate was lower than that of the unfilled polymer. With the addition of 5%PTFE to this composition, the wear rate decreased even further providing an overall reduction in wear rate of about 50% compared to that of unfilled PPS. Though this reduction is not very dramatic, this could still be economically advantageous if bentonite is cheaper than PPS on volume basis. The coefficient of friction decreased in all the cases with nanoscale bentonite filler because of its hygroscopic behavior. The lowest value of the coefficient of friction was obtained with the addition of 5%PTFE to PPS+5%bentonite (100 nm), supporting the role of PTFE as a solid lubricant.

Travertine was another mineral from Armenia. It is mostly $CaCO_3$ along with traces of some other compounds (Table 3.1) which on incineration decomposes into CaO and CO_2 gas. Its properties are similar to that of bentonite (Table 3.2) and so its wear behavior was also expected to be similar. Wear and friction plots of untreated 45 μm travertine-filled PPS composites are shown in Fig. 3.8. With filler proportions of 5% and 10% both, wear increased linearly with sliding distance. The coefficient of friction was slightly lower because of the possibility of moisture absorption in the filler. Figure 3.9 shows the wear behavior of PPS filled with micro and nanosize travertine, untreated and treated in different ways, as indicated in the figure. The wear rate is higher than that of the unfilled PPS in all cases. From the initial shape of the plots, it so appears that transfer film is rapidly formed so that wear rate in the early part of sliding is low. After about 3 km sliding, wear rate increases rapidly and linearly, which is again indicative of abrasive action. The observed wear behavior was

unexpected because this filler has been reported to improve the wear resistance of CFD [8]. The coefficient of friction for PPS filled with 10% 80 nm travertine was slightly lower than that of PPS possibly because of the large proportion of hygroscopic travertine. In other cases, there was no significant difference in friction coefficient with the use of the filler.

The other two fillers were the oxides of molybdenum: MoO_3 and MoO_2. Figure 3.10 shows the variation of wear rate with sliding distance for PPS filled with these compounds. When MoO_3 was used as the filler material, wear rate was excessive and so sliding test was stopped after sliding over a distance of 7.5 km. Similar behavior for MoO_3 filler was also reported by Clauss [9] who attributed it to the impurities or other side effects rather than the inherent abrasiveness of MoO_3. The coefficient of friction for this composite was about the same as that of the unfilled PPS in steady state sliding condition.

For the composite with 7%MoO_2 in 1 μm size, steady state wear rate was lower than that of the unfilled PPS. A much greater reduction in steady state wear rate was obtained with the addition of 5%PTFE to this PPS+MoO_2 composite, as seen in Fig. 3.10. Next, 50 nm MoO_2 powder was used in different volume proportions. As may be seen in Fig. 3.10, steady state wear rate of PPS with 2%MoO_2 was about the same as that of the unfilled PPS. It decreased with the addition of 7%MoO_2 powder but increased with 12%MoO_2. It is possible that 12%MoO_2 in nanosize made the composite material fragile. The lowest steady state wear rate was observed with the addition of 5%PTFE to PPS+7% nano MoO_2. The coefficient of friction of PPS in steady state sliding was lowered with the addition of MoO_2. The higher the proportion of MoO_2, the smaller was the steady state coefficient of friction. This behavior shows the lubricating ability of MoO_2 material. The effect of PTFE as the solid lubricant in the presence of MoO_2 was not significant in terms of the reduction in the coefficient of

friction.

3.4.2 Abrasiveness of minerals

In most cases, the wear volume versus sliding distance plots showed a linear variation indicating the possibility of abrasion in the sliding wear behavior. It was, therefore, decided to test the abrasiveness of minerals by an improvised set-up, as described earlier. The results from these tests are shown in Fig. 3.11. In the case of 80 μm particles, tuff was the most abrasive and bentonite the least abrasive mineral. Travertine was also highly abrasive and its abrasive wear volume was lower than that of tuff but higher than that of bentonite. Bentonite in suspension in the liquids used formed a slippery material which could have reduced the abrasivity of particles than what it would be under dry condition. Wear rates of bentonite-filled composites were fairly high, as shown in Fig. 3.6. The abrasivity test results for 45 μm size particles are also shown in Fig. 3.11. With the reduction in particle size, the abrasivity was reduced considerably. In this case, the abrasive wear loss for tuff and travertine was considerably greater than that of bentonite. The abrasivity tests on MoO_2 and MoO_3 powders could not be done because of the insufficient amounts of material available.

3.4.3 Transfer film studies

Figure 3.12 shows the optical micrographs of transfer films for typical PPS composites filled with tuff particles. In all the cases, there is evidence of transfer films being formed on the counterface. In the case of PPS+3% 80 μm tuff composite, the film is very thick and appears to be lumpy. The steady state wear rate increased slightly with the addition of tuff to PPS (Fig. 3.2). With 10%tuff encapsulated with HDPE, the film became uniform but the abrasion was quite significant and so the wear rate increased (Fig. 3.3). With the addition of

10% CuO to PPS+10%tuff composition, the film became thinner but the abrasion was still significant. When Ag_2S was added instead of CuO to PPS+10%tuff composition, the surface became much smoother but the abrasion was still there. Compared to all the compositions with tuff in Fig. 3.12, Ag_2S was the best for wear resistance (Fig. 3.5), but the improvement was insignificant.

The transfer film micrographs of PPS filled with treated and untreated nanoscale bentonite particles are shown in Fig. 3.13. The abrasion grooves in Fig. 3.13(c), which is for 7% 35 μm size bentonite particles treated with Katamin AB-18, are the deepest. The wear rates for the composites made with all microsize particles were very high, as seen in Fig. 3.6. With 100 nm bentonite particles, the wear rates were either compatible or lower than that of PPS (Fig. 3.7). The transfer film for 100 nm 5% bentonite-filled PPS in Fig. 3.13(a) is much smoother. The steady state coefficient of friction and wear rate for this composite are also lower than that of the unfilled PPS. With the addition of 5%PTFE to this composite, wear rate was further reduced and the coefficient of friction was also fairly low (Fig. 3.7). The transfer film for this case in Fig. 3.13(b) was smooth and so thin that the abrasion marks from the finishing operation of the disk can be seen. There are no abrasion marks seen on the transfer film in the direction of sliding.

The high wear rates for travertine-filled PPS (Figs. 3.8-3.9) are supported by the shape of wear particles and the transfer film shown in Fig. 3.14 for a typical composition. Thin and uniform transfer film initially developed but was rapidly removed with further sliding. Counterface abrasion was also observed. Roll-like wear debris, as seen in Fig. 3.14(a), was formed. The transfer film here is fairly thick and lumpy, and the abrasion grooves can be seen in the sliding direction.

A fairly thick, non-uniform, and lumpy transfer film was observed in the case of PPS+17%MoO_3 composite, as shown in Fig. 3.15(a). The wear rate for this composition was very high (Fig. 3.10). The shape of the wear particles generated in sliding of this composite revealed that the lumps were being removed during sliding. In contrast, lower ware rates were observed for MoO_2-filled composites. Figures 3.15(b), (c), and (d) show the transfer films for these three cases. The transfer film shown in Fig. 3.15(b) appears to be continuous and shows grooves possibly formed by the abrasive action of microsize MoO_2 particles. With the substitution of nanoscale MoO_2 particles, the transfer film became thinner and more uniform, and there are no abrasion grooves in the sliding direction. The wear rate was also lower in this case (Fig. 3.10). When 5%PTFE was added to PPS+7%MoO_2, the transfer film provided a better coverage, as seen in Fig. 3.15(d). The wear rate in this case was the lowest.

3.5 Conclusions

1. The fillers such as tuff, travertine, and bentonite were abrasive. With the reduction in size from 80 μm to 45 μm, the abrasiveness of particles decreased significantly.
2. Wear rate of PPS composite filled with tuff increased as the proportions of tuff increased from 3 to 15 vol.%. The surface treatments on both micro and nano scale tuff particles were not effective in lowering the wear rate. A slight improvement in wear resistance compared to that of unfilled PPS was observed when 4-5 vol.% CuO or 5 vol.% Ag_2S micro particles were added to PPS+10 vol.% tuff, but it was not significant from a practical standpoint.
3. The surfactant treatment on microsize bentonite particles with Katamin AB-18 was not effective in lowering the wear rate of bentonite-filled PPS composites. However, friction

was lowered with untreated bentonite particles. The steady state wear rates were lower than that of unfilled PPS when nanosize bentonite particles were used as the fillers. The lowest wear rates were observed with 100 nm 5 vol.% filler with and without 5 vol.% PTFE.

4. Travertine-filled PPS composites showed very high wear rates irrespective of the particles size and applied surface treatment. Wear was also dominated by abrasive action as seen in tuff.
5. 17 vol.% MoO_3 as the filler showed the highest wear rate in this study. On the other hand, PPS composite with 7 vol.% micro (or nano) and 5 vol.% PTFE showed the lowest steady state wear rate of 0.032 mm^3/km. This wear rate was $1/9^{th}$ to that of unfilled PPS.
6. In all the cases for which transfer films are reported, abrasion was observed except for PPS+7 vol.% MoO_2 (1μm)+5 vol.% PTFE and PPS+5 vol.% bentonite (100nm)+ 5% PTFE. Abrasion appears to be the most important factor responsible for wear rates of the composites reported in this study.
7. Small proportions of tuff and travertine filler particles did not affect the coefficient of friction regardless of the particle size and surface treatment. The reduction in the coefficient of friction with larger filler proportions occurred because of the hygroscopic nature of tuff particles. The coefficients of friction for bentonite-filled PPS composites were generally lower than those for the composites filled with tuff and travertine.
8. The coefficients of friction of PPS composites filled with MoO_2 were in general lower than those of the other composites, indicating the lubricating ability of MoO_2 particles.

9. In view of the results from these fillers in formaldehyde and dioxolane copolymer, additional innovative treatments of fillers are needed to improve further their effectiveness in increasing the wear resistance of PPS.

3.6 References

1. C. Sunkara, The role of particulate inorganic fillers on the tribological behavior of polyphenylene sulfide, MS thesis, Iowa State University, Ames, 2000.
2. Q. Zhao, S. Bahadur, A study of the modification of the friction and wear behavior of polyphenylene sulfide by particulate Ag_2S and PbTe fillers, Wear 217 (1998) 62-72.
3. L. Yu, S. Bahadur, Q. Xue, Investigation of the friction and wear behaviors of ceramic particle filled polyphenylene sulfide composites, Wear 214 (1998) 54-63.
4. Q. Wang, Q. Xue, W. Shen, The friction and wear properties of nanometer SiO_2 filled polyetheretherketone, Tribology International 1998; 30(3): 193-197.
5. F. Yang, V. Hlavacek, Improvement of PVC wearability by addition of additives, Powder technology 103 (1999) 182-1888.
6. C. J. Schwartz, S. Bahadur, Studies on the tribological behavior and transfer film-counterface bond strength for polyphenylene sulfide filled with nanoscale alumina particles, Wear 237 (2000) 261-273.
7. A.K. Pogosian, S. Bahadur, K.V. Hovhannisyan, A.N. Karapetyan, Investigation of the Tribological and Physico-Mechanical Processes in Sliding of Mineral-Filled Formaldehyde Copolymer Composites against Steel, Journal of Wear (2004): Submitted for Publication.

8. A.K. Pogosian, K.V. Hovhannisyan, A.R. Isajanyan, Self-lubricating mechanism of polymer-based composites with mineral fillers, World Tribology Congress, Vienna, 2001, 101-104.

9. F.J. Clauss, Solid lubricants and Self-Lubricating Solids, Academic Press, 1972.

Table 3.1 Chemical constituents of mineral deposits.

	Tuff	Bentonite	Travertine
SiO_2	63.5	60.40	0.40
Al_2O_3	16.7	16.27	0.02
$CaCO_3$	-	-	99.0
TiO_2	0.20	0.82	-
Fe_2O_3	2.20	5.51	0.10
FeO	0.98	0.61	-
MnO	0.40	0.14	-
CaO	2.65	2.78	-
MgO	2.10	3.45	0.50
Na_2O	3.84	2.23	-
K_2O	4.40	0.56	-
P_2O_5	-	-	0.05
H_2O	1.00	6.74	-
SO_3	-	-	0.10

Table 3.2 Mechanical properties of mineral deposits.

	Tuff	Bentonite	Travertine
Density, g/cc	2.50	2.60	2.40
Compressive strength, MPa	11-35	20-60	50-150
Tensile strength, MPa	-	-	-
Flexural strength, MPa	-	-	-
Moisture absorption, %	20.0	11.0	1.5-10.0
Porosity, %	15-48	-	3-4
Thermal stability, °C	1200	550	600
Thermal conductivity, J/m·s·°C	0.29	0.32	0.42
Mohs hardness	4-6	3	3-4

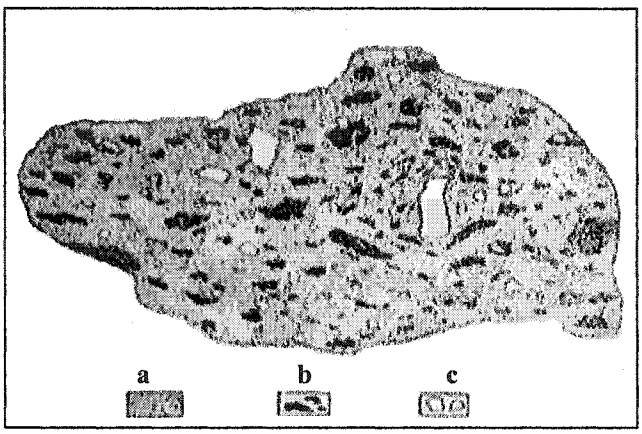

Figure 3.1 Structure of tuff; a) bulk fragmentary-ashes, b) embedded black glass fragments, and c) other rock fragments.

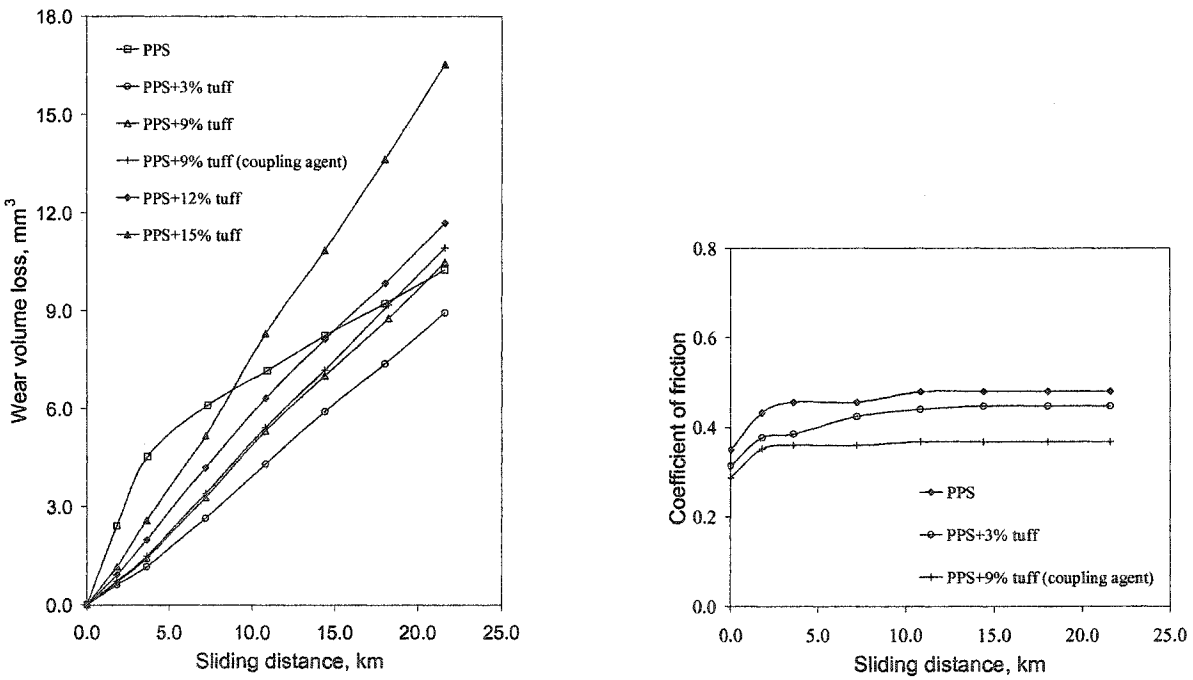

Figure 3.2 Variation of wear and coefficient of friction with sliding distance for PPS filled with 80 μm microscale tuff particles. Test conditions: sliding speed 1.0 m/s, nominal pressure 0.65 MPa, counterface roughness 0.09-0.11 μm Ra. Filler proportions are by volume.

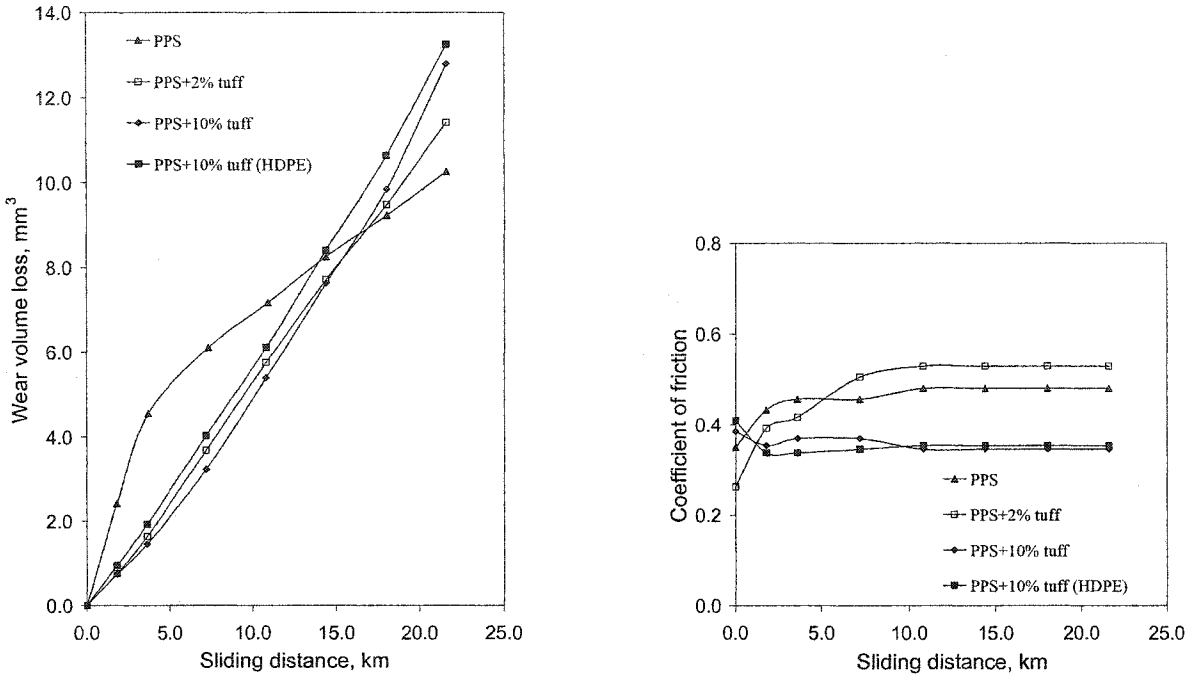

Figure 3.3 Variation of wear and coefficient of friction with sliding distance for PPS filled with 45 μm tuff particles. Test conditions same as in Fig. 3.2. Filler proportions are by volume.

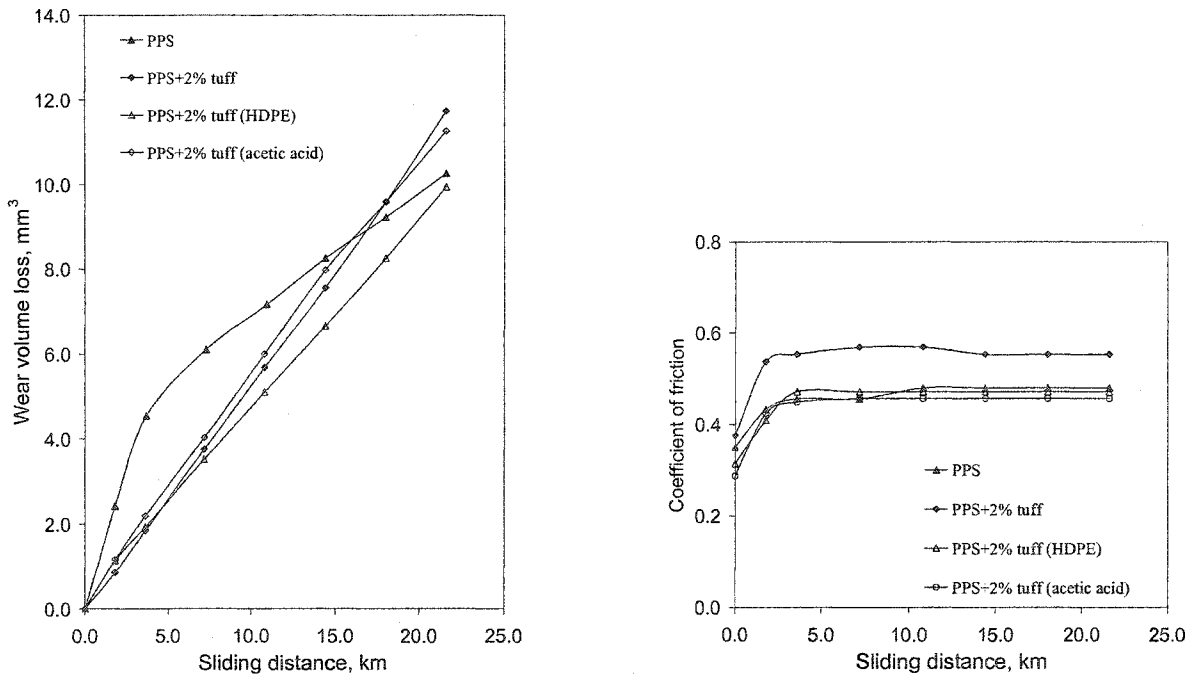

Figure 3.4 Variation of wear and coefficient of friction with sliding distance for PPS filled with 80 nm tuff particles. Test conditions same as in Fig. 3.2. Filler proportions are by volume.

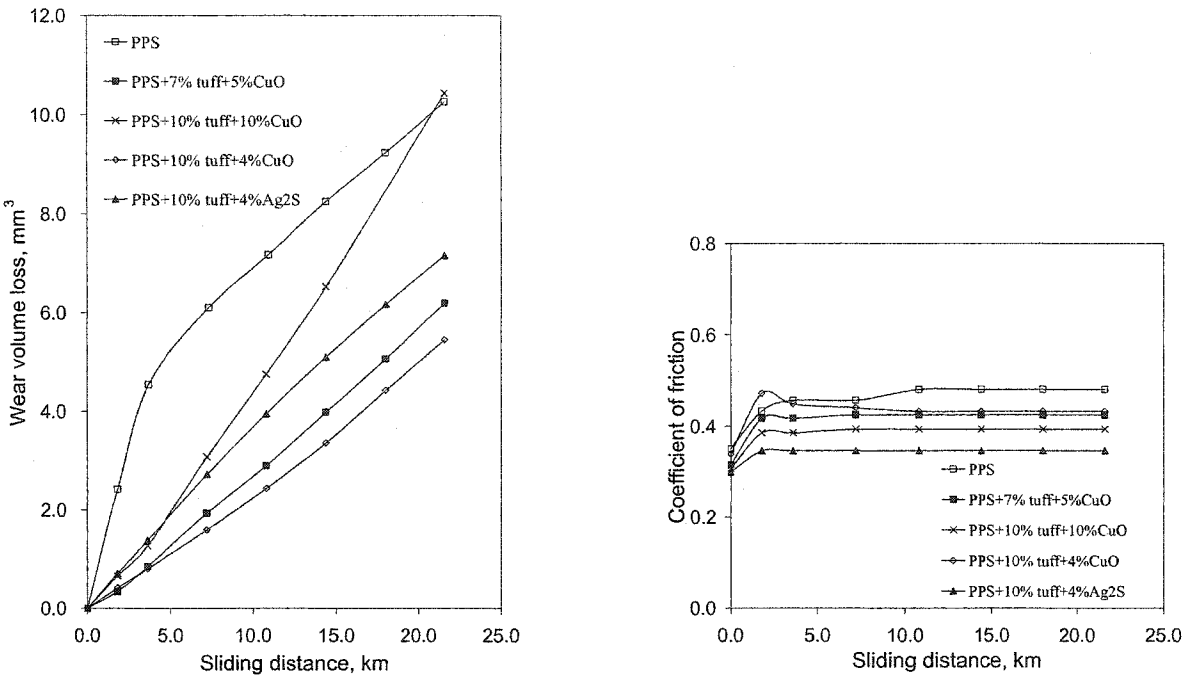

Figure 3.5 Variation of wear and coefficient of friction with distance for PPS filled with microsize tuff and fillers. Particle size; tuff: 80 μm, CuO: 5 μm, and Ag_2S: 44~150 μm. Test conditions same as in Fig. 3.2. Filler proportions are by volume.

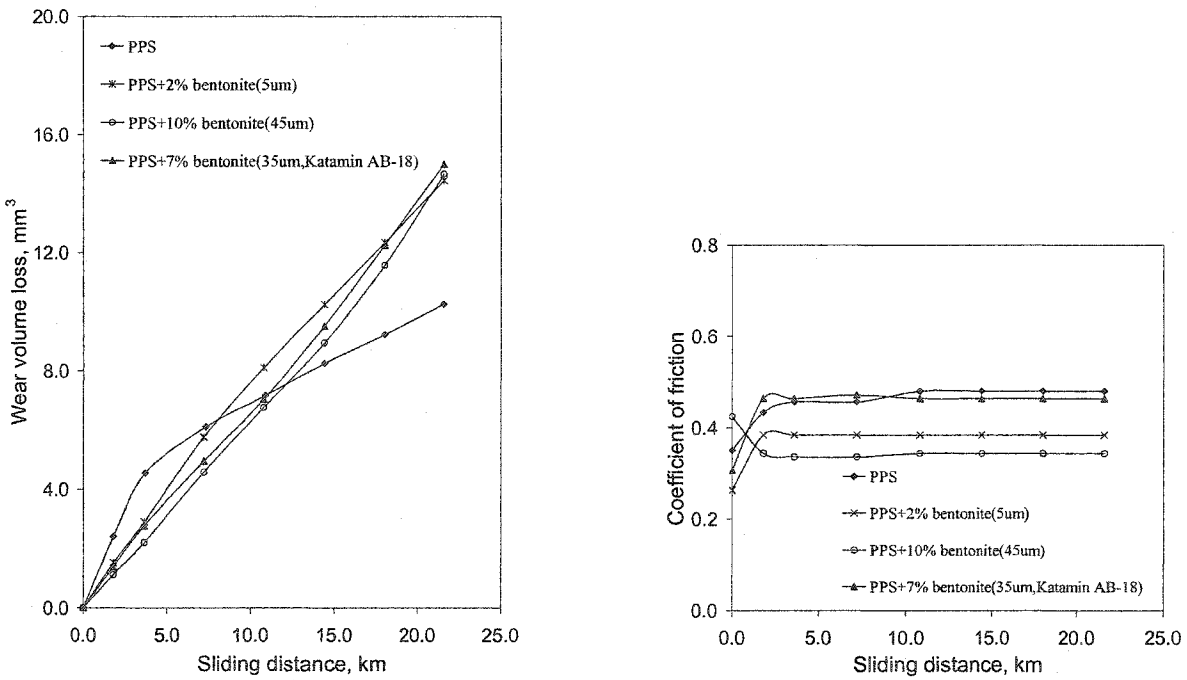

Figure 3.6 Variation of wear and coefficient of friction with sliding distance for PPS composites filled with untreated and treated microscale bentonite particles. Test conditions same as in Fig. 3.2. Filler proportions are by volume.

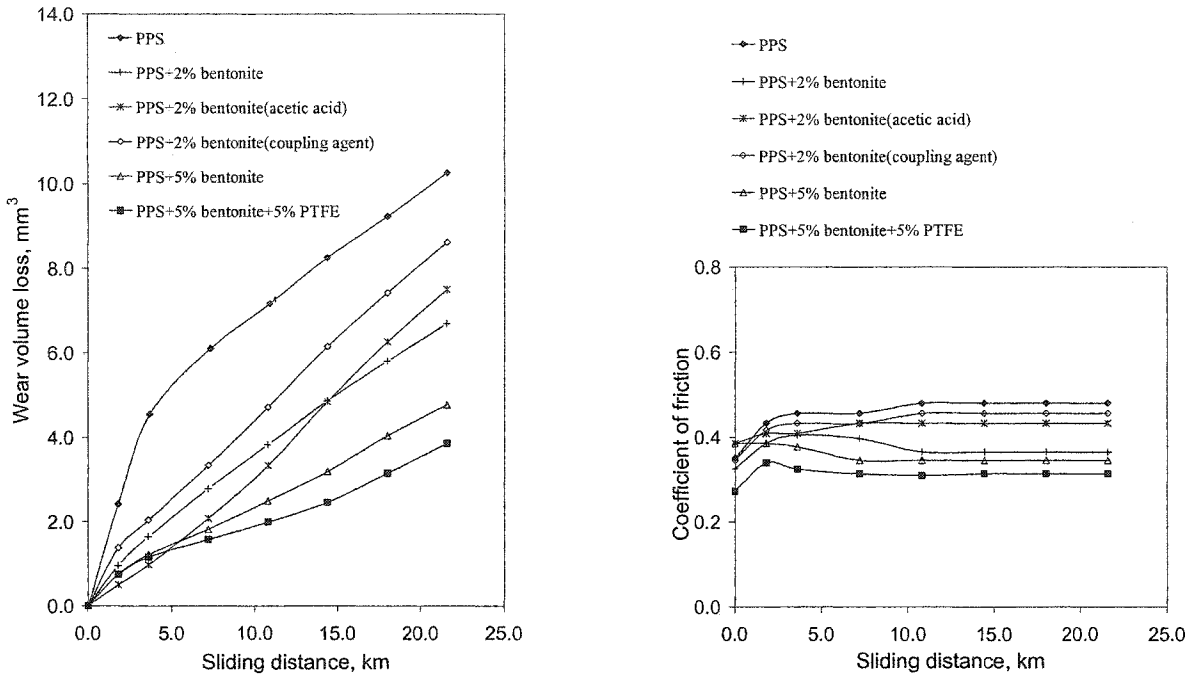

Figure 3.7 Variation of wear and coefficient of friction with sliding distance for PPS composites filled with treated and untreated 100 nm bentonite particles. Test conditions same as in Fig. 3.2. Filler proportions are by volume.

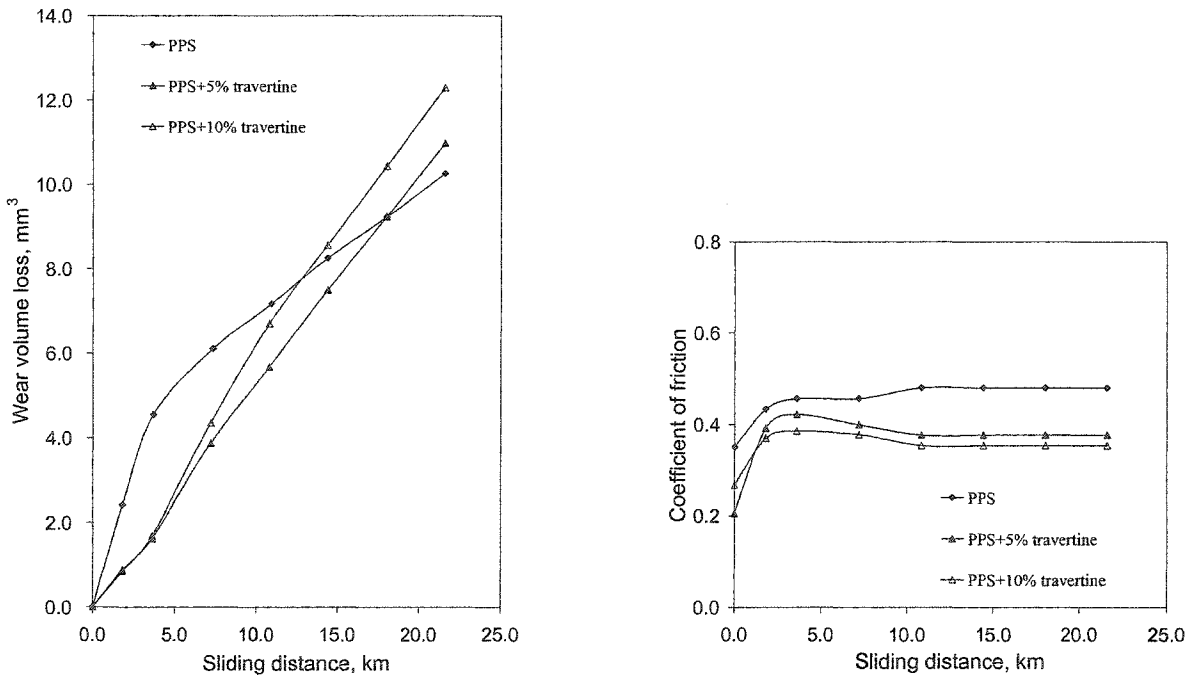

Figure 3.8 Variation of wear and coefficient of friction with sliding distance for PPS filled with untreated 45 μm travertine particles. Test conditions same as in Fig. 3.2. Filler proportions are by volume.

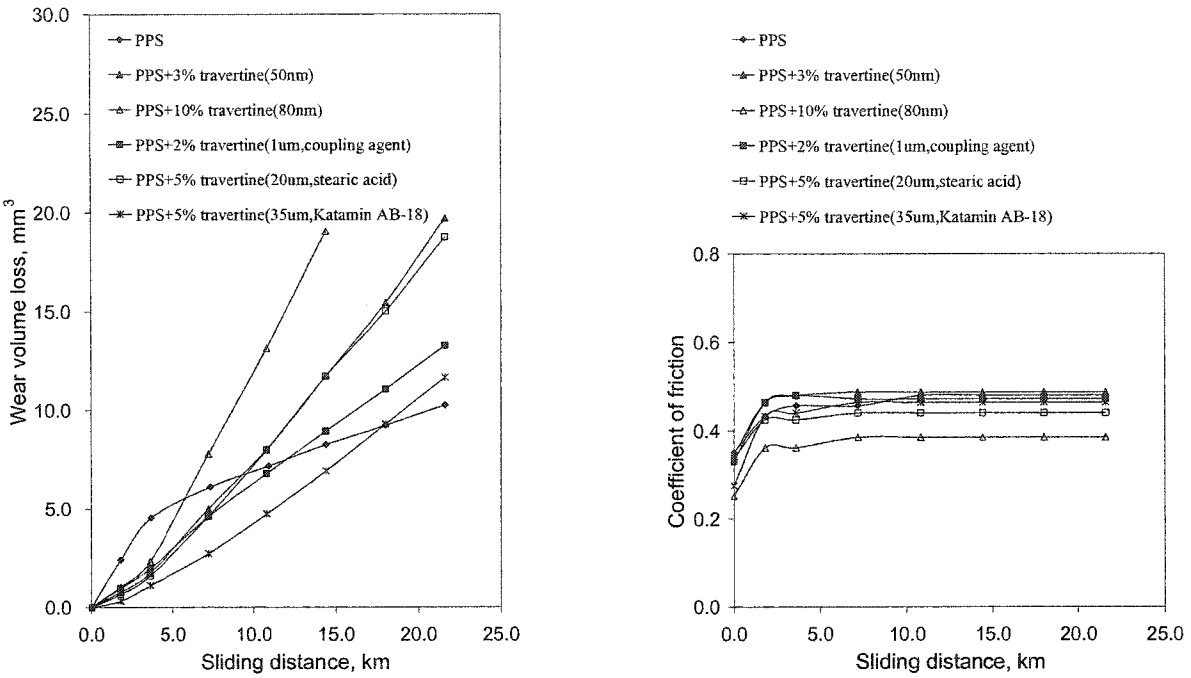

Figure 3.9 Variation of wear and coefficient of friction with sliding distance for PPS filled with untreated nano and treated microsize travertine particles. Test conditions same as in Fig. 3.2. Filler proportions are by volume.

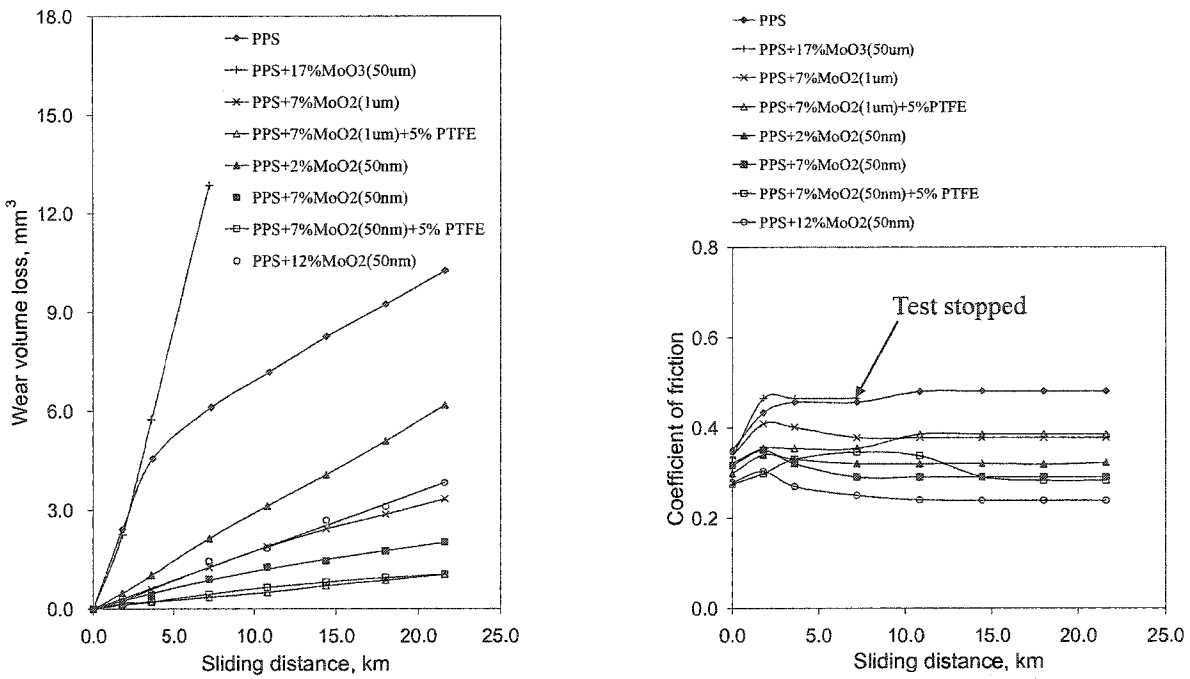

Figure 3.10 Variation of wear and coefficient of friction with sliding distance for PPS filled either with MoO_2 or with MoO_3 composites. Test conditions same as in Fig. 3.2. Filler proportions are by volume.

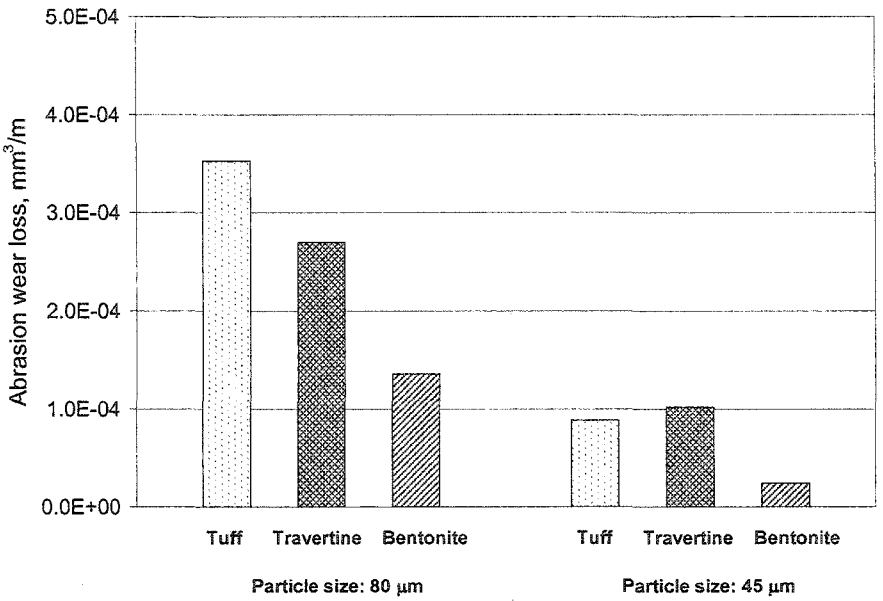

Figure 3.11 Results on the abrasiveness of minerals. Sliding speed 0.8 m/s and contact load 0.25 N.

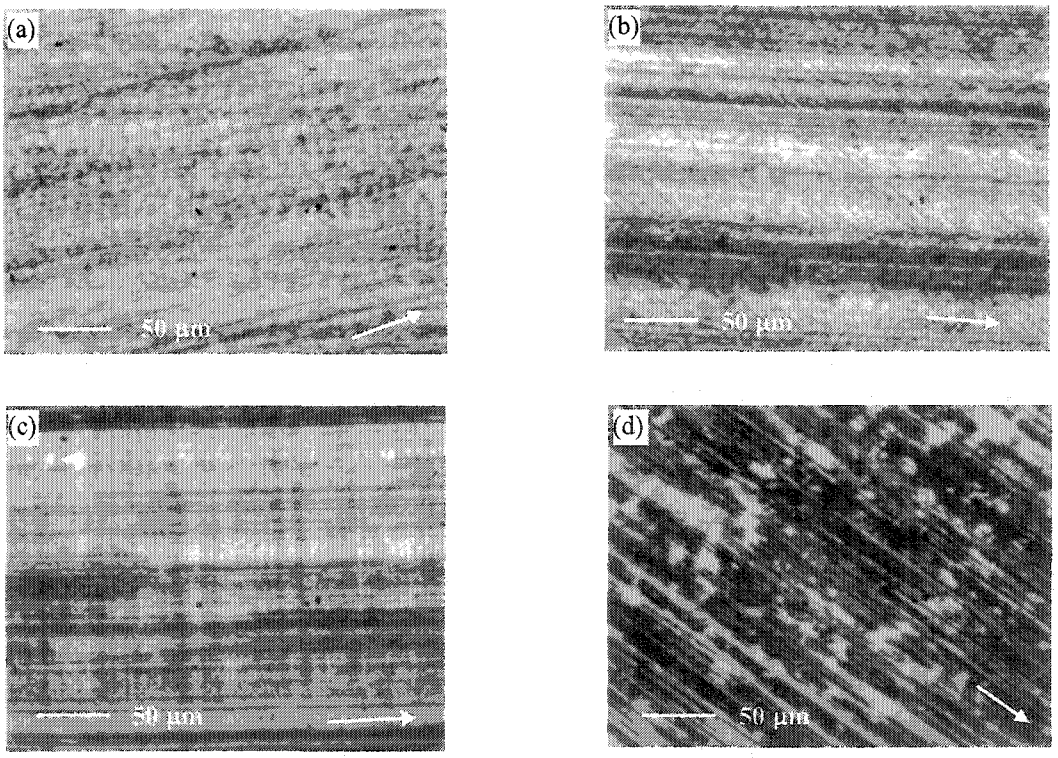

Figure 3.12 Optical micrographs of transfer films; (a) PPS+3% 80 μm tuff, (b) PPS+10% 45 μm tuff encapsulated with HDPE, (c) PPS+10% 80 μm tuff+10% microsize CuO, and (d) PPS+10% 80 μm tuff+4% Ag_2S. Test conditions same as in Fig. 3.2. Arrow indicates sliding direction.

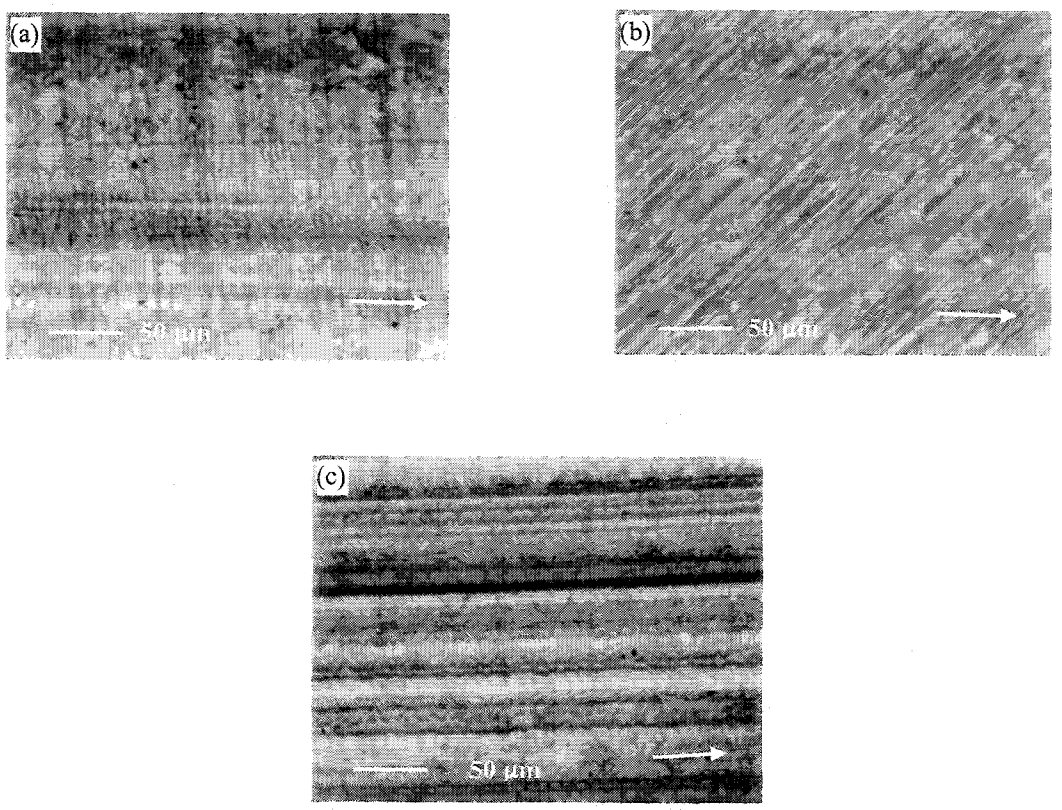

Figure 3.13 Optical micrographs of transfer films; (a) PPS+5% 100 nm bentonite, (b) PPS+5% 100 nm bentonite+5% PTFE, and (c) PPS+7% 35 μm bentonite treated with Katamin AB-18. Test conditions same as in Fig. 3.2. Arrow indicates sliding direction.

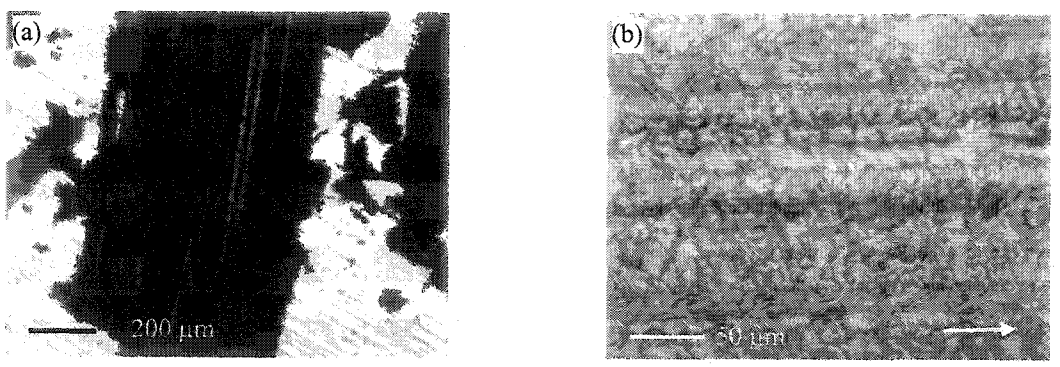

Figure 3.14 (a) Worn particles of PPS+10% 45 μm travertine and a large fragment of separated transfer film, and (b) optical micrograph of the transfer film of PPS+5% 35 μm travertine treated by Katamin AB-18. Test conditions same as in Fig. 3.2. Arrow indicates sliding direction.

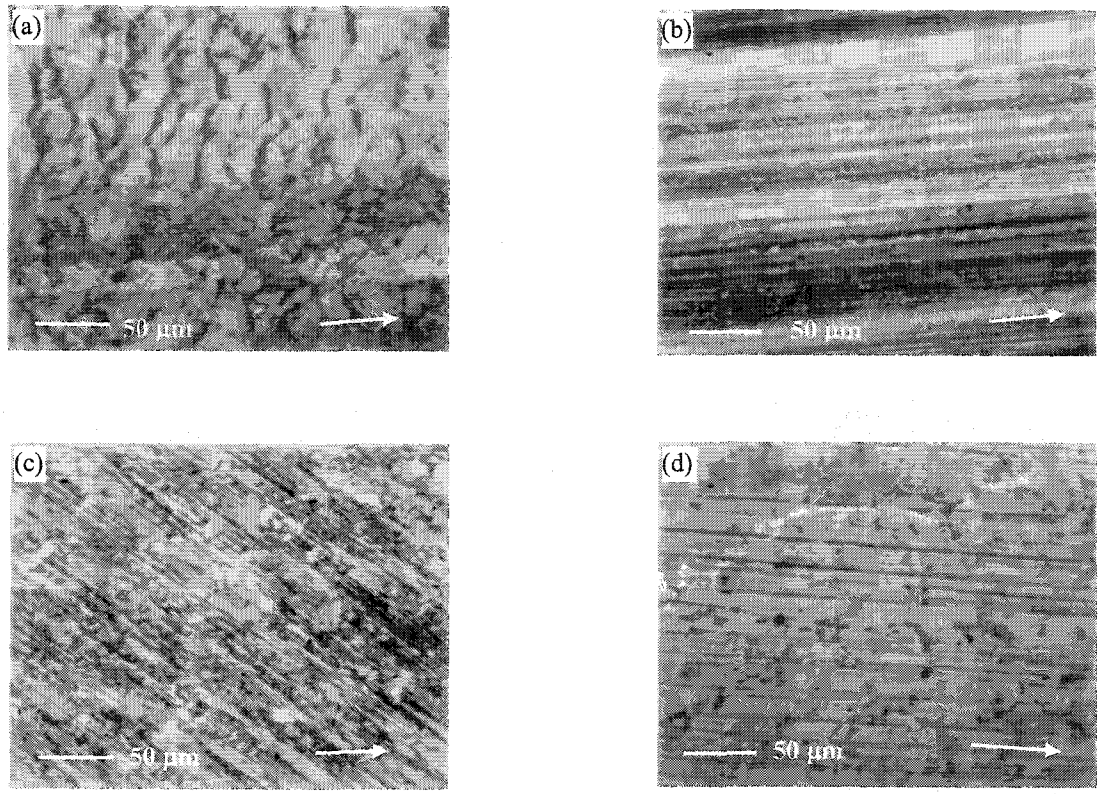

Figure 3.15 Optical micrographs of transfer films; (a) PPS+17%MoO_3(50μm), (b) PPS+17%MoO_2 (1μm), (c) PPS+7%MoO_2(50nm), and (d) PPS+7%MoO_2(1μm) +5%PTFE. Test conditions same as in Fig. 3.2. Arrow indicates sliding direction.

CHAPTER 4
FRICTION AND WEAR STUDIES USING TAGUCHI METHOD ON POLYPHENYLENE SULFIDE FILLED WITH A COMPLEX MIXTURE OF MoS_2, Al_2O_3, AND OTHER COMPOUNDS

A paper submitted to *Wear*

Minhaeng Cho and Shyam Bahadur

4.1 Abstract

The tribological behavior of PPS filled with molybdenum-concentrate (MC) deposit from Armenia was studied. The deposit MC was a complex mixture of compounds such as MoS_2, SiO_2, CuS, Al_2O_3, and others. Whereas MC as the filler in particulate form reduced the steady state wear rate of PPS, the optimum reduction in wear was found to occur with the addition of PTFE along with PPS. The behavior of PPS composites made with MC and PTFE sliding against a steel counterface was investigated as a function of the MC and PTFE proportions, sliding speed, and counterface roughness. For this purpose, pin-on-disk configuration and the design of experiments approach utilizing Taguchi's orthogonal arrays were used. Of all the above factors, the change in MC proportion, while PTFE was also present, had the greatest effect on the reduction in wear rate. The variation of the coefficient of friction was found to be in the narrow range of 0.27-0.33. The lowest wear rate was found in the case of PPS+17vol.%MC+10vol.%PTFE composite sliding at 1.5 m/s against a counterface roughness of 0.1 μm Ra. Optical and scanning electron microscopy of the transfer films were performed for observation of the features such as coverage, thickness, topography, and bonding. Friction and wear results are discussed in terms of these observations.

4.2 Introduction

The modification of the tribological behavior of polymers by the addition of filler materials has shown a great promise and so has lately been a subject of considerable interest. The filler materials include organic, inorganic, and metallic particulate materials in both macro and nano sizes. Most studies on filler action in the case of polymer composites sliding against metal counterfaces have focused on the reduction of wear rate and the coefficient of friction. Solid lubricants such as graphite, MoS_2, and polytetrafluoroethylene (PTFE) when added to polymers have proven effective in reducing the coefficient of friction but their action on wear resistance is not that specific. It is well known that the wear rate of unfilled PTFE is very high [1], but low wear rate and the coefficient of friction have been obtained by the addition of PTFE to various polymeric materials. For example, Yamaguchi [2] showed that wear rate was reduced with the addition of PTFE to polymers such as polyphenylene sulfide (PPS), polyvinylchloride, polyarylate, polyoxymethylene, polyimide, and diallyl-phthalate. Mens *et al.* [3] reported that PTFE when filled in PPS reduced the wear rate of the polymer remarkably. The role of PTFE filler in modifying the tribological behavior has also been reported for fiber-reinforced composites. Bolvari *et al.* [4] reported that a considerable reduction in wear and the coefficient of friction of polyamide 6,6 reinforced with aramid fiber was obtained when PTFE was added to it. Bahadur *et al.* [5] reported that the steady state wear rates of polyamide reinforced with glass fabric or CuO alone, or in combination, were further lowered by the addition of PTFE. In contrast to the above observations, Jacobs *et al.* [6] reported that in the case of epoxy resin PTFE did not improve its wear resistance. It thus seems that wear reduction by PTFE is specific to the polymer and the reasons for the anomaly are not known. It is also not known how PTFE would affect the tribological

behavior of a polymer in the presence of a complex mixture of inorganic fillers such as molybdenum-concentrate (MC).

Studies [3,7-10] have been reported on the effect of MoS_2 addition in terms of the tribological behavior of PTFE, nylon 6/6, and PPS. Whereas MoS_2 reduced the wear rates of these polymers, the reduction of the coefficient was not observed. Conversely, MoS_2 increased the wear rate of nylon 1010 [11] but the coefficient of friction decreased with one exception. It was further reported that the effect of MoS_2 in terms of wear reduction was meager when MoS_2 was used together with carbon fiber in nylon 1010. Ridson *et al.* [7] reported that the addition of graphite to MoS_2/PTFE system resulted in a very low wear rate and also the coefficient of friction. Tanaka *et al.* [9] also showed that PTFE filled with graphite exhibited much lower wear rate than when filled with MoS_2, ZrO_2, and TiO_2 fillers.

Apart from the polymer composition, wear rate and coefficient of friction depend upon counterface roughness and sliding speed. This dependence has been extensively studied by many researchers. Anderson [12] reported that the steady state wear rate of ultrahigh molecular weight polyethylene (UHMWPE) increased with the increase in sliding speed. Dickens and Sullivan [13] found that steady state wear rate increased with the increase in sliding speed for PPO, PEEK, and PTFE, but the coefficient of friction was not greatly affected in the case of PPO and PEEK whilst it increased in the case of PTFE. Bahadur and coworkers [14,15] reported that the wear rate of nylon increased at a high counterface roughness of 0.3 μm Ra due to the absence of transfer film on the counterface. They showed that abrasive action was dominant when the counterface was rough thereby resulting in high wear rate and wear rate increased due to thermal softening of the polymer when the sliding speed was increased to 2 m/s. In the case of PPS, steady state wear rate increased at both low

and high sliding speeds. Thermal softening was observed at the sliding speed of 2 m/s thereby resulting in higher wear rate. The coefficient of friction of PPS decreased as the sliding speed was decreased from 1.0 to 0.25 m/s, but the highest sliding speed of 2 m/s showed the lowest friction of coefficient because of thermal softening [16,17]. It was also shown that the development of transfer film was associated with counterface roughness, and the transfer films were patchy and discontinuous when the counterface roughness was either very low or very high.

The present work was done with the objective of exploring the effectiveness of large mineral deposits in Armenia as the fillers in polymers in terms of the desirable tribological behavior. The utilization of these deposits for industrial purposes is vital for the economy of the country in post-Soviet era. Of the many deposits, a mineral called Mo-concentrate was selected for this study. Whereas earlier studies on the tribological behavior of PPS filled with single compounds have been done, no study on the effect of a complex deposit, which is a mixture of many compounds, has been performed. In addition, the objective was to develop a composition utilizing this filler and PPS that would be promising for industrial usage of the material. The tribological behavior of a few typical compositions was also studied as a function of sliding speed and counterface roughness, using the design of experiments approach.

4.3 Experimental Details

4.3.1 Materials

Mo concentrate (MC) is a complex mineral whose composition is given in Table 4.1. It has a large 82 wt.% MoS_2, 9 wt.% SiO_2, 1.6 wt. % CuS, 1.2 wt.% Al_2O_3, a small proportion

of Fe_2O_3, and the traces of elements such as Na, K, Pb, Sn, Re, etc. It is hygroscopic and contains traces of oil as well. Because of the latter, it is known to have antifriction characteristics. The dark and shiny mineral filler in the as-received form consisted of a wide particle size distribution. It was therefore pulverized and later sieved to a size less than 45 μm. The use of larger size particles was avoided because they could cause abrasion of the steel counterface during sliding experiments.

The matrix polymer material used was polyphenylene sulfide (PPS) which was supplied in powder form by the Phillips Chemical Company. The tribological behavior of PPS filled with this filler was modified by adding PTFE (FLUON® as Grade G163 powder in 25 μm mean size) which was supplied by Asahi Glass Fluoropolymer Co.

4.3.2 Specimen preparation

PPS powder and the mineral filler were dried in an electric oven at 125°C for 5 hours. PTFE powder was kept in a desiccator overnight. The materials were then weighted in the proportions needed and the mixture was blended in an ultrasonic bath of acetone for 30 minutes. Acetone was expected to wash out oil and moisture in the mineral without having any adverse effect on PPS and PTFE. The mixture was dried by exposure to atmosphere as acetone evaporates rapidly. The dried mixture was loaded in a cylindrical mold in order to obtain 6.35 mm diameter and 11.00 mm long pins. The mixture was compacted by applying pressure. A maximum pressure of 36 MPa was applied for one minute to the compacted material in the mold heated to 310°C so as to expel the entrapped air out of the mold. The pressure was then lowered to 18 MPa and maintained at this level for 10 minutes. It was further lowered to 9 MPa and maintained for 5 minutes. Afterwards, heat was turned off and

the molded material was left to cool in the mold for 1 hour prior to opening. The cylindrical sample, 6.35 mm in diameter and 11 mm long, was machined to 6.2 mm in diameter and 10 mm in length. The latter was the specimen size used in sliding tests.

4.3.3 Sliding tests

Sliding tests were performed in a pin-on-disk configuration with the pin end of 62 mm diameter resting on a rotating counterface. The latter was in the form of a disk, 5 mm thick and 76 mm in diameter, and was made of quench-hardened tool steel with a hardness of HRC 55-60. Three different surface roughnesses were chosen for the counterface: 0.06, 0.1, and 0.14 μm Ra. The disks were finished by unidirectional abrasion against SiC papers. They were washed with soap and water, dried with a jet of air, and stored in a dessicator. Sliding tests were performed at three speeds: 0.5, 1.0, and 1.5 m/s. They were run over a distance of 21.6 km irrespective of the sliding speed. The contact surface of the pin was finished to ensure maximum contact with the counterface. The nominal contact pressure of 0.65 MPa was applied during sliding. Sliding tests in the case of 1 m/s sliding speed were interrupted twice every half hour and later every hour for gravimetric measurements with an accuracy of 10 μg. The tests at other sliding speeds were also interrupted at the same sliding distances. Mass loss was converted into volume loss for plotting the wear data using the computed density values based on the composition. Friction force was measured from the output of strain gages mounted on the specimen-loading arm. A minimum of two tests were run for each condition. If the difference between wear was more than 15 %, a third test was also performed. The maximum variation in wear and the coefficient of friction was less than 15% and 10%, respectively, between test to test for the same sliding conditions.

4.3.4 Design of experiment by Taguchi analysis

The purpose of the design of experiments was to investigate the tribological behavior of the composites for different test conditions. Since the tests were performed under ambient conditions at a fixed contact pressure, the only sliding variable was sliding speed. The latter was limited to 1.5 m/s in order to avoid excessive temperature rise at the sliding interface. The other test variables were counterface roughness and composite compositions. It is well documented that wear and the coefficient of friction vary with counterface roughness [14-17]. The counterface roughness values chosen in our investigation were 0.06, 0.10, and 0.14 μm Ra, representing from a real smooth to a moderately rough surface topography. The composites were comprised of Mo-concentrate (MC), PTFE, and PPS. Based on earlier experience, PTFE was limited to 15 vol.%, and three volume proportions of PTFE were used. Similarly, three proportions of MC were also used. Here the total amount of both fillers was kept below 35 vol.% because an excessive amount of filler makes the molded composite specimen fragile. The selection was also guided by the findings that 20-25 vol.% microfillers in polymer composites provide an optimum wear reduction [18,19]. The details of the parameters and their values are given in Table 4.2. We have four parameters and three levels for each parameter. From the consideration of these experimental conditions, a pre-designed orthogonal array, called $L_9(3^4)$, developed by Taguchi was applied to this study. Table 4.3 describes the detailed orthogonal arrays used in this study. Here, each row represents the test conditions and the column represents a test parameter. With 4 parameters and three levels for each, a full factorial experiment would require 3^4=81 runs. On the other hand, Taguchi's fractional factorial experiment approach reduces the requirement to nine runs and hence offers a great advantage.

Based on the results from the above experiments, confirmation tests were also carried out using each parameter value at its lowest wear rate level. This was to confirm whether the result was optimized or not. This test is not always included in the original test set-up arrays. If this is the case, an additional test using the optimized level from each parameter must be carried out with the combination of both the sample and the test conditions that provided the lowest wear rate.

4.4 Results and discussions

4.4.1 Effect of fillers on friction and wear

Friction and wear results for PPS filled with MC are shown in Fig. 4.1. The percent compositions used throughout the paper are by volume. It should be noted that the filler MC reduced the coefficient of friction of PPS by 50% to a value of 0.33 which is comparable to that of the coefficient of PTFE (a solid lubricant) at 1 m/s sliding speed. The reduction in the coefficient of friction was brought about by a large proportion (82 wt.%) of MoS_2, but this could not be said a priori because the other constituents in MC such as SiO_2, Al_2O_3, and Fe_2O_3 would be expected to increase friction. There was also a reduction in wear rate but it was still too high for practical usage. It was decided, therefore, to add a small amount of PTFE to this filled composition which produced a dramatic reduction in wear while keeping the coefficient of friction low. Both the transient and steady wear states are clearly seen for all the compositions, but the effect of transient state on the wear of PPS+17%MC+5%PTFE is negligible and the steady state wear rate of 0.01 mm^3/km is very low. On the whole, it was therefore a very desirable result. Furthermore, these observations led us to include PTFE

along with the mineral filler in subsequent studies and hence the experimental design used in this study.

Figure 4.2 shows the plots of wear loss and the coefficient of friction for the design set-up arrays given in Table 4.3. The wear results for the first five combinations are given in Fig. 4.2(a) and for the remainder four in Fig. 4.2(c). This split-up was done to avoid jumbling of the test results. For the same reason, the coefficient of friction plots were also split up in Fig. 4.2(b) and 4.2(d). In all the cases, both transient and steady states of wear are seen but the transition state is mild for 15%PTFE irrespective of the MC proportion. Furthermore, 17% MC along with any of the three PTFE proportions was quite effective in reducing the steady state wear rate. Steady state wear rates with 5%MC and any proportion of PTFE were in general very high. The coefficient of friction for all the compositions was 0.3 ± 0.03.

4.4.2 Taguchi analysis of wear rate and friction

In order to perform Taguchi analysis, steady state wear rates are plotted in Fig. 4.3 as a function of the parameters used in this study. Here, each point represents the mean of the three wear rate values obtained for a particular parameter while using different values of the other parameters. From Fig. 4.3, it is seen that the steady state wear rate decreased significantly as the proportion of the mineral filler MC increased from 5 to 10%. The change in the wear rate was insignificant when the mineral filler proportion increased from 10 to 17%. Thus, this plot indicates the effectiveness of this mineral filler for lowering the wear rate of the composites. It also indicates that using a MC proportion greater than 17% would serve no useful purpose in terms of wear reduction. Furthermore, it would make the composite material fragile. From the plot of steady state wear rate vs. PTFE %, it is seen that

10% PTFE proportion is most effective and a greater proportion would be undesirable in view of the composite getting fragile. It is also not needed for lowering the coefficient of friction because no significant reduction with the increase in PTFE is either observed or expected.

As for the effect of sliding speed, steady state wear rates were about the same in the range of 0.5 to 1 m/s but decreased as the sliding speed increased to 1.5 m/s, as seen from Fig. 4.3. The decrease in wear rate at high speed occurred because of thermal softening as was reported in another study [16]. The polymer did so well in terms of the wear resistance up to 1 m/s because it is a high temperature polymer. The variation of the coefficient of friction with sliding speed was not significant in our experiments (Fig. 4.4). This observation is in agreement with that reported earlier [15,16].

As for the counterface roughness, the reduction in steady state wear rate was observed from 0.06 to 0.10 μm Ra and slight increase from 1.0 to 1.5 μm Ra. This behavior is also in agreement with the results reported earlier on polymers such as polyamide and PPS [14-16]. The coefficient of friction against very smooth surfaces (such as 0.06 μm Ra used in this work) is high because of high adhesion between the mating surfaces. The counterface roughness for the minimum wear has been reported to be different for different polymers. Figure 4.4 shows the plots of the coefficient of friction with the change in parameters. The variation is not significant as indicated by the upper and lower boundary lines which were determined by the scatter in the coefficient of friction data.

The confirmation test was done for the levels that provided the lowest steady state wear rate for each parameter. These were 17%MC, 10%PTFE, 1.5 m/s sliding speed, and 0.1 μm Ra. The test gave the lowest steady state wear rate of 0.0024 mm^3/km. The corresponding

coefficient of friction was 0.31 which is the average value of all the test results. This indicates that the design of experiments as used in this work was valid.

4.4.3 Transfer film studies

The transfer films were studied because their role in the tribological behavior of polymers is important. It has been reported [20] that wear depends upon the capability of the material to form a uniform and thin transfer film on the counterface and the thickness and texture of the transfer film. PPS, which is the matrix material used in this work, is known to form a thick and grainy transfer film on the counterface [21, 22], as seen in Fig. 4.5(a). Figure 4.5(b-d) shows the transfer films formed on the counterface during steady state sliding for three compositions: PPS and the mineral filler, and two compositions with both PTFE and the mineral filler. In the case of PPS+17%MC composite (Fig. 4.5b), the transfer film is fairly thick because abrasion marks from the finishing operation of the disk cannot be seen at all. The surface exhibits deep furrows which are produced on the soft and thick polymer transfer film surface due to sliding action. It was observed during sliding test that the transfer film formed quickly at the onset of sliding and the wear track was covered with a dark and thick transfer film. The transfer film was being peeled from the surface thereby generating large wear particles. This behavior indicated that adhesion between the film and the metal surface was poor. A behavior like this can be associated with high wear rate.

The transfer films were also examined for all of the nine conditions given in Table 4.3. It was found that transfer films formed on the counterface in all cases. Figure 4.5(c-d) shows the transfer films for two typical cases. These transfer films are much thinner and much more uniform than observed in Fig. 4.5(b) and this change is because of the addition of PTFE to

PPS+MC composite. The deep grooves are no longer seen here and the surface topography is fairly smooth. The abrasion marks by the finishing operation are seen, which indicates that the transfer film is almost transparent. The latter is the case because the film is too thin. The transfer film is covering the entire track uniformly and it appears to be mechanically locked into the grooves on the metal counterface. The latter promotes strong adhesion between the film and the counterface. The film is thus not peeled easily during sliding so that it is not depleted and so the loss of material contributing to wear is greatly diminished.

In order to provide support to the observations stated above, the transfer films of two mineral-filled compositions, with and without PTFE, were studied by scanning electron microscopy. Figure 4.6 shows the SEM micrographs of the transfer films for these two compositions. As may be seen in Fig. 4.6(a), the transfer film of PPS+17%MC composite is grainy and fairly thick. This feature was also seen in the corresponding optical micrograph. Figure 4.6(b) shows the edge of transfer film on the counterface which appears to be well-defined. It is clearly seen that the transfer film is thick and loosely bonded along its edge to the counterface. Figure 4.6(c) shows wear particles and the transfer film of PPS+17%MC +5%PTFE composite. The tiniest wear particles are of the size of about one micron. There are some bigger particles which were presumably formed by the compaction of these small particles. Unlike the case of PPS+17%MC composite, the transfer film in this case is thin and coherent, as may be seen in Fig. 4.6(c). The abrasion marks on metal counterface are well covered by this coherent and smooth transfer film. The edge of wear track for this composite is seen in Fig. 4.6(d). It shows clearly that the transfer film is strongly adhering to the counterface and the film is much thinner than that observed in the earlier case when PTFE was not in the composite material.

4.4.4 XPS analysis of transfer film

The transfer films of MC-filled PPS composites, with and without PTFE, were analyzed by XPS in order to detect the chemical compounds if any formed near the sliding interface. XPS analyses were carried out for both the top layer of the transfer film and at a location closer to the steel substrate. For the latter case, transfer film was mildly scraped by a razor blade.

The XPS spectra of both the unscratched and scratched transfer films of PPS+17%MC composite are given in Fig. 4.7. The identified compositions along with their binding energies are listed in Table 4.4. This was done with the help of the Handbook of X-ray Photoelectron Spectroscopy [23] and an earlier reported XPS study of PPS [22]. These results revealed that certain chemical reactions occurred during sliding. It was found that MoS_2 in the mineral filler decomposed to both the elemental Mo and S. It seems that the elemental Mo reacted with O_2 and H_2O in atmosphere, thereby generating MoO_3 compound. The generation of MoO_3 when MoS_2 is used as the filler material in polymer has been reported earlier [11,24]. It is also known that MoO_3 is derived by heating MoS_2, and so it can be thought that temperature at the interface increased considerably during sliding action. The active S from the decomposition of MoS_2 could react with Fe in the counterface metal so that $FeSO_4$ would form. Elemental S is believed to be from the decomposition of MoS_2 and not PPS during sliding. This is so because no sulfur compounds were detected in the transfer film of PPS filled with PbTe or PbSe [22,25]. This indicates that the decomposition of PPS did not occur in these composites. S(2p) spectra show the binding energies for MoS_2, $FeSO_4$, and for S in PPS. Fe_2O_3 is formed from the oxidation of steel counterface with atmospheric O_2.

In case of the scratched transfer film of PPS+17%MC composite, the configuration of

spectra is about the same with the exception of the intensity of each element. Specifically speaking, all intensities decreased at the interface except for Fe(2p) peak. It was so because the data was taken nearer to the steel substrate. It should, however, be noted that the compound $FeSO_4$ is still detected though its intensity decreased, which means that the decomposition of the filler occurred and the chemical reaction between elemental S and counterface Fe took place throughout the transfer film. Additionally, oxidation of the steel counterface occurred because Fe_2O_3 was detected.

XPS spectra of the transfer film of PPS+17%MC+5%PTFE composite are given in Fig. 4.8. The identified compositions along with their binding energies are listed in Table 4.5. As before, MoS_2 in the composite decomposed into elemental Mo and S and MoO_3 was formed. The peaks at 162.5 eV and 168.8 eV in the S(2p) spectrum correspond to S in MoS_2 and $FeSO_4$, respectively. The intensity of S at a location between the transfer film and the metal substrate was about the same as in the previous case. This indicates that the concentration of $FeSO_4$ was fairly constant through the transfer film. Thus the presence of PTFE helped in some ways in promoting the formation of $FeSO_4$. The latter has been reported [15,25] to promote a stronger bonding between the transfer film and the counterface which would account for lower wear. F in PTFE was detected but the spectra did not indicate the presence of any compound with F in it. The intensity of F spectrum decreased closer to the interface but was still high.

The above discussion of XPS analysis of transfer films led to the conclusion that some tribochemical reactions occurred during sliding. In case of both composites, MoS_2 decomposed to elemental Mo and S. The presence of MoO_3 in the spectrum shows that elemental Mo reacted either with O_2 or H_2O, or both, in the atmosphere thereby producing

MoO_3. Elemental S reacted with Fe in the steel counterface and formed $FeSO_4$ in the presence of O_2. The presence of PTFE in the material made this process more vigorous. As reported earlier [15,16], this compound promotes the adhesion of transfer film to counterface. The development of thin and uniform transfer film which bonded well to the counterface was responsible for low wear rates in the case of the composites with PTFE.

4.5 Conclusions

1. Mo-concentrate mineral from Armenia as the filler in PPS lowered the steady state wear rate of PPS by a small amount. The reduction was, however, much greater when PTFE was also included as the filler.
2. The coefficient of friction of PPS was lowered from 0.48 to 0.33 with the addition of MC filler. Further addition of PTFE lowered the coefficient of friction by an insignificant amount. The coefficient of friction for all the filled composites was in the range of 0.27 - 0.33.
3. PPS+17%MC+10%PTFE composite sliding at 1 m/s speed, against a steel counterface of 0.1 μm Ra counterface roughness, provided the lowest steady state wear rate of 0.0024 mm^3/km in this study. The steady state wear rate of the unfilled PPS was 0.29 mm^3/km.
4. Design of experiments approach by Taguchi method enabled us to analyze successfully the friction and wear behavior of composites with two fillers, sliding velocity, and counterface roughness as the variables with fewer experiments that would otherwise be needed.

5. The transfer films formed on the steel counterface in the case of PPS+MC composite with PTFE were very thin and uniform. These features were responsible for a very low wear rate.
6. XPS analysis of transfer films revealed that MoS_2 decomposed to Mo and S so that the compounds MoO_3 and $FeSO_4$ were formed. The presence of $FeSO_4$ in transfer film indicates the tribochemical reaction between S and Fe in the counterface, which presumably promoted adhesion between the transfer film and the counterface. The adhesion retarded the loss of transfer film from the counterface, which contributed to the reduction in wear rate.

4.6 References

1. K. Tanaka, Y. Uchiyama, S. Toyooka, The mechanism of wear of polytetrafluoroethylene, Wear 23 (1973) 153-172.
2. Y. Yamaguchi, Tribology of plastic materials, Tribology Series, Elsevier, Vol. 16, 1990, 156-193.
3. J.W.M. Mens, A.W.J. de Gee, Friction and wear behavior of 18 polymers in contact with steel in environments of air and water, Wear 149 (1991) 255-268.
4. A. Bolvari, S. Glenn, R. Janssen, C. Elliset, Wear and friction of aramid fiber and PTFE filled composites. Sealing Technology, 1997 (47) 7-9.
5. S. Bahadur, V.K. Polineni, Tribological studies of glass fabric-reinforced polyamide composites filled with CuO and PTFE, Wear 1996 (200) 95-104.
6. O. Jacobs, R. Jaskulka, F. Yang, W. Wu, Sliding wear of epoxy compounds against different counterparts under dry and aqueous conditions, Wear 256 (2004) 9-15.

7. T.J. Ridson, R.D. Loban, Effect of molybdenum disulfide on the wear rates of polymer composites. ASLE proceedings, 2nd International Conference on Solid Lubrication, 1978, 230-236.
8. B. Arkles, J. Theberge, M. Schireson, Wear behavior of thermoplastic polymer-filled PTFE composites, ASLE, 1977, 33(1), 33-38.
9. K. Tanaka, S. Kawakami, Effect of various fillers on the friction and wear of polytetrafluoroethylene-based composites, Wear 79 (1982) 221-234.
10. D. Gong, Q. Xue, H. Wang, Study of the wear of filled polytetrafluoroethylene, Wear 134 (1989) 283-295.
11. Junxiang Wang, Mingyuan Gu, Bai Songhao, Shirong Ge, Investigation of the influence of MoS_2 filler on the tribological properties of carbon fiber reinforced nylon 1010 composites, Wear 255 (2003) 774-779.
12. Anderson, J.C., High density and ultra-high molecular weight polyethenes: their wear properties and bearing applications, Tribology International, 1982. 15: p. 43-47.
13. P.M. Dickens, J.L. Sullivan, Speed effects on the dry and lubricated wear of polymers, Wear 112 (1986) 273-289.
14. S. Bahadur, D. Gong, The transfer and wear of nylon and CuS-nylon composites: filler proportion and counterface characteristics, Wear 162-164 (1993) 397-406.
15. A. Kapoor, S. Bahadur, Transfer film bonding and wear studies on PbS-nylon composite sliding against steel, Tribology International, 1993. 27(5): p. 323-329.
16. Q. Zhao, S. Bahadur, Investigation of the transition state in the wear of polyphenylene sulfide sliding against steel, Tribology Letters, 2002. 12(1): p. 23-33.

17. C.J. Schwartz, S. Bahadur, Studies on the tribological behavior and transfer film-counterface bond strength for polyphenylene sulfide filled with nanoscale alumina particles, Wear 237 (2000) 261-273.

18. S. Bahadur, D. Tabor, Role of fillers in the friction and wear behavior of high density polyethylene, Polymer wear and its control, ACS Symposium Series, ed. L.H. Lee. Vol. 287. 1985. 253-268.

19. L. Yu, S. Bahadur, An investigation of the transfer film characteristics and the tribological behaviors of polyphenylene sulfide composites in sliding against too steel, Wear 214 (1998) 245-251.

20. S. Bahadur, The development of transfer layers and their role in polymer tribology, Wear 245 (2000) 92-99.

21. Q. Zhao, S. Bahadur, The mechanism of filler action and the criterion of filler selection for reducing wear, Wear 225-229 (1999) 660-668.

22. Q. Zhao, S. Bahadur, A study of the modification of the friction and wear behavior of polyphenylene sulfide by particulate Ag_2S and PbTe fillers, Wear 217 (1998) 62-72.

23. C.D. Wagner, W.M. Riggs, L.E. Davis, J.F. Moulder, G.E. Muilenberg, Handbook of X-ray photoelectron spectroscopy: A reference book of standard spectra for identification and interpretation of XPS data, ed. J. Chastain, 1992. Perkin-Elmer Corp.

24. Laigui Yu, Shengrong Yang, Weimin Liu, Qunji Xue, An investigation of the friction and wear behaviors of polyphenylene sulfide filled with solid lubricants, Polymer Engineering and Science, 2000. 40(8). 1825-1832.

25. Q. Zhao, S. Bahadur, The mechanism of filler action and the criterion of filler selection for reducing wear, Wear 225-229 (1999) 660-668.

Table 4.1 Major constituents of Molybdenum-concentrate.

Constituents	Contents, weight %
MoS_2	82
SiO_2	9
CuS	1.6
Al_2O_3	1.2
Fe_2O_3	0.54
P	0.008
Pb	0.02
Bi	0.0075
Na + K	0.29
As	0.03
Sn	Traces only
Re	280 grams/ton
Moisture + Oil	5.0

Table 4.2 Filler contents and experimental conditions: 4 parameters and 3 levels.

Levels	Parameters			
No	Mo concentrate (MC) vol.%	PTFE vol.%	Sliding speed m/s	Roughness μm, Ra
1	5	5	0.5	0.06
2	10	10	1.0	0.10
3	17	15	1.5	0.14

Table 4.3 $L_9(3^4)$ Orthogonal arrays designed by Taguchi method.

Runs required	Fillers		Test Conditions	
Test No.	MC, vol.%	PTFE, vol.%	Speed, m/s	Roughness, μm
1	5	5	0.5	0.06
2	5	10	1.0	0.10
3	5	15	1.5	0.14
4	10	5	1.0	0.14
5	10	10	1.5	0.06
6	10	15	0.5	0.10
7	17	5	1.5	0.10
8	17	10	0.5	0.14
9	17	15	1.0	0.06

Table 4.4 Identified species in the XPS spectra of the transfer film of PPS+17%MC composite.

Species	Binding energies of peaks				
	C(1s)	O(1s)	S(2p)	Fe(2p)	Mo(3d)
Contaminated C	284.8				
C in PPS	284.8				
S in PPS			163.7		
Fe				707.0	
Mo					228.0
MoO_3		531.7			232.6
MoS_2			162.5		229.6
Fe_2O_3		529.6		710.8	
$FeSO_4$		532.4	168.8	712.1	

Table 4.5 Identified species in the XPS spectra of the transfer film of PPS+17%MC+ 15%PTFE composite.

Species	Binding energies of peaks					
	C(1s)	O(1s)	F(1s)	S(2p)	Fe(2p)	Mo(3d)
Contaminated C	284.8					
C in PPS	284.8					
S in PPS				163.7		
$(CF_2=CF_2)n$	292.2		689.0			
Fe					707.0	
Mo						228.0
MoO_3		531.7				232.6
MoS_2				162.5		229.6
Fe_2O_3		529.6			710.8	
$FeSO_4$		532.4		168.8	712.1	

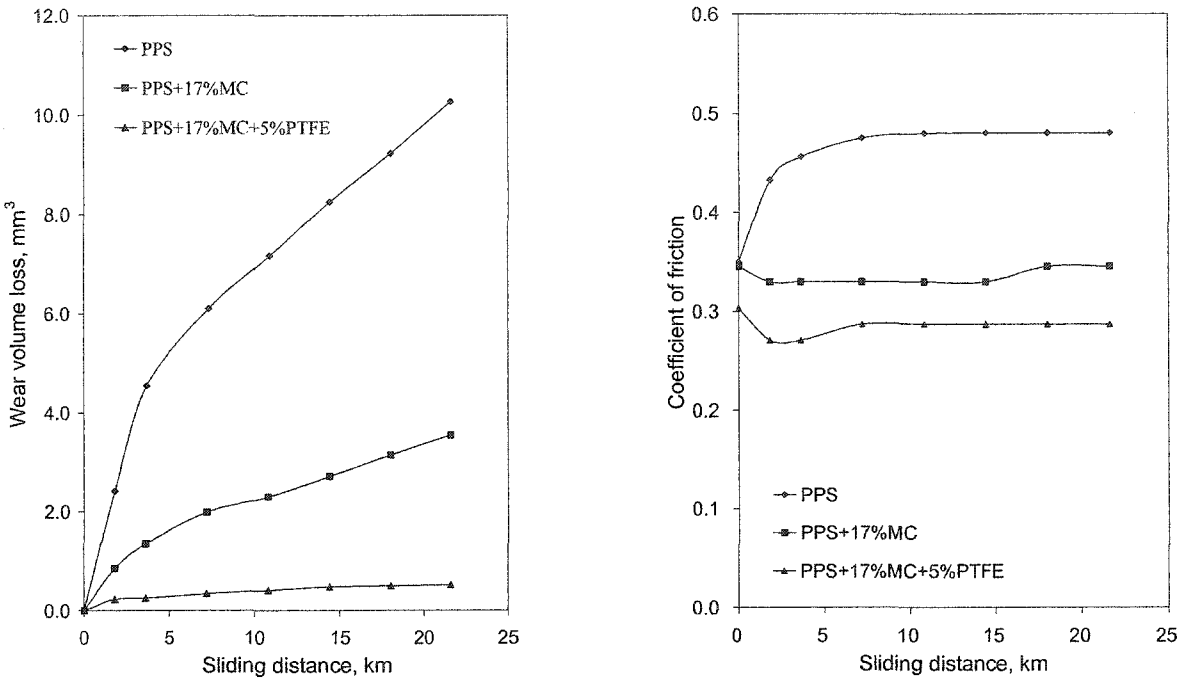

Figure 4.1 Variation of wear volume loss vs. slidin1g distance and coefficient of friction vs. sliding distance. Test conditions: sliding speed 1.0 m/s, nominal pressure 0.65 MPa, counterface roughness 0.10 μm Ra.

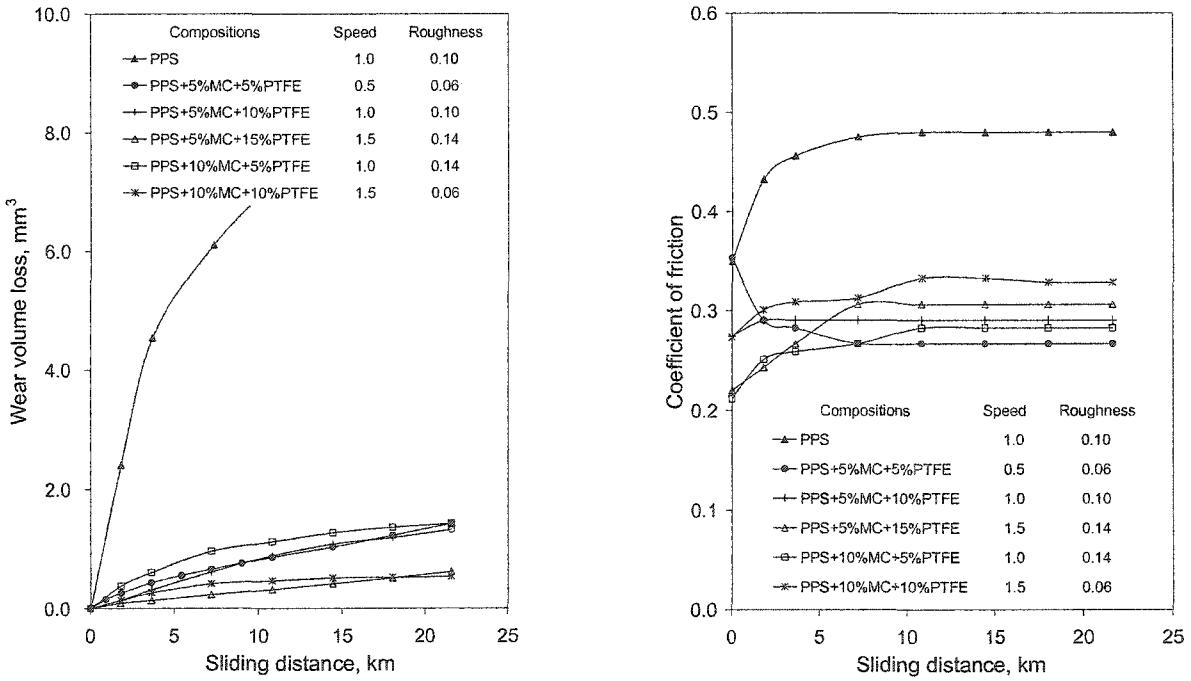

(a) (b)

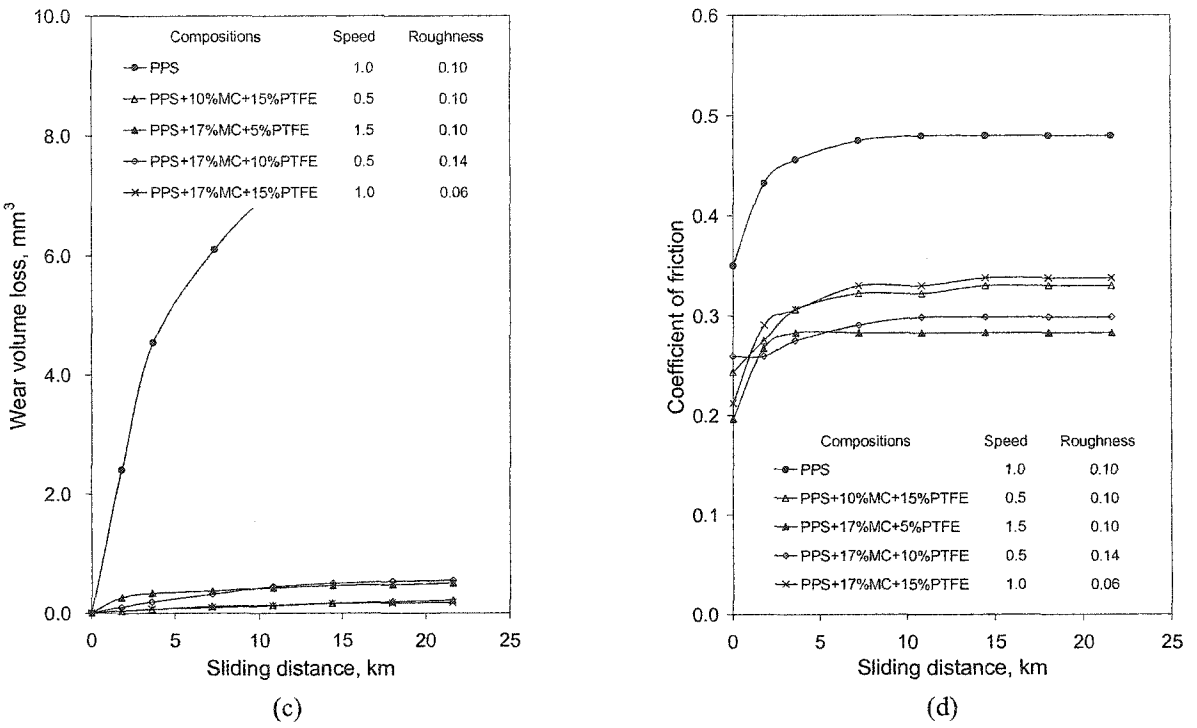

Figure 4.2 Variation of (a) and (c) wear volume loss vs. sliding distance, and (b) and (d) coefficient of friction vs. sliding distance. Refer to Table 4.3 for compositions and test conditions.

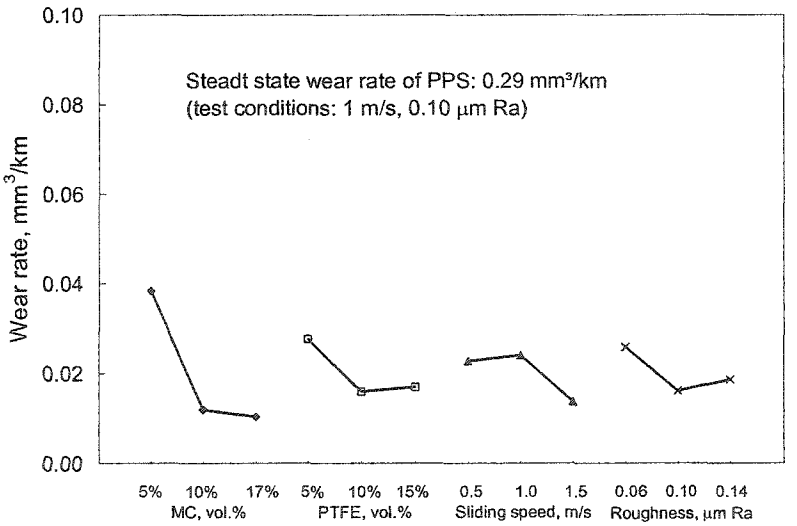

Figure 4.3 Plot of steady state wear rates with the variation of parameters.

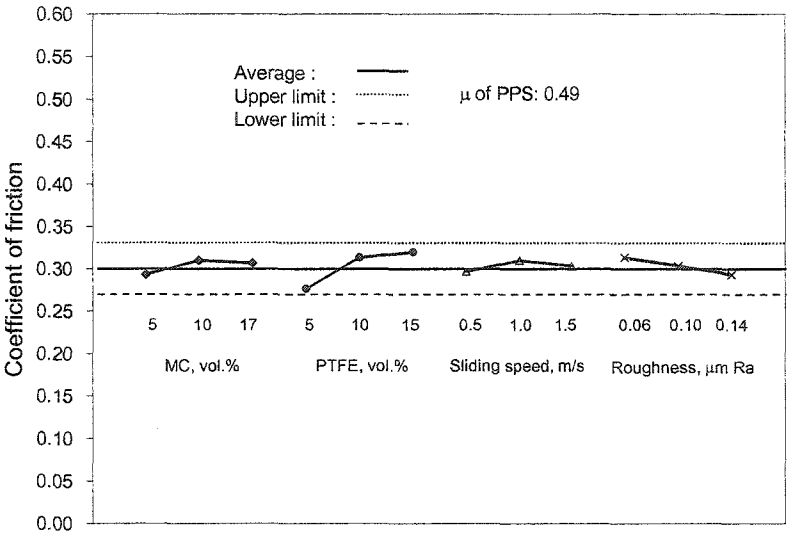

Figure 4.4 Plot of the coefficient of friction with the variation of parameters.

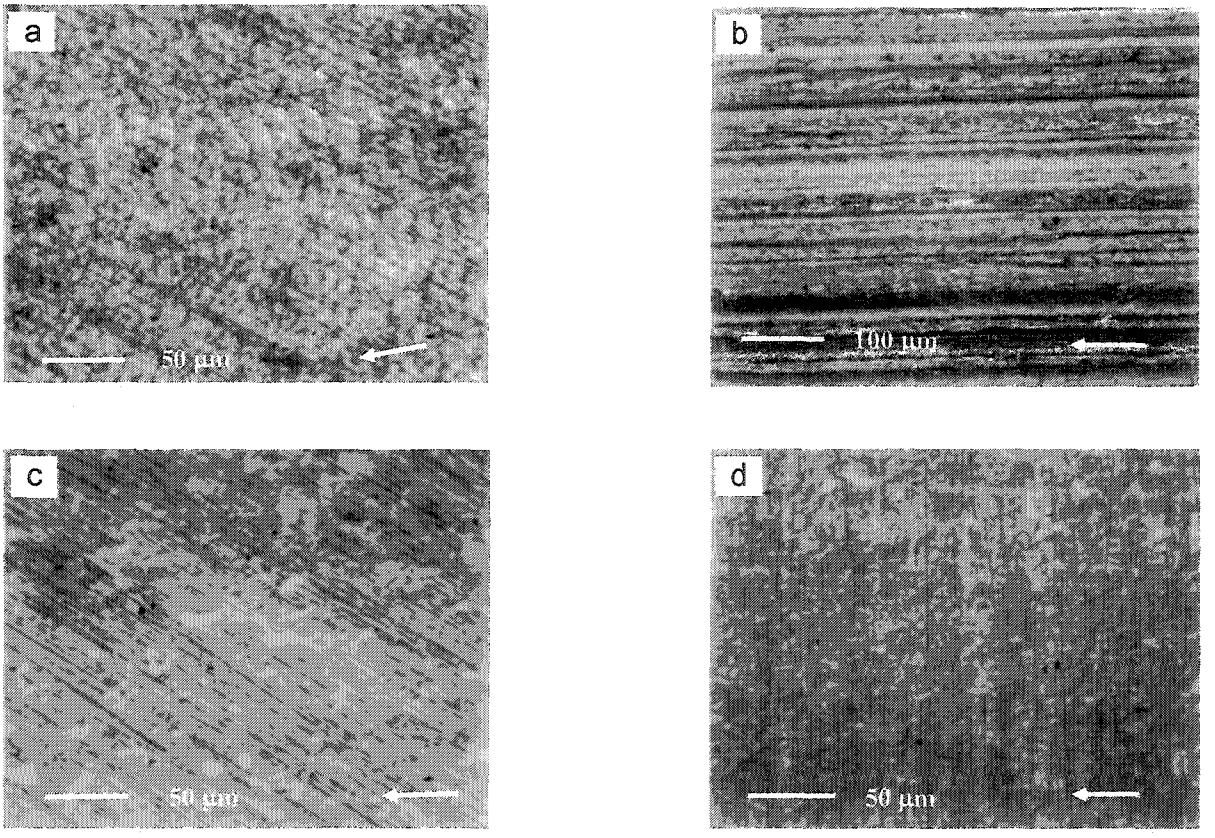

Figure 4.5 Optical micrographs of transfer film and test conditions; (a) PPS: 1.0 m/s , 0.1 μm Ra, (b) PPS+17% MC: 1.0 m/s, 0.1 μm Ra, (c) PPS+10%MC+10%PTFE: 1.5 m/s, 0.06 μm Ra and (d) PPS+17%MC +15%PTFE: 1.0 m/s, 0.06 μm Ra. Arrow indicates sliding direction.

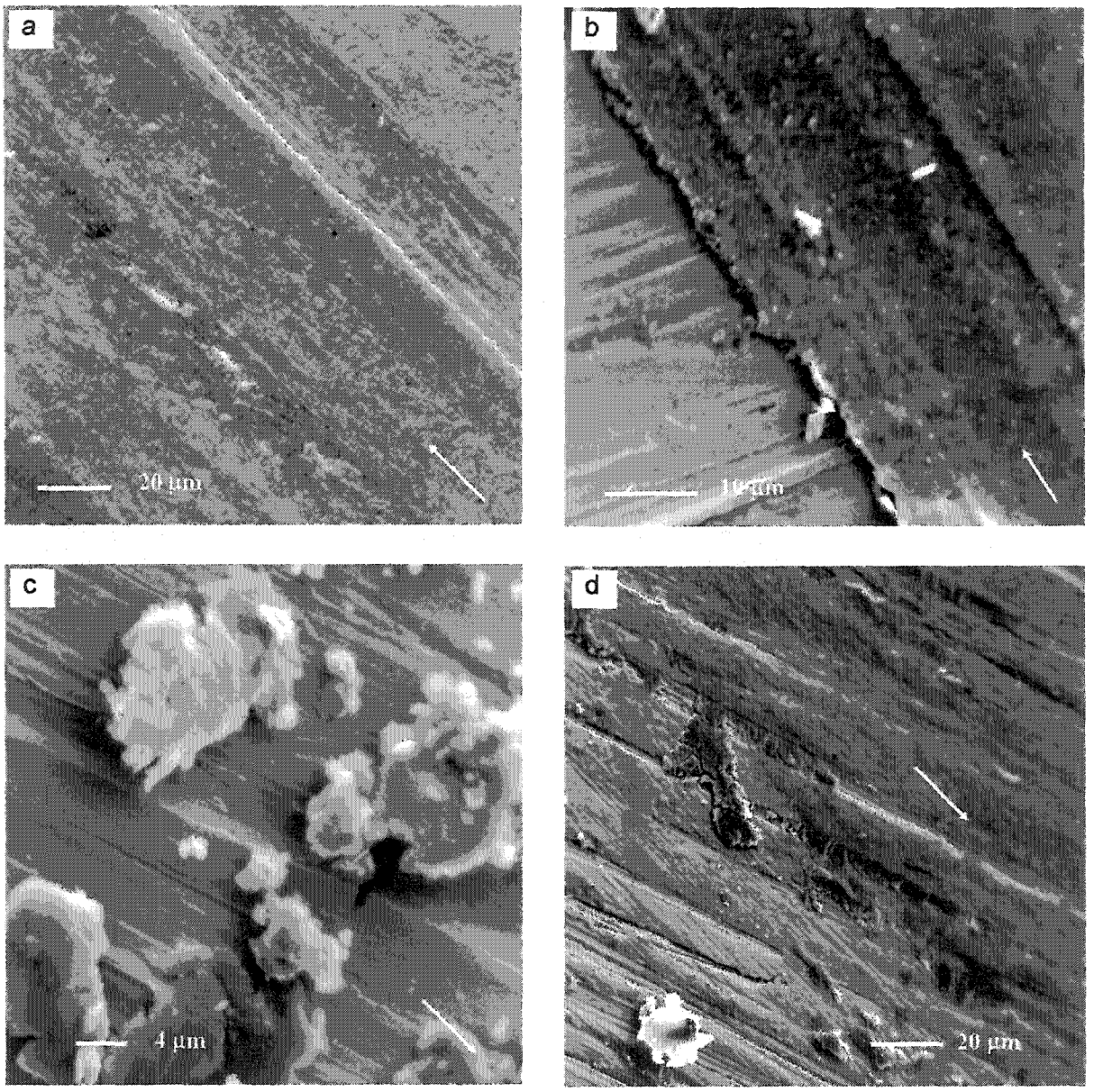

Figure 4.6 SEM micrographs of transfer film; (a-b) PPS+17%MC, (c-d) PPS+17%MC+5%PTFE composites. Sliding speed 1.0 m/s, contact pressure 0.65 MPa, and counterface roughness 0.09-0.11 μm Ra.

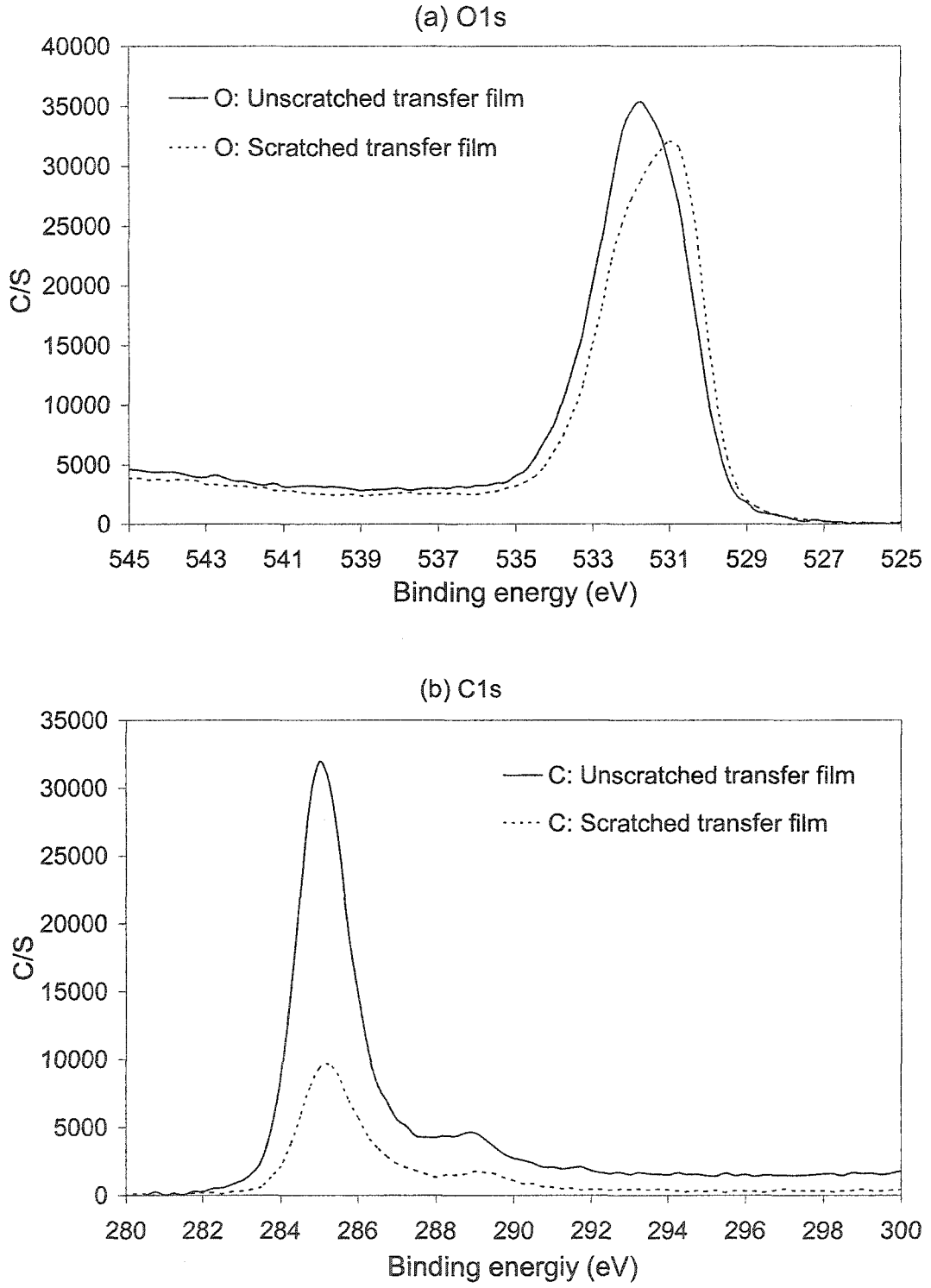

Figure 4.7 XPS spectra of the unscratched and scratched transfer films formed on the steel counterface by PPS+17%MC composite. (a) O1s; (b) C1s; (c) Fe2p; (d) Mo3d; (e) S2p.

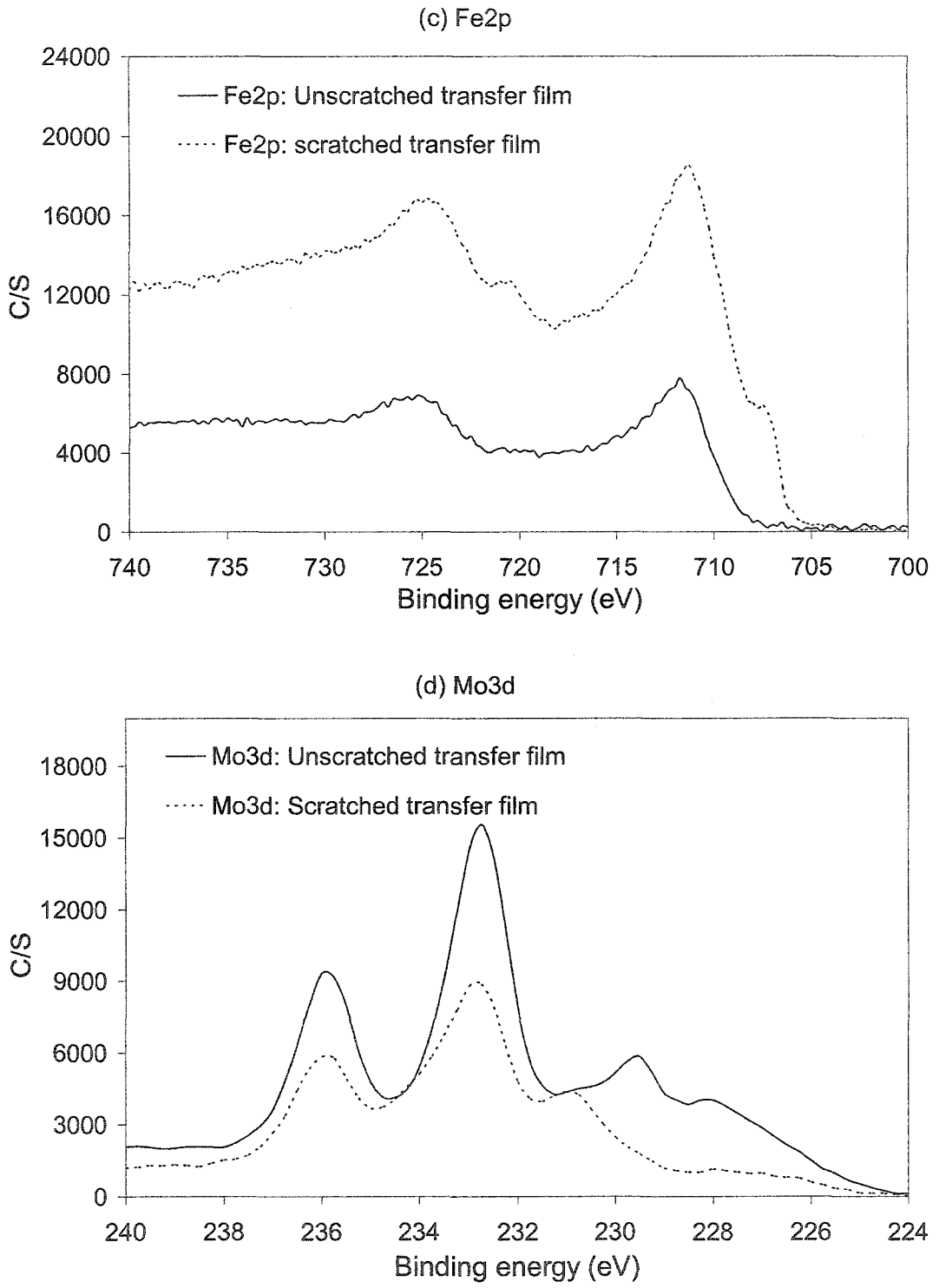

Figure 4.7 continued. XPS spectra of the unscratched and scratched transfer films formed on the steel counterface by PPS+17%MC composite. (c) Fe2p; (d) Mo3d.

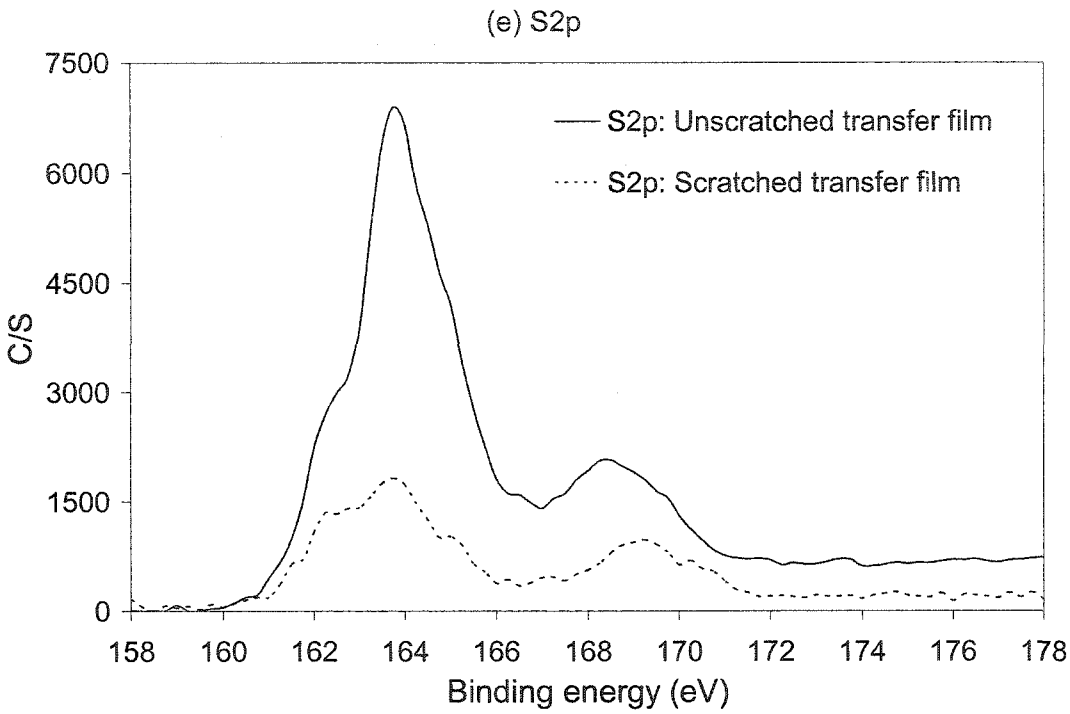

Figure 4.7 continued. XPS spectra of the unscratched and scratched transfer films formed on the steel counterface by PPS+17%MC composite. (e) S2p.

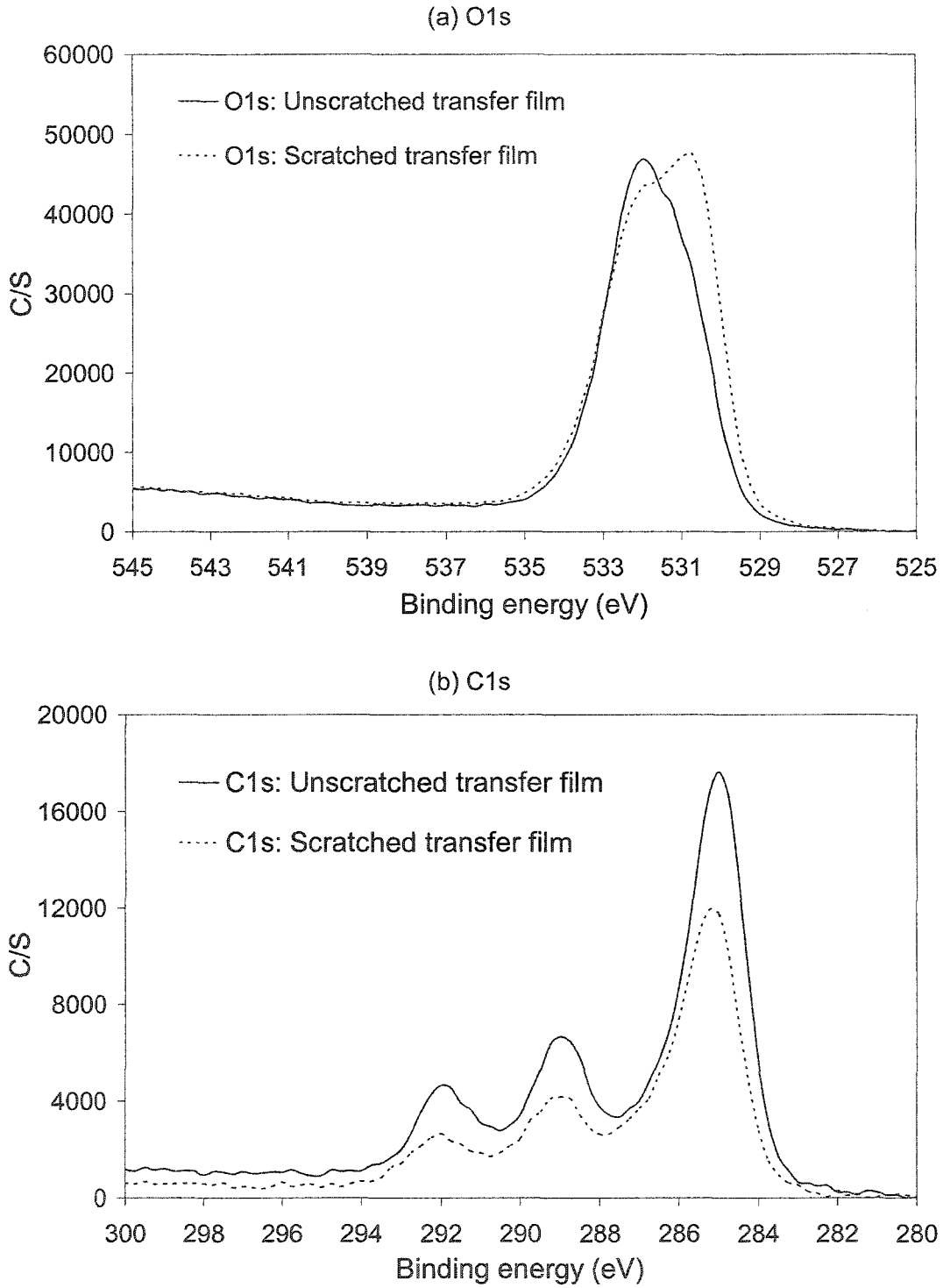

Figure 4.8 XPS spectra of the unscratched and scratched transfer films formed on the steel counterface by PPS+17%MC+5%PTFE composite. (a) O1s; (b) C1s; (c) Fe2p; (d) Mo3d; (e) S2p; (f) F1s.

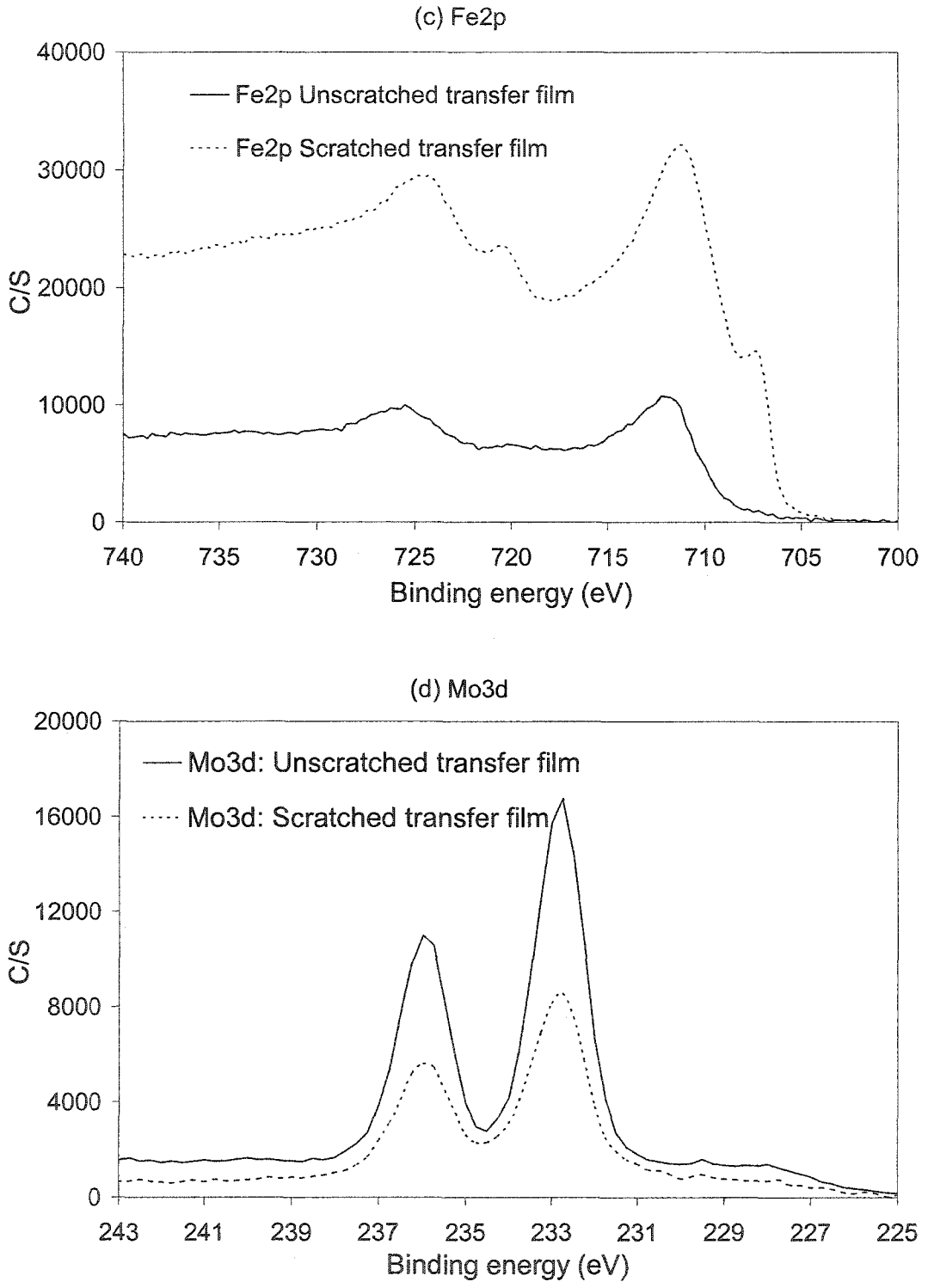

Figure 4.8 continued. XPS spectra of the unscratched and scratched transfer films formed on the steel counterface by PPS+17%MC+5%PTFE composite. (c) Fe2p; (d) Mo3d.

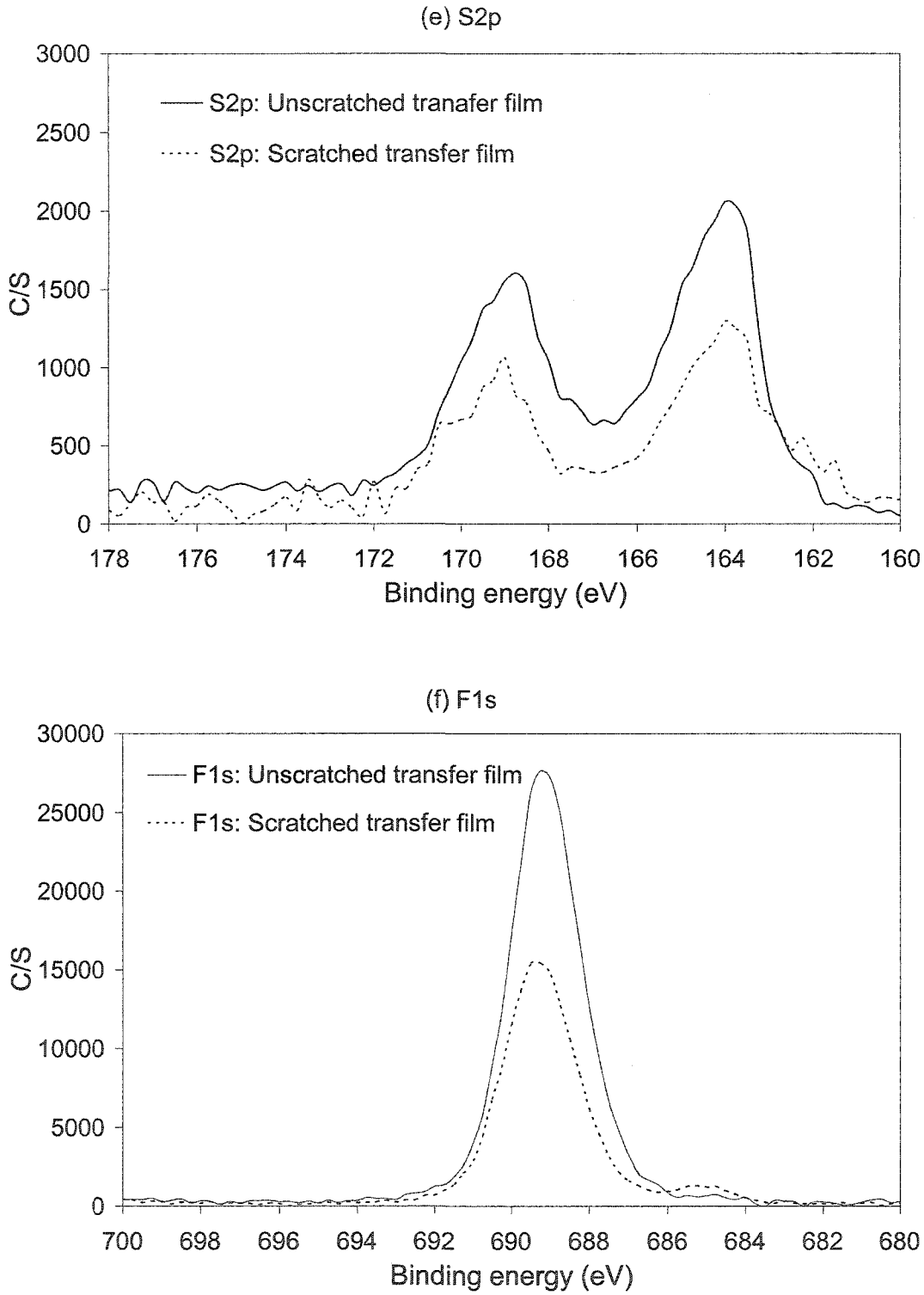

Figure 4.8 continued. XPS spectra of the unscratched and scratched transfer films formed on the steel counterface by PPS+17%MC+5%PTFE composite. (e) S2p; (f) F1s.

CHAPTER 5
DESIGN OF EXPERIMENTS APPROACH TO THE STUDY OF TRIBOLOGICAL PERFORMANCE OF Cu-CONCENTRATE-FILLED PPS COMPOSITES

A paper submitted to *Tribology International*

Minhaeng Cho and Shyam Bahadur

5.1 Abstract

The tribological performance of copper-concentrate (CC) mineral deposit as the filler in polyphenylene sulfide (PPS) was studied as a function of the filler proportions and sliding test variables. CC is a complex mixture of CuS, Fe_xO_y, SiO_2, Al_2O_3, and other trace materials. The design of experiments based upon L_9 (3^4) orthogonal arrays by Taguchi was used. Sliding tests were performed in the pin-on-disk configuration against a hardened tool steel (55-60 HRC) disk. The improvement in wear resistance of PPS was considerable with the use of fillers. The lowest steady state wear rate of 0.0030 mm^3/km was obtained for PPS+20%CC+15%PTFE composition. It was two orders of magnitude lower than that of unfilled PPS. The variations in steady state coefficient of friction with the changes in filler proportions and sliding test variables were small. The transfer film was studied by atomic force microscopy (AFM) and scanning electron microscopy (SEM). X-ray photoelectron microscopy (XPS) was used to detect chemical reactive species developed during sliding, especially in the interface between transfer film and its counterface. Wear particles and the polymer worn surfaces were analyzed by energy dispersive spectroscopy (EDS) for elemental distribution.

5.2 Introduction

The improvement of mechanical and/or tribological properties of polymers by incorporation of particulate filler materials and short fibers has been widely studied [1]. It has been noticed that there is synergism between the filler and fiber materials when both are simultaneously present, and such hybrid composites provide tribological properties unachievable by the filler or the fiber alone [2]. An alternative to these hybrid composites would be the composites filled with minerals which consist of a complex mixture of inorganic compounds. The tribological behavior of such composites has not been studied. The interaction of these compounds with the counterface due to high pressure and heat at the sliding interface could make the tribological behavior of these composites very complex.

Studies have been carried out using a variety of inorganic filler materials in order to reduce wear and increase or decrease the coefficient of friction of polymer composites. One of the inorganic filler materials which is pertinent to this study is CuS. The reduction in wear rate with the addition of micro CuS filler has been reported in the case of high-density polyethylene [3], polyetheretherketone [4], polytetrafluoroethylene [5], and polyamide 11 [6]. Yu and Bahadur [7] reported that the wear rate of PPS was significantly reduced by the addition of 35 vol.% CuS. In addition, the synergism effect was also reported when CuS and short carbon fibers as reinforcement material were used together in nylon [2]. It was also shown that the development of a thin and uniform transfer film on the counterface during sliding was associated with the reduction in wear rate.

In addition to filler type and its proportions, sliding variables such as counterface roughness, sliding speed, and applied load have been known to affect the tribological behavior of polymer composites. As for the sliding speed, the faster the sliding speed, the

higher was the wear rate in the case of ultra-high molecular weight polyethylene, polyphenylene oxide, polyetheretherketone, and polytetrafluoroethylene where sliding speed was varied from 0.001 to 10.0 m/s [8,9]. However, the coefficient of friction did not follow the same pattern as observed for the wear rate. A high sliding speed of 2 m/s caused thermal softening in case of the polymers [10]. Bahadur and Gong [11] showed that wear rate of nylon and nylon filled with 35% CuS increased when the counterface roughness was increased from 0.04 to 0.30 μm Ra. It was so because of the incomplete coverage of transfer film on the rougher counterface. The wear of polymer composites was found to be closely related with sliding variables, but no regular pattern between the variables was found to exist.

Studies showing the relationship between transfer film formed on a counterface during sliding and wear behavior of polymer composites have been reported [2-7]. Yu and Bahadur [7] reported that wear resistance was substantially increased when transfer film was thin and smooth. Furthermore, poor cohesion and adhesion of the transfer film to the counterface contributed to increased wear rate.

5.3 Experimental details

5.3.1 Materials

Polyphenylene sulfide (PPS) was used as base material due to its low coefficient of friction, high strength, and high temperature capability. The latter was important because sliding tests were run at high sliding speeds. PPS in the form of powder was supplied by the Philips Chemical Company. PTFE (FLUON® Grade G163) in powder form was supplied by Asahi Glass Fluoropolymer Co. It was used as a solid lubricant in PPS composites.

The mineral filler used in this study was copper-concentrate (abbreviated as CC) which is

composed of a mixture of inorganic compounds and iron oxides. The major constituents in this mineral are CuS, FeO, Fe_2O_3, Al_2O_3, CaO, and SiO_2. The proportions of these and other constituents are given in Table 5.1. The filler used was in the form of powder of 45 μm maximum size.

5.3.2 Sample Preparation

PPS, CC, and PTFE were dried at 125°C before weighing to prepare the specimens with desired proportions. The mixture was mechanically blended in an ultrasonic bath of acetone. It was dried and compacted in a cylindrical mold 6.35 mm in diameter and 11.00 mm long. The specimen was compression molded at 310°C as described elsewhere [7]. A total of nine specimens with the compositions given in Table 5.2 were prepared.

5.3.3 Pin-on-disk sliding tests

Pin-on-disk sliding tests were performed on a hardened tool steel counterface (55-60 HRC). The specimen for wear test was 6.2 mm in diameter and 10 mm long. The test surface was finished by abrasion, washed, and dried. As shown in Table 5.2, wear tests were performed at the sliding speeds of 0.5, 1.0, and 1.5 m/s. A nominal contact pressure of 0.65 MPa was used. The counterfaces were finished by abrasion to provide three roughnesses. The combinations of the sliding speed and counterface roughness for each composition are given in Table 5.2. Sliding tests were performed over a distance of 21.6 km regardless of the sliding speed. The long duration tests ensured steady state wear which is emphasized in this study. The mass loss was measured with an accuracy of 10 μg at the sliding distances of 1.8 km and 3.6 km for the first two data points and at every 3.6 km thereafter. It was converted to volume loss using the density of the specimen. The coefficient of friction was also measured

using strain gages which were mounted on the loading arm. Three wear tests for each composition were carried out and were averaged. The results were within a scatter range of ±15% for wear and ±10% for friction.

5.3.4 Design of experiments

In order to investigate the tribological behavior of the composites with the variables used in this study, design of experiments approach was employed. The variables included were sliding speed, counterface roughness, and CC and PTFE proportions. The parameter values and the experimental setup by Taguchi's orthogonal arrays are shown in Table 5.2. In the case of counterface roughness, an extremely smooth or a rough surface was avoided since it has been reported [12] to provide high wear rate. The highest sliding speed was limited to 1.5 m/s in order to avoid considerable thermal softening of the polymer at contact surface. The total filler content was limited to 35 vol. % because higher proportions make the sample fragile.

5.4 Results

5.4.1 Effect of fillers on wear and friction

Figure 5.1 shows wear volume loss and the coefficient of friction plots as a function of sliding distance for PPS filled with CC at the sliding speed of 1.0 m/s against a counterface of 0.1 μm Ra roughness. The percentage compositions used in this work are by volume. It should be noted that steady state wear rate increased as the CC proportion increased from 10 to 20%. The steady state wear rate of PPS+20%CC was higher than that of unfilled PPS but slightly lower for 10 and 15% filler proportions. This indicates that the effect of CC as a filler material to reduce the wear rate of PPS is marginal. No transient wear state was observed in

the case of PPS+20%CC composite but in the other two cases it was noticeable. It took a sliding distance of about 12 km for the onset of steady state for PPS+15%CC, but in the case of PPS+10%CC it commenced very early. A rapid decrease in wear rate for the latter composition was observed possibly because of the formation of transfer film. A much greater reduction in wear rate (by a factor of about 20) was obtained with the addition of 5%PTFE to PPS+10%CC composite, as seen in Fig. 5.1. In view of this result, it was decided to add PTFE along with CC filler in the design of experiments. As for the coefficient of friction, it decreased from 0.48 for unfilled PPS to 0.32 with the addition of 10%CC and 5%PTFE. This result supports the role of PTFE as a solid lubricant in addition to wear reduction. The steady state coefficients of friction with the addition of 10, 15, and 20%CC to PPS were about the same but lower than that of unfilled PPS.

Figure 5.2 shows the wear and friction plots for PPS filled with 10, 15, and 20%CC along with 5, 10, and 15%PTFE. Here, for each composition, the sliding speed and counterface roughness combinations given in Table 5.2 were used. Steady wear state was observed in all the cases and the wear rates were considerably lower than that of unfilled PPS. These wear rates are given in Table 5.2. The composites filled with 10%CC showed similar steady state wear rates (0.010-0.014 mm^3/km) regardless of the PTFE proportion and other test parameters. When CC proportion increased to 15% and 20%, the proportion of PTFE needed for minimum wear also increased. The lowest steady state wear rate was observed for PPS filled with 15-20%CC and 15%PTFE. It was lower by a factor of 100 as compared to that of unfilled PPS. Along with the earlier observation, this indicates that PTFE had a significant role in terms of wear reduction. It should further be noted that larger proportions of PTFE were needed for optimum wear resistance with larger proportions of CC. From these

observations, it was concluded that the addition of both copper-concentrate and PTFE as the filler was very effective in lowering the steady state wear rate of PPS.

As for the steady state coefficient of friction, it decreased with the addition of any amount of PTFE. For the case of 10%CC-filled composites, the coefficient of friction decreased as the proportion of PTFE increased. For 15 and 20%CC, the coefficient of friction values were about the same irrespective of the PTFE volume fraction.

Apart from the above general observations, it would not be reasonable to compare wear or friction results for varying compositions because the sliding speed and counterface roughness are also changing.

5.4.2 Taguchi analysis of wear and friction

The level average analysis of the steady state wear rates with the variation of parameters such as filler proportions, siding speed, and counterface roughness is presented in Fig. 5.3. It can be seen that wear resistance increases with the increase in CC proportion from 10 to 15% but decreases when increased to 20%. It increases continuously with the increase in PTFE proportion from 5% to 15%. During sliding tests, it was observed that PTFE promoted the development of a thin and uniform transfer film on the counterface during sliding. Wear rate is relatively high at both the low and high sliding speeds, being the lowest at 1.0 m/s. As for the counterface roughness, the lowest wear rate was obtained for 0.06 μm Ra and there was practically no difference in the wear rates for 0.10 and 0.15 μm Ra.

The results on the coefficient of friction based on the level average analysis are presented in Fig. 5.4. The steady state coefficient of friction decreased as the level of each parameter increased. It should, however, be noted that this variation is insignificant being

within a scatter range of ±10%. It indicates that the effect on the coefficient of friction by the addition of PTFE to CC-filled PPS composites is pretty consistent regardless of the test parameters. Also, the coefficients of friction of all the composites decreased by 10-35% as compared to that of unfilled PPS.

5.4.3 Wear particle, transfer film, and worn surface studies

In order to investigate the reasons for the tribological behavior reported above, transfer films along with wear particles were studied. With the addition of 15%PTFE to PPS+20%CC, the size of wear particles was reduced considerably, as seen in Fig. 5.5. Figure 5.5(c) shows wear particles at higher magnification generated in the case of PPS+20%CC +15%PTFE composite. Finer wear particles contribute to a thin and coherent transfer film on the counterface which has been attributed to the reduction in wear rate.

Figure 5.6 shows optical micrographs of the transfer films formed on counterface during sliding of some typical compositions. As can be seen from Fig. 5.6(a), the transfer film of PPS+10%CC composite shows abrasion marks in the sliding direction. These marks were presumably generated during sliding by the abrasive action of CC particles which contained abrasive compounds such as Al_2O_3 and SiO_2. The transfer film appears to be thick because the abrasion marks from the finishing operation of the counterface cannot be seen. This type of film was contributed by the wear particles whose size was large as indicated above. The texture of transfer films changed when PTFE was added, as seen in Figs. 5.6(b-d). The abrasion finishing marks of the counterface through the transfer film are seen in these cases. The transfer films show that the worn particles are embedded into the valleys of abrasion grooves. The transfer films are fairly thin and uniform regardless of the CC composition and

the test conditions. The thin films were generated because the size of wear particles with PTFE addition was much smaller. A considerable reduction in the wear rate of PPS was contributed by these films, as has been reported widely earlier [7,12].

Figures 5.7 shows the transfer films for PPS+20%CC composite with and without PTFE. The transfer film without PTFE is rougher and thicker as compared to that with PTFE. Thus, sliding in the latter case would be smoother than in the former case. This characteristic sliding feature along with thin transfer film would be conducive to lower wear.

Figure 5.8 shows 3-dimensional AFM topographic images of the transfer films for PPS+20%CC composite with and without PTFE. The transfer film in the case of PPS+20%CC composite shows deep trenches indicating significant abrasive action. In the case of PPS+20%CC+15%PTFE, deep furrows are no longer seen. Instead, the transfer film became thinner and more uniform. The latter is supported by the AFM sectional analysis results presented in Fig. 5.9. In the case of PPS+20%CC composite, high peaks and deep valleys normal to the sliding direction are seen on the transfer film. The extent of the severity of abrasiveness is seen from the peak-to-valley vertical distance. With the addition of PTFE, the transfer film became much more uniform. There are still some spikes, but their relative size and distribution is minute compared to that of PPS+20%CC composite.

Figure 5.10(a) shows SEM micrograph of the worn surface of PPS+20%CC+15%PTFE composite. In addition to the tiny wear particles, plowing tracks along the sliding direction are seen. There is an indication of cracking on the bottom surface of the grooves. The orientation of cracks perpendicular to the sliding direction indicates that cracks developed because of tensile stress in that direction. The pin surface has a uniform distribution of the elements such as Fe, Cu, F, and S, as seen in Fig. 5.10(b). On the surface, there is a large CC

particle because the concentrations of Cu and Fe in its location are very high.

5.4.4 XPS studies of transfer films

Chemical interaction between the composite transfer film and steel counterface was studied by means of XPS analysis. The latter was done for PPS+20%CC and PPS+20%CC +15%PTFE composites at two levels in the transfer film, the surface of transfer film as well as the interface between transfer film and its substrate. For the latter case, transfer film was gently scraped in order to expose the interface.

The XPS spectra of the unscraped and scraped transfer film of PPS+20%CC composite are given in Fig. 5.11 and the identified species are listed in Table 5.3. Some of the species detected are Fe, Cu, CuS, Fe_2O_3, and $FeSO_4$. The broad peak in Fe(2p) spectrum around 710 eV for both the unscraped and scraped transfer film indicates the existence of Fe_xO_y species, which is because of the presence of high percentages of iron oxides in copper-concentrate. The Fe(2p) peak in the scraped spectrum is more pronounced because of iron oxide on the counterface surface. An earlier study [13] has shown that PPS does not decompose during sliding. Thus, the element S in $FeSO_4$ is believed to be from the decomposition of CuS to Cu and S.

Figure 5.12 shows the XPS spectra of the unscraped and scraped transfer films of PPS+20%CC+15%PTFE composite. Table 5.4 shows the identified species for these spectra. $FeSO_4$ was detected here as well, indicating the decomposition of CuS to Cu and S during sliding. As expected, fluorine in PTFE was detected. In addition, F(1s) peak at 685 eV was observed. This peak corresponds to FeF_2, as reported earlier [14]. Because of FeF_2, an improved adhesion of transfer film to the steel counterface could be expected. As discussed

in the earlier case, Fe_xO_y species were also detected. With the exception of C(1s) and Cu(2p) peaks, the peak intensities in the spectra of scraped transfer film were higher than those observed for the unscraped transfer film. This indicates that FeF_2 and $FeSO_4$ concentrations were greater closer to interface than on the surface of transfer film. In other words, the chemical interaction between the composite constituents and those of the steel counterface occurs more vigorously closer to the sliding interface. The generation of these species provides a mechanism for stronger bonding of transfer film to the counterface. It also provides the basis for a mechanism of increased wear resistance by reducing the loss of transfer film for the counterface surface because of enhanced bonding between the two.

5.5 Discussion

The investigation of wear with the proportions of two fillers, counterface roughness, and sliding speed as the variables would have required a large number of tests if all combinations of the test variables were used. The design of experiments based upon Taguchi method enabled us to perform this study using only 9 tests as given in Table 5.2. For wear tests which require long times, this is thus a very effective approach.

This work revealed that even a very small amount of PTFE (5 vol.%) produced a dramatic reduction in wear rate in combination with copper-concentrate mineral from Armenia. Since this mineral is cheaply and abundantly available in Armenia, the economic benefits of this study for this country are tremendous. In addition to that, the study led to the understanding of wear in terms of the processes that affect the wear behavior. Whereas a small reduction in wear rate was observed with 10 and 15 vol.%CC, wear rate with 20 vol.%CC became higher than that of the unfilled PPS. The wear rate with 15 vol.%CC filler

was higher than with 10 vol.%. These observations indicated that whereas the filler in small quantities was beneficial for wear reduction by virtue of supporting the load as has been advocated in the literature [15], it became harmful in larger quantities because it started producing abrasion as observed by microscopic examination of the surfaces. The addition of PTFE to the PPS+CC composite helped in the formations of a thin and uniform transfer film. The role of this film became dominant in controlling the wear behavior. PTFE also contributed to the adhesion of transfer film to counterface by the formation of FeF_2 as observed by XPS studies. The reduction in the coefficient of friction by the adhesion of PTFE could have also been beneficial because it resulted in reduced dissipation of energy at the interface thereby resulting in lower temperature rise so that the composite material had a better ability to support stresses induced at the interface.

5.6 Conclusions

1. The reduction in wear rate of PPS filled with 10-15% copper-concentrate was marginal as compared to that of unfilled PPS. Wear resistance was considerably enhanced with the addition of PTFE to PPS+CC. With the addition of 10%CC, the coefficient of friction of PPS was lowered from 0.48 to 0.40, when sliding occurred at 1 m/s against a counterface of 0.1 μm Ra. It was further lowered to 0.32 by the addition of 5%PTFE.
2. The lowest steady state wear rate of 0.0030 mm^3/km was observed for PPS+20%CC+ 15%PTFE composition. The wear rate for PPS+15%CC+15%PTFE was also about the same. This wear rate was 100^{th} of that of unfilled PPS.

3. Wear rate in the design of experiments was minimum for 15% copper-concentrate filler and 15%PTFE. As for the test variables, 1 m/s and 0.06 μm Ra showed the minimum wear rate.
4. In the design of experiments, the changes in the coefficient of friction with CC and PTFE proportions, sliding speed, and counterface roughness were found to be insignificant.
5. The examination of transfer film by optical and scanning electron microscopy and AFM showed abrasion marks on the transfer film of PPS+CC. With the addition of 15%PTFE, the transfer film became smoother and more uniform.
6. The examination of the worn surface of PPS+20%CC+15%PTFE showed deep plowing marks and microcracking on the bottom surface of grooves.
7. XPS analysis of transfer films indicated the decomposition of CuS to Cu and S and the formation of $FeSO_4$ and FeF_2. This tribochemical reaction provides a mechanism for enhanced bonding of transfer film to the counterface, which serves as a basis for the reduction in wear rate.

5.7 References

1. J. Bijwe, C. M. Logani, U. S. Tewari, Influence of fillers and fiber reinforcement on abrasive wear resistance of some polymeric composites, Wear 138 (1990) 77-92.
2. S. Bahadur, Q. Fu, D. Gong, The effect of reinforcement and the synergism between CuS and carbon fiber on the wear of nylon, Wear 178 (1994) 123-130.
3. S. Bahadur, D. Tabor, Role of filers in the friction and wear behavior of high-density polyethylene, in: L.H. Lee (Ed.), Polymer wear and its control, ACS Symposium Series 287 (1985) 253-268.

4. S. Bahadur, D. Gong, J.W. Anderegg, The investigation of the action of fillers by XPS studies of the transfer films of PEEK and its composites containing CuS and CuF_2, Wear 160 (1993) 131-138.
5. S. Bahadur, D. Tabor, The wear of filled polytetrafluoroethylene, Wear 98 (1984) 1-13.
6. S. Bahadur, D. Gong, Tribological studies by XPS analysis of transfer films of Nylon 11 and its composites containing copper compounds, Wear 165 (1993) 205-212.
7. L. Yu, S. Bahadur, An investigation of the transfer film characteristics and the tribological behaviors of polyphenylene sulfide composites in sliding against tool steel, Wear 214 (1998) 245-251.
8. J.C. Anderson, High density and ultra-high molecular weight polyethylene: their wear properties and bearing applications, Tribology international, 1982 (15) 43-47.
9. P.M. Dickens, J.L. Sullivan, J.K. Lancaster, Speed effects on the dry and lubricated wear of polymers, Wear 112 (1986) 273-289.
10. A. Kapoor, S. Bahadur, Transfer film bonding and wear studies on CuS-nylon composite sliding against steel, Tribology International, 1993. **27**(5) 323-329.
11. S. Bahadur, Deli Gong, The transfer and wear of nylon and CuS-nylon composites: filler proportion and counterface characteristics, Wear 162-164 (1993) 397-406.
12. Q. Zhao, S. Bahadur, Investigation of the transition state in the wear of polyphenylene sulfide sliding against steel, Tribology Letters, Vol. 12, No. 1, January 2002, 23-33.
13. Q. Zhao, S. Bahadur, The mechanism of filler action and the criterion of filler selection for reducing wear, Wear 225-229 (1999) 660-668.
14. D. Gong, Q. Xue, H. Wang, ESCA study on tribochemical characteristics of filled PTFE, Wear 148 (1991) 161-169.
15. G.W. Stachowiak, A.W. Batchelor, Engineering Tribology, Tribology series 24, 715-771.

Table 5.1 Constituents of copper-concentrate.

Constituents	Contents, %
CuS	46
Fe_2O_3	24
FeO	13
SiO_2	7.3
Al_2O_3	2.3
CaO	1.1
MgO	0.46
MoS_2	0.02
Pb	0.40
As	0.50
Zn	0.35
Ag	65.5 grams/ton
Au	4.0 grams/ton

Table 5.2 $L_9(3^4)$ Orthogonal arrays designed by Taguchi method.

Test runs	Fillers		Test conditions		Steady state wear rate*
No.	CC, vol.%	PTFE, vol.%	speed, m/s	roughness, μm Ra	mm^3/km
1	10	5	0.5	0.06	0.0140
2	10	10	1.0	0.10	0.0104
3	10	15	1.5	0.15	0.0118
4	15	5	1.0	0.15	0.0101
5	15	10	1.5	0.06	0.0074
6	15	15	0.5	0.10	0.0033
7	20	5	1.5	0.10	0.0345
8	20	10	0.5	0.15	0.0259
9	20	15	1.0	0.06	0.0030

* Steady state wear rate of unfilled PPS at 1.0 m/s sliding speed and 0.1 μm Ra counterface roughness was 0.29 mm^3/km.

Table 5.3 Identified species in the XPS spectra of unscraped and scraped transfer film of PPS+20%CC composite.

Species	Binding energies of peaks, eV				
	C(1s)	O(1s)	S(2p)	Fe(2p)	Cu(2p)
Contaminated C	284.8				
C in PPS	284.8				
S in PPS			163.7		
Fe				707.0	
Cu					932.7
CuS			162.0		935.0
$FeSO_4$		532.4	168.8	712.1	
Fe_2O_3		530.2		710.8	

Table 5.4 Identified species in the XPS spectra of unscraped and scraped transfer film of PPS +20%CC+15%PTFE composite.

Species	Binding energies of peaks, eV					
	C(1s)	O(1s)	S(2p)	F(1s)	Fe(2p)	Cu(2p)
Contaminated C	284.8					
C in PPS	284.8					
S in PPS			163.7			
$(CF_2=CF_2)n$	292.2			689.0		
Fe					707.0	
Cu						932.7
CuS			162.0			935.0
$FeSO_4$		532.4	168.8		712.1	
FeF_2				685.0	711.3	
Fe_2O_3		530.2			710.8	

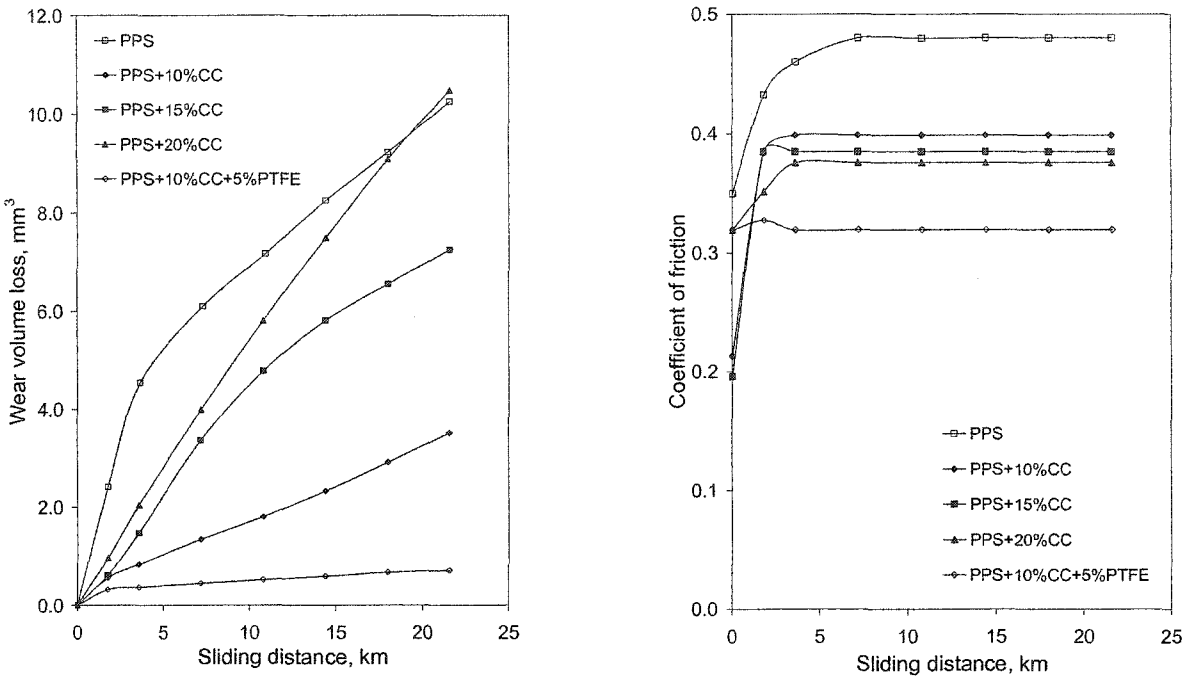

Figure 5.1 Variation of wear and coefficient of friction for PPS filled with different proportions of CC, with and without PTFE. Test conditions: sliding speed 1.0 m/s, nominal pressure 0.65 MPa, counterface roughness 0.10 μm Ra.

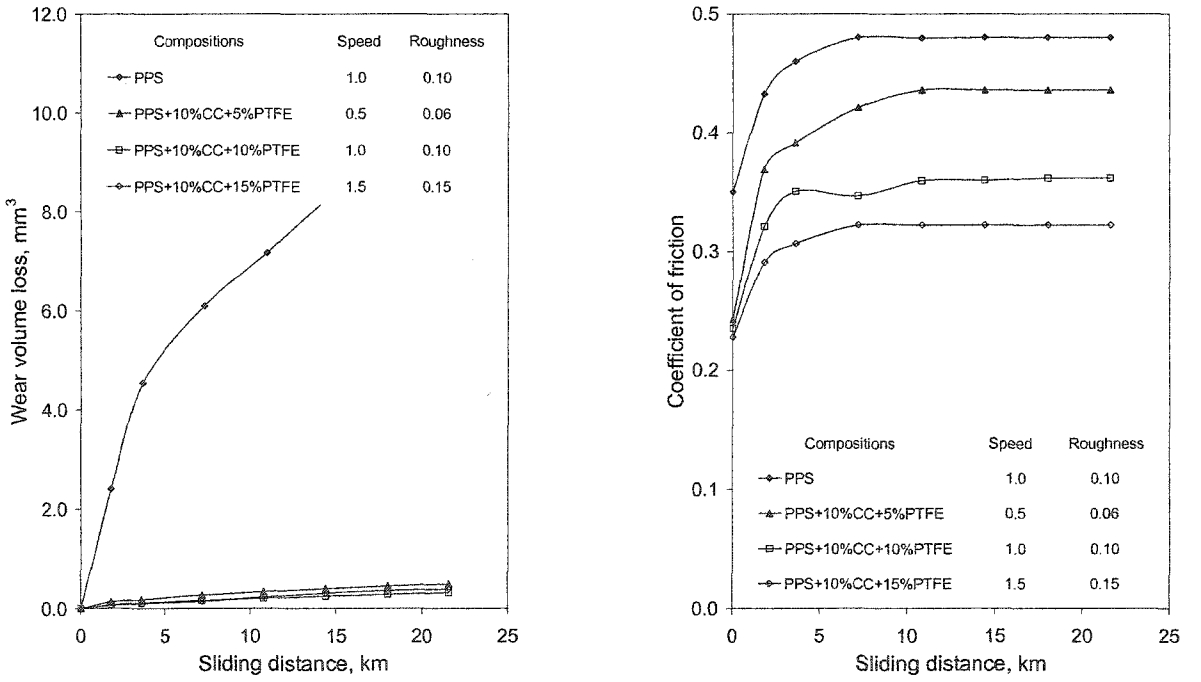

Figure 5.2 Variation of wear and coefficient of friction with different compositions and sliding parameters as given in Table 5.2. Unit: Speed m/s, roughness μm Ra.

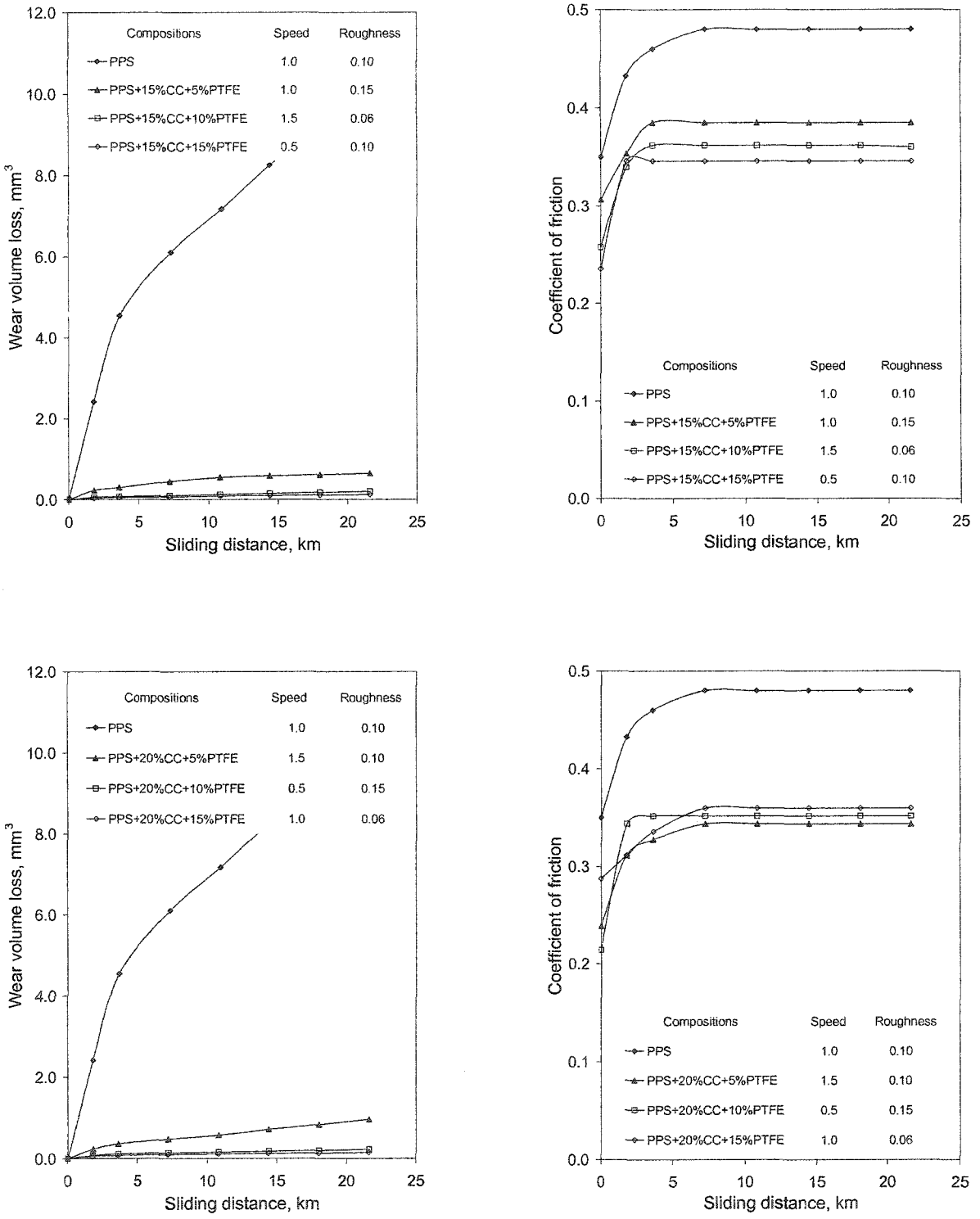

Figure 5.2 continued. Variation of wear and coefficient of friction with different compositions and sliding parameters as given in Table 5.2. Unit: Speed m/s, roughness μm Ra.

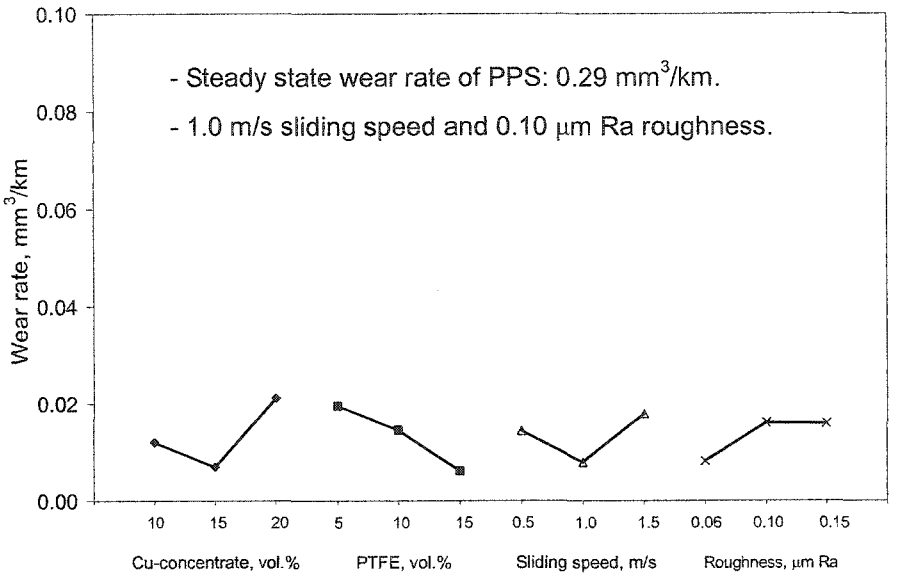

Figure 5.3 Plot of steady state wear rates with the variation of parameters by level average analysis.

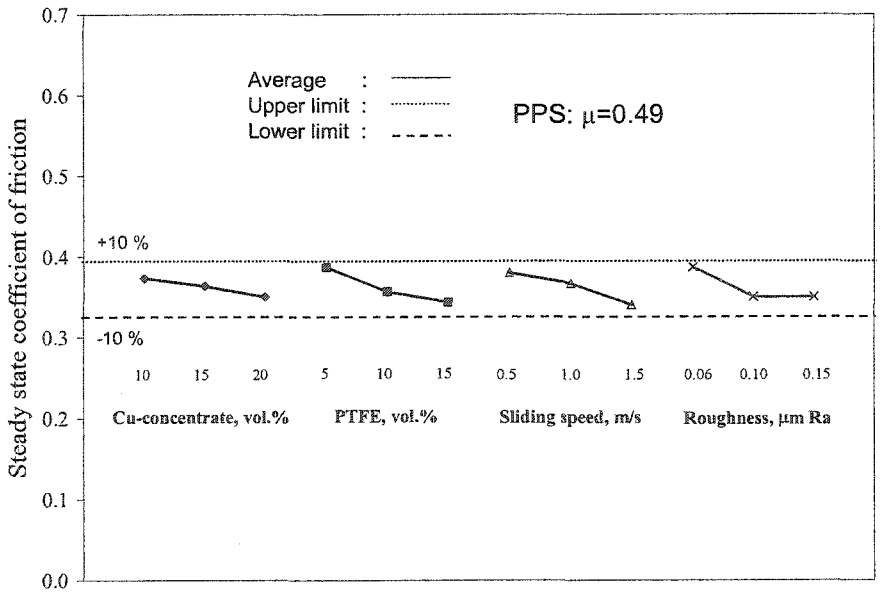

Figure 5.4 Plot of the coefficient of friction with the variation of parameters by level average analysis.

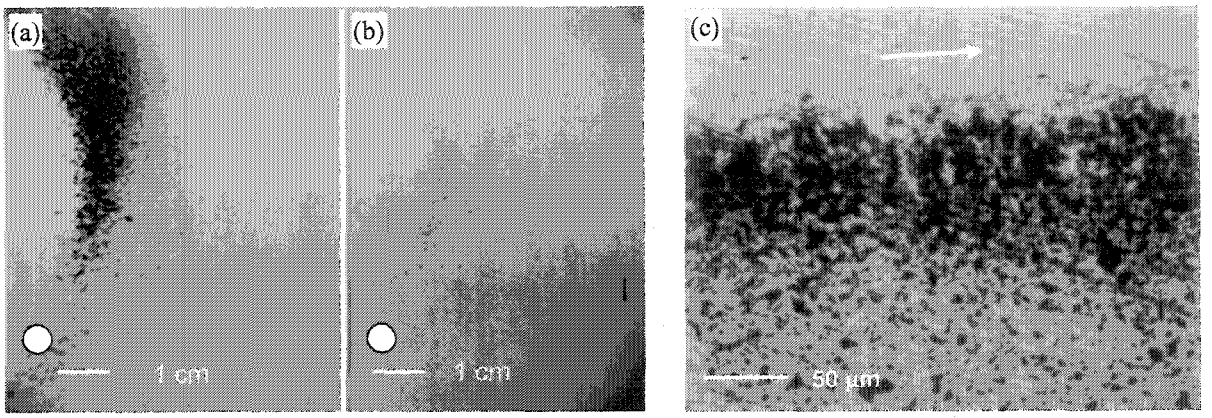

Figure 5.5 Optical micrographs of wear particles for (a) PPS+20%CC, (b) PPS+20%CC+15%PTFE, and (c) wear debris of (b) on the counterface at higher magnification after sliding. Test conditions same as in Fig. 5.1. Solid circle indicates the location of pin sample. Arrow indicates sliding direction.

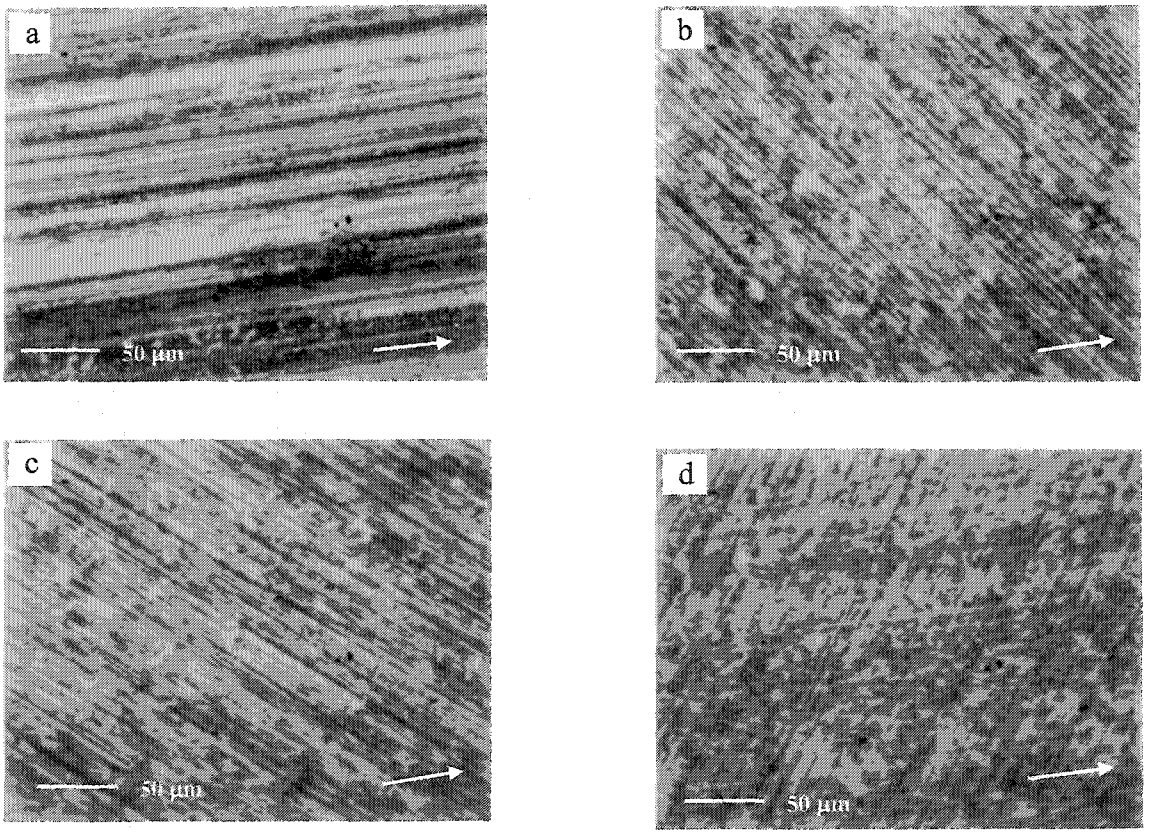

Figure 5.6 Optical micrographs of transfer film: (a) PPS+10%CC; 1.0 m/s, 0.10 μm Ra, (b) PPS+10%CC+15% PTFE; 1.5 m/s, 0.15 μm Ra, (c) PPS+15%CC+15%PTFE; 0.5 m/s, 0.10 μm Ra, and (d) PPS+20%CC+15% PTFE; 1.0 m/s, 0.06 μm Ra. Arrow indicates sliding direction.

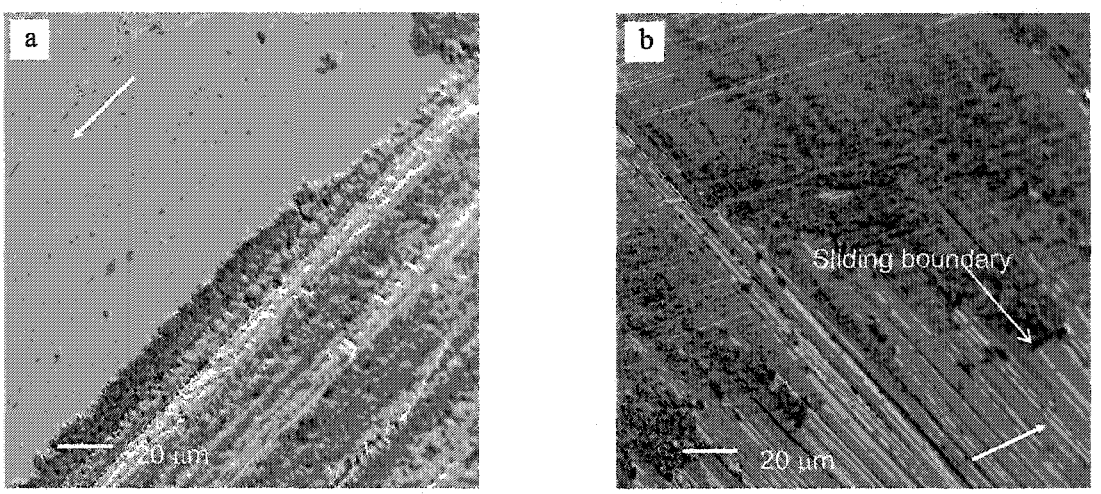

Figure 5.7 SEM micrographs of transfer films for (a) PPS+20%CC and (b) PPS+20%CC+15%PTFE composite. Sliding conditions same as Fig. 5.1. Arrow indicates sliding direction.

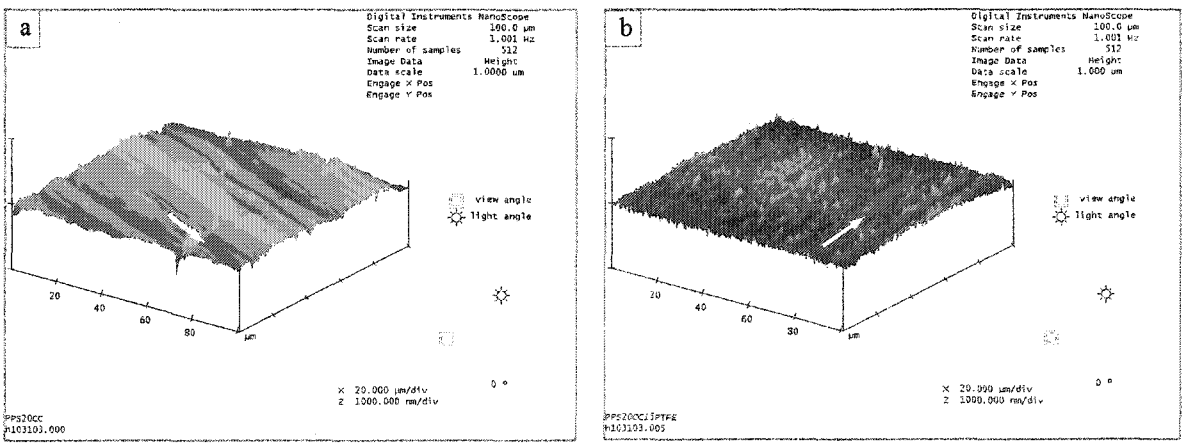

Figure 5.8 3-Dimensional AFM images of transfer film for (a) PPS+20%CC and (b) PPS+20%CC +15%PTFE composite. Sliding conditions same as Fig. 5.1. Arrow indicates sliding direction.

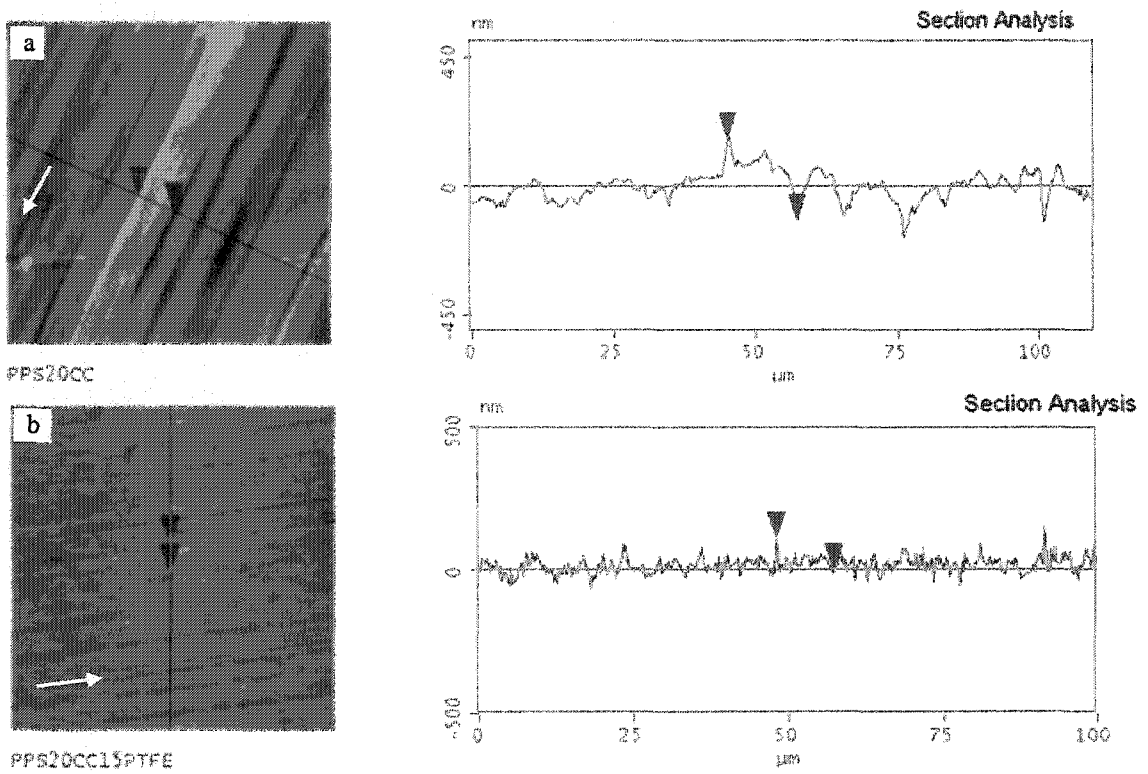

Figure 5.9 AFM sectional analysis images of (a) PPS+20%CC and (b) PPS+20%CC+15%PTFE composite. Sliding conditions same as Fig. 5.1. Arrow indicates sliding direction.

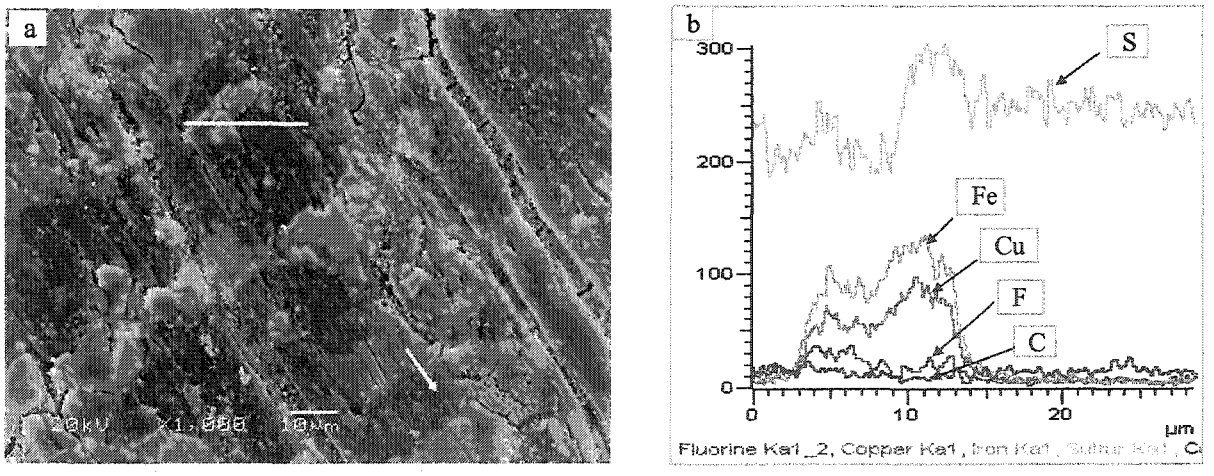

Figure 5.10 SEM micrograph of the worn surface of PPS+20%CC+15%PTFE composite: (a) SE image and (b) EDS intensity plot. Solid line in (a) indicates scanning line. Sliding conditions same as Fig. 5.1. Arrow indicates sliding direction.

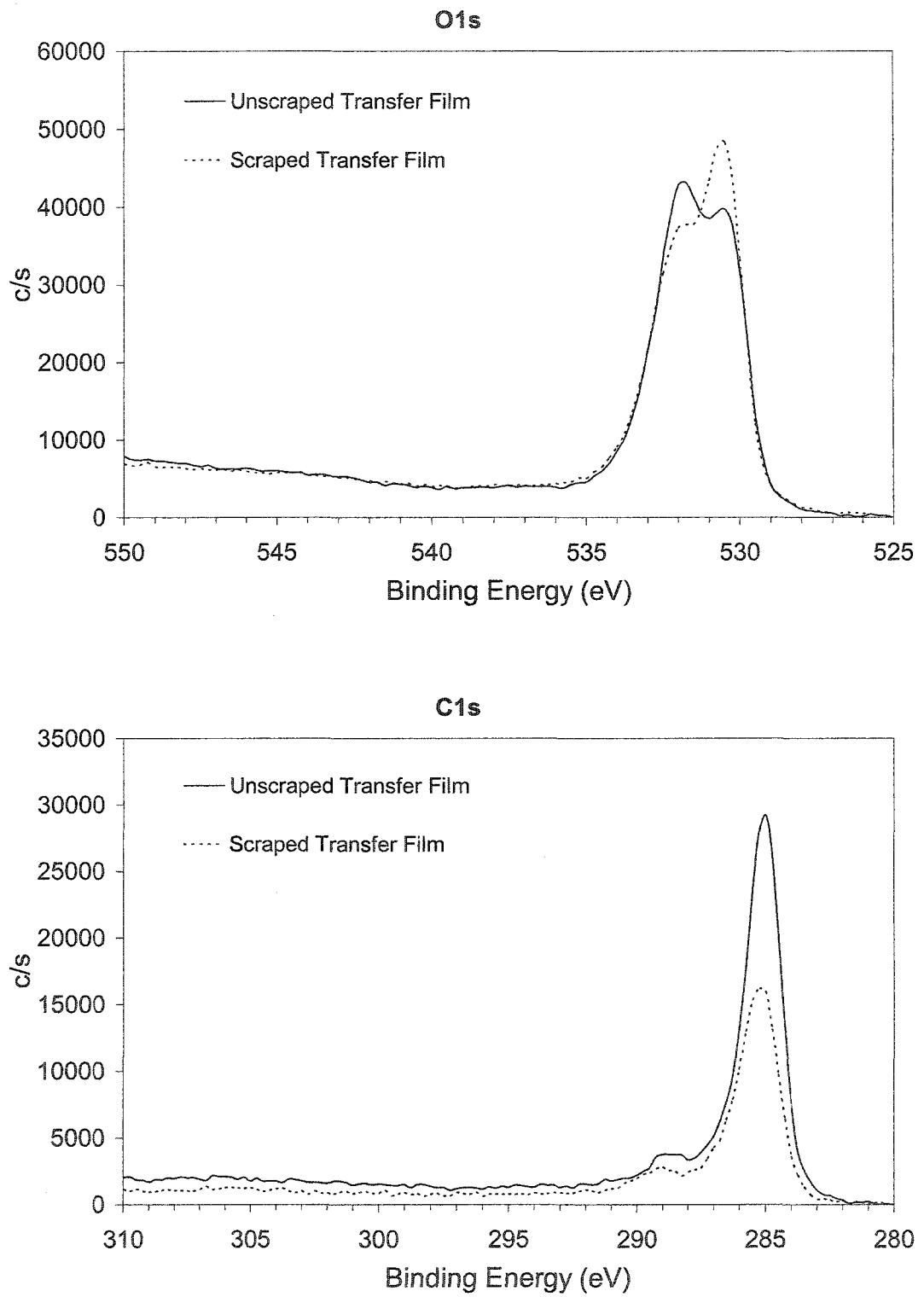

Figure 5.11 XPS spectra plots of transfer film of PPS+20%CC composite. Solid line indicates unscraped transfer film and dashed line indicates scraped transfer film.

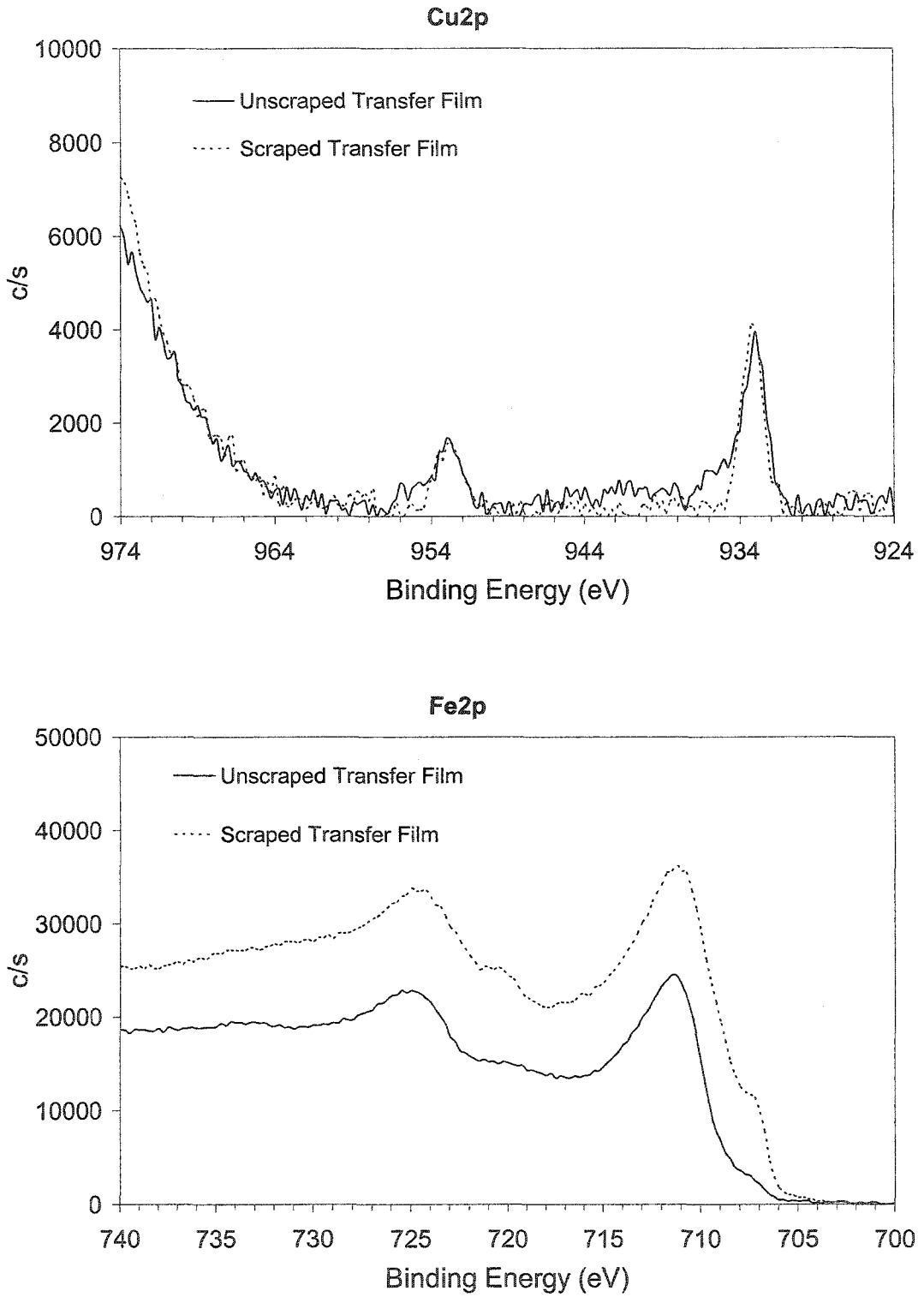

Figure 5.11 continued. XPS spectra plots of transfer film of PPS+20%CC composite. Solid line indicates unscraped transfer film and dashed line indicates scraped transfer film.

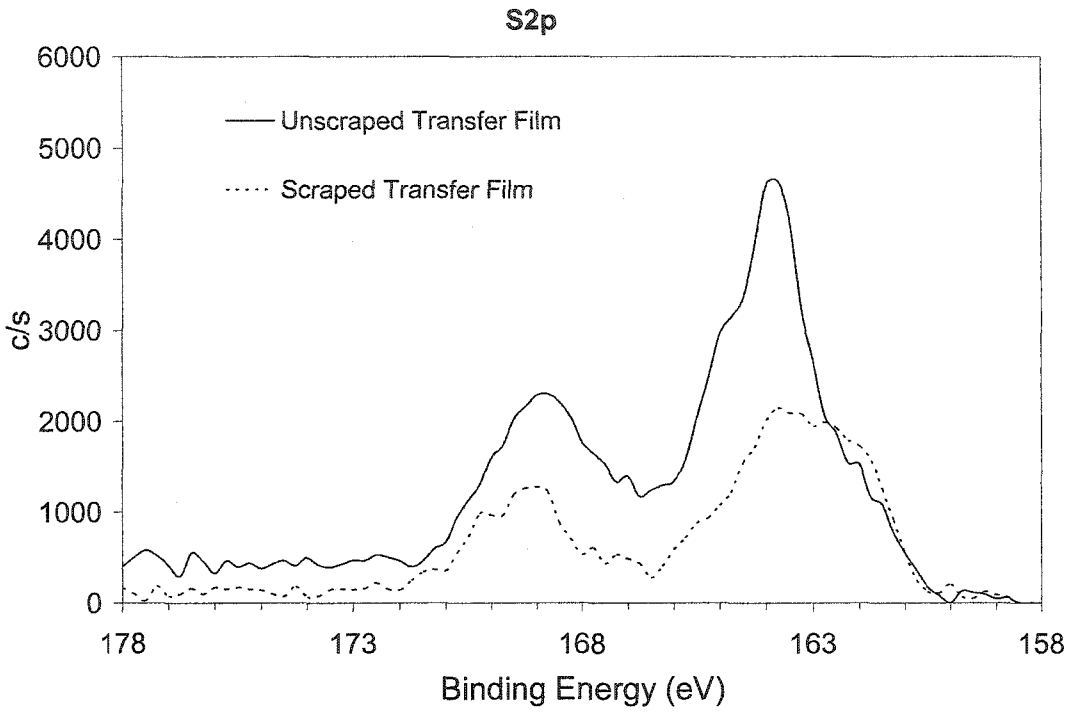

Figure 5.11 continued. XPS spectra plots of transfer film of PPS+20%CC composite. Solid line indicates unscraped transfer film and dashed line indicates scraped transfer film.

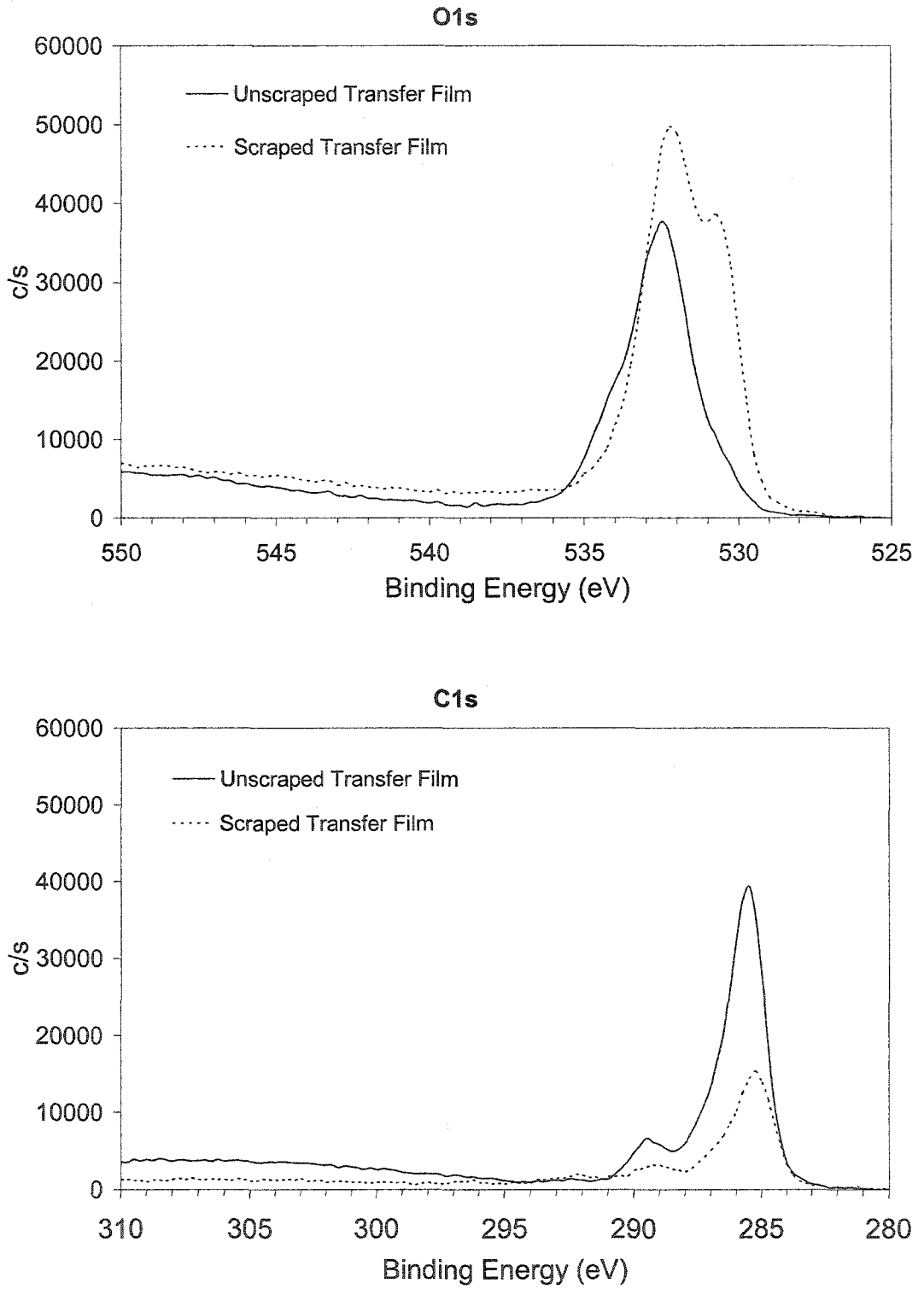

Figure 5.12 XPS spectra plots of transfer film of PPS+20%CC+15%PTFE composite. Solid line indicates unscraped transfer film and dashed line indicates scraped transfer film.

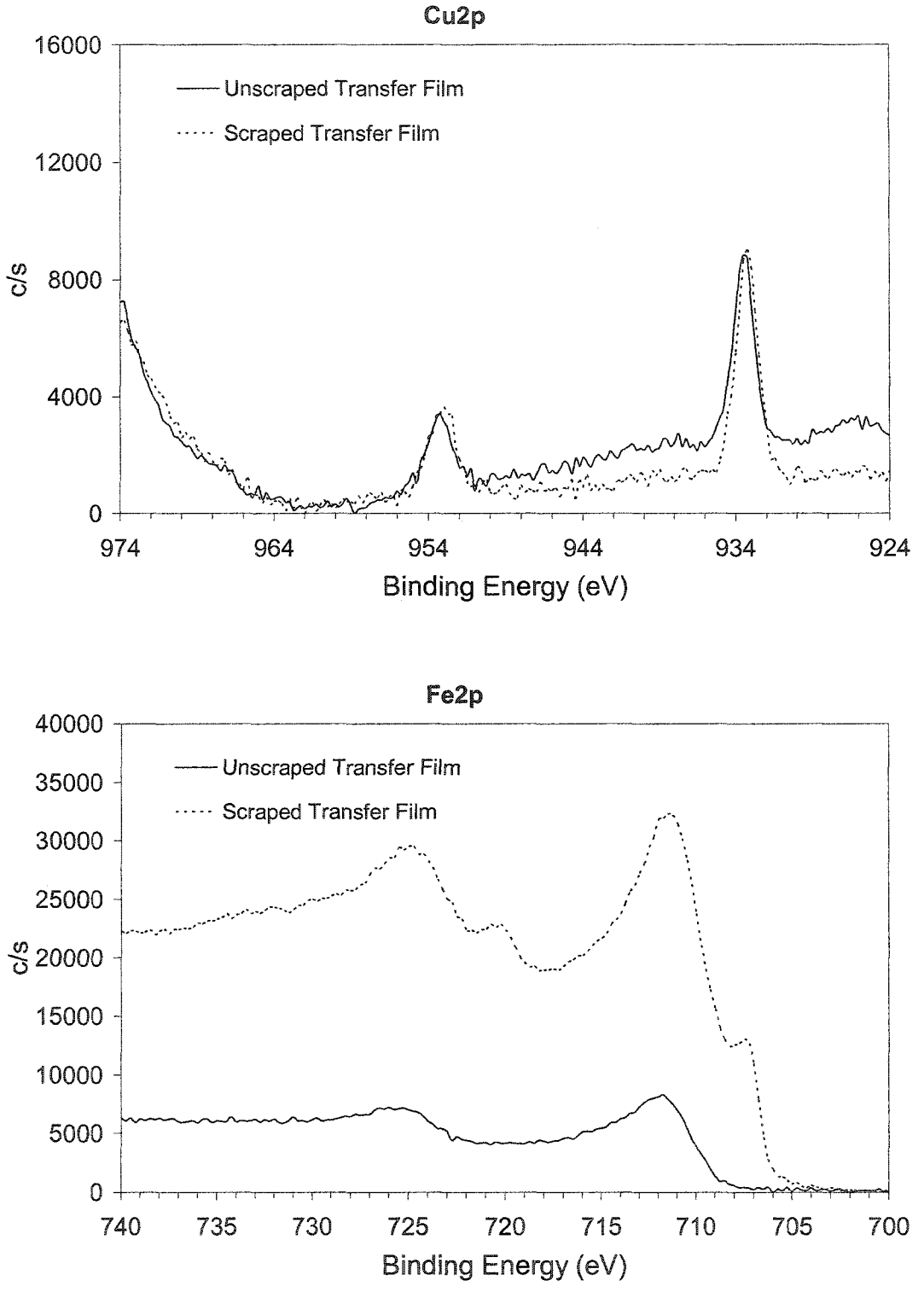

Figure 5.12 continued. XPS spectra plots of transfer film of PPS+20%CC+15%PTFE composite. Solid line indicates unscraped transfer film and dashed line indicates scraped transfer film.

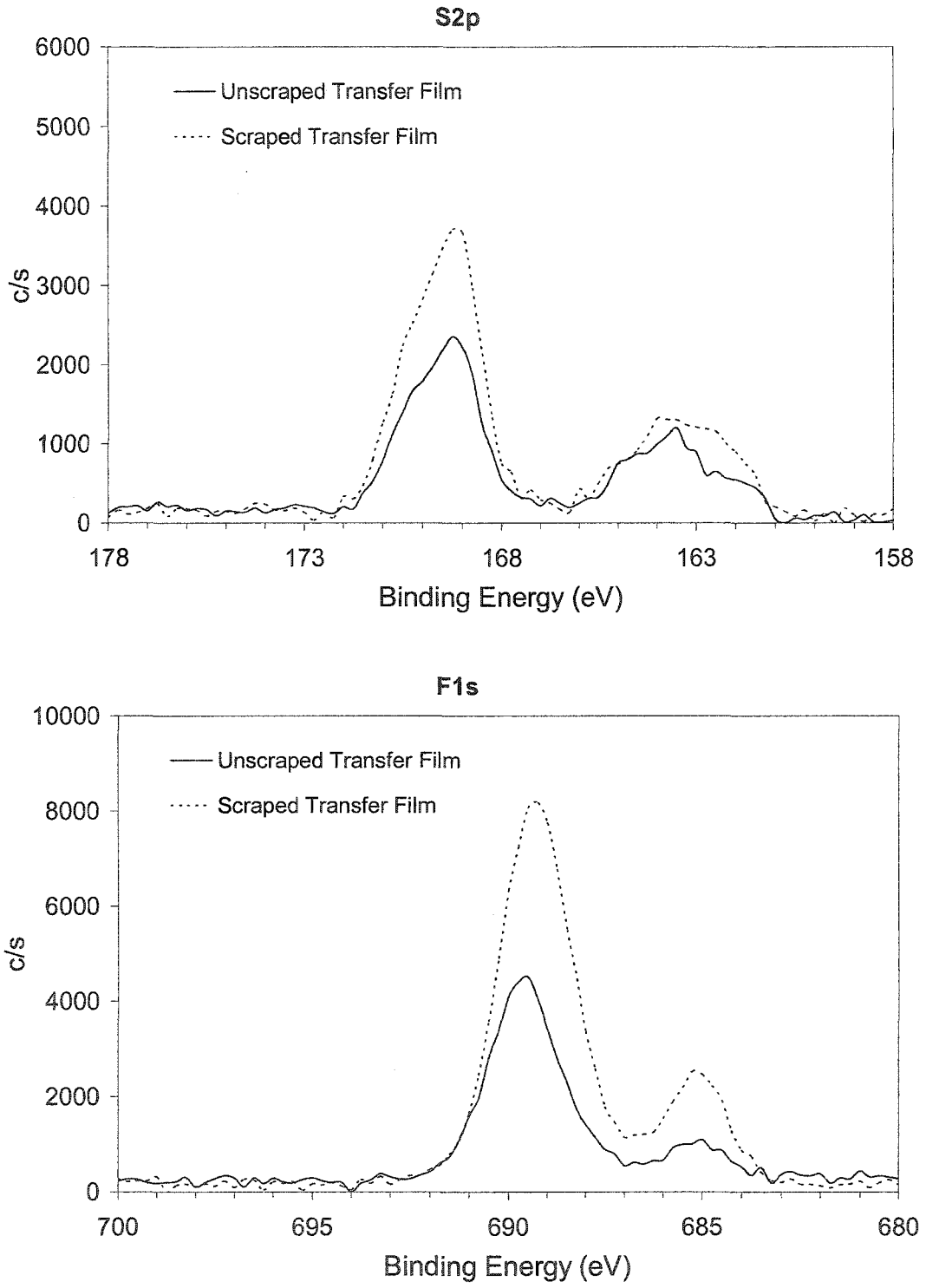

Figure 5.12 continued. XPS spectra plots of transfer film of PPS+20%CC+15%PTFE composite. Solid line indicates unscraped transfer film and dashed line indicates scraped transfer film.

CHAPTER 6
A STUDY OF THE THERMAL, MECHANICAL AND TRIBOLOGICAL PROPERTIES OF POLYPHENYLENE SULFIDE COMPOSITES REINFORCED WITH CARBON NANOTUBES AND CARBON NANOFIBERS

A paper to be submitted to *Wear*

Minhaeng Cho and Shyam Bahadur

6.1 Abstract

The thermal, mechanical and tribological properties of polyphenylene sulfide (PPS) composites reinforced with carbon nanotube (CNT) and carbon nanofiber (CNF) were studied. Dynamic mechanical thermal analysis (DMTA) and differential scanning calorimetry (DSC) were used to study the viscoelastic properties and thermal transitions. Three-point flexure tests were performed to the study the flexural properties. In order to study the tribological properties, sliding tests in a pin-on-disk configuration were performed. The changes in melting point, crystallization temperature and glass transition temperature were small as a result of reinforcement. The flexural properties had slight improvement with some proportions of CNT but worsened in the case of reinforcements. The wear rate of reinforced composites in the early part of sliding was lower than that of PPS but over extended sliding the reinforcement was not effective in reducing the wear rate. The coefficient of friction was not greatly affected by the presence of CNF and CNT. The transfer films formed on counterfaces during sliding were examined by atomic force microscopy (AFM) and were found to be lumpy and rugged for 10 vol.% CNT and 2-10 vol.% CNF. The lack of transition from run-in to steady state wear was attributed to the increased wear rates of PPS composites.

6.2 Introduction

The reinforcement of polymers with glass, carbon, and aramid fibers has proven to be very beneficial in terms of the improved physical, mechanical, and tribological properties [1-3]. It has led to the wide use of these composites in industry. The advent of carbon nanotubes (CNT) and carbon nanofibers (CNF) offers an alternative to the reinforcement of polymers with these materials. As expected, there is considerable interest and high expectation that such reinforced polymer composites could be superior to the conventional polymer composites hitherto used. It was with this perspective that this study was undertaken.

The advantages of reinforcement in terms of the enhancement in mechanical properties greatly diminish when short fibers instead of the continuous fibers are used [4]. However, short fibers have been reported to increase wear resistance and affect the coefficient of friction [5]. The reinforcement with CNT and CNF would be akin to the reinforcement with conventional short fibers in terms of the physical structure and processing capabilities. CNT and CNF have excellent properties in terms of the high strength and high modulus [6,7] which would be expected to be beneficial attributes for reinforcement in terms of the superior mechanical properties of the composite. This possibility would be further enhanced considering that these nano reinforcing materials have aspect ratios much larger than those of the conventional fibers and would be more compatible to the polymer resulting in superior interfacial adhesion. It is difficult to say how the reinforcement with these nanotubes and nanofibers would affect the tribological behavior of the polymer.

Dong *et al.* [8] studied the tribological behavior of CNT-reinforced copper composites and found that reinforcement lowered the coefficient of friction and increased the wear rate of copper. It was also reported that porosity in the composite increased as the volume fraction

of nanotubes increased. Shaffer and Windle [9] observed by dynamic mechanical thermal analysis (DMTA) that the storage modulus of polyvinyl alcohol (PVA) matrix reinforced with carbon nanotubes was unaffected with CNT proportions up to about 20 wt.% but increased for higher proportions. The onset of glass transition was also not greatly affected for any nanotube fraction. Like nanotubes, carbon nanofibers have also been used as reinforcement in metal- and polymer-matrix composites. Chen *et al.* [10] studied the tribological behavior of carbon nanofiber-reinforced polymeric coatings on aluminum/alumina based composites. They found the formation of a lubricious carbon layer and its transfer to the steel counterface occurred during sliding and this resulted in providing a low coefficient of friction of 0.2-0.3. Mechanical tests on PEEK reinforced with carbon nanofiber [11] showed that the elastic modulus of the composites increased as the CNF fraction increased, but the strain-to-failure decreased abruptly at 15 wt.% CNF, showing brittle fracture behavior. Dynamic mechanical property measurements showed that storage modulus of the composite increased with the increase in CNF proportion both below and above the glass transition temperature, but CNF did not affect the onset of glass transition.

In this study, carbon nanotube and carbon nanofiber-reinforced polyphenylene sulfide (PPS) composites were studied in terms of their thermal, mechanical, viscoelastic, and tribological properties. The thermal properties were studied by differential scanning calorimetry (DSC), viscoelastic properties by dynamic mechanical testing, and mechanical properties by flexure test. There is no known work related to this kind of study for PPS reinforced with carbon nanotubes and nanofibers.

6.3 Experimental details

6.3.1 Materials

PPS in the form of powder, supplied by Phillips Chemical Company, was used as the matrix material due to its superior mechanical properties and high temperature capability. Multi-wall carbon nanotube (CNT) and carbon nanofiber (CNF) were purchased from Nanotech Company. They were produced by chemical vapor deposition (CVD) method. The size of nano-tubes was 15-40 nm in diameter and 30-50 μm long and of nanofibers 100-120 nm in diameter and 30-50 μm long. Their purity based upon the manufacturer's specification, which is the weight ratio of CNT or CNF to the total weight, was over 95 %. It is well known that CNT contain a number of by-products such as amorphous carbon, fullerene, etc. Because of such by-products, the purification process for CNT with less impurity is required, which is a complex, costly, and lengthy process. The latter was not needed in this work because of the high purity of CNT and CNF as received.

6.3.2 Sample preparation

PPS powder was dried at 125°C for 6 hours. Carbon nanotube and nanofiber were used in the as-received form, and so 5 wt.% of these was basically amorphous carbon. In order to separate CNT from their lumps, the agglomerates of CNT were crushed gently in order to minimize damage to the structure of CNT. The crushing process was not needed for CNF which were not agglomerated. PPS and nanotubes or nanofibers were weighted in required proportions and the mixture was blended in an ultrasonic bath of acetone for 2 hours. When most of acetone evaporated in air, the blend was dried at 125°C for 1 hour in an electric oven. The proportions of CNT or CNF ranged from 1.0 vol.% to 10.0 vol.% in this study. The specimen from blended mixture was prepared by compression molding, following the steps

described elsewhere [12]. The molded blocks were in two sizes: cylinder 6.35mm in diameter and 11 mm long; slab 36 mm x 27 mm x 4 mm.

6.3.3 DSC and DMTA studies

Differential scanning calorimetry (DSC) and dynamic mechanical thermal analysis (DMTA) tests were performed on composites with 0, 2, and 10 vol.% proportions of CNT and CNF each. The materials for DSC test were quenched in ice-water following molding at 310°C. This was done to ensure that transitions appeared distinctly. A small fragment weighing about 7 mg ± 0.8 mg was cut from the material and used as sample for the DSC test. The sample was heated at the rate of 10°C/min to a temperature of 310°C.

The three-point flexure method was employed for DMTA test. The sample size for this test was 25.0 mm x 6.5 mm x 3.2 mm. The specimen support span in sample chamber was 20 mm. The test was started at 35°C and stopped around 260°C due to severe deflection of the specimen as it approached the melting temperature of PPS. The heating rate of 10°C/min and the frequency of 1 Hz were used for the test. The static and dynamic forces used for the loading were 500 mN and 400 mN, respectively. The static force was well within the elastic deformation range of the specimen.

6.3.4 Flexural test

The effect of reinforcement on mechanical properties was studied by three-point flexure tests performed at room temperature. The specimen support span was 24.5 mm and the radius of the loading nose was 3.175 mm. The specimen rested on supports which provided line contacts. The test was run with the crosshead speed of 1 mm/min and load as a function of displacement was recorded. For each composition, the test was repeated 4-5 times.

6.3.5 Pin-on-disk sliding tests

Sliding tests were performed in a pin-on-disk configuration against a hardened tool steel (55-60 HRC) disk. The steel counterface was abraded with 320-grit SiC paper to provide a counterface roughness of about 0.10 μm Ra. The polymer composite specimen was finished by abrasion against 240-grade emery paper in running water, washed with soap and water, and dried in air. It was stored overnight in a dessicator prior to testing. Full contact between the counterface and the specimen during sliding was ensured by abrading the specimen lightly against emery paper mounted on a rotating disk. Sliding tests at the sliding speed of 1.0 m/s and nominal contact pressure of 0.65 MPa were performed over a duration of 6 hrs. Sliding tests were performed for 6 hours. They were interrupted for gravimetric measurement of wear loss at the intervals indicated in the wear and friction plots reported later. Wear loss was measured to an accuracy of 10 μg and converted to wear volume loss using the density of the composite. For each composition, 2-3 tests were repeated and the average value was used to find steady state wear rate and the coefficient of friction. The scatter in data was within ±10 %.

6.4 Results and discussion

6.4.1 Differential scanning calorimetry

The crystallization features of PPS and its composites made by the addition of CNT and CNF were studied using DSC measurements. Anisothermal thermograms were recorded during the heating process and these are given in Fig. 6.1. From these, the thermal crystallization temperature (T_c), melting temperature (T_m), heat of fusion (ΔH_m), and percent crystallinity (X_c) were obtained and they are given in Table 6.1. The degree of crystallization,

X_c, was calculated from the equation:

$$X_c\ (\%) = [(\Delta H_m - \Delta H_c) / (\Delta H^\circ_f W_f)] \cdot 100$$

where ΔH_m is the melting enthalpy from DSC scan, ΔH_c is cold crystallization enthalpy, W_f is the weight fraction of PPS in the composite, and ΔH°_f is the melting enthalpy of 100% crystallized PPS which was taken as 105 J/g. The melting enthalpy ΔH_m and crystallization enthalpy ΔH_c were obtained from the areas of melting and crystallization peaks, respectively, using compute software. The heat of melting and cold crystallization are in terms of J/g. It should be noted that the crystallization temperatures decreased slightly with the addition of CNT or CNF. Lozano *et al.* [13] reported that T_c increased slightly with CNT or CNF in PP and was not affected with CNF in PEEK matrix. Since crystallization involves the development of orderly arrangement of polymer molecules, the delay in crystallization during cooling indicates that the presence of nanotubes and nanofibers interfered in this process. Since nanotube and nanofiber surfaces could provide heterogeneous nucleation sites, an opposite effect in terms of the recrystallization occurring earlier could also prevail. These opposing factors could account for why recrystallization occurs earlier in some systems and later in others. The crystallization peak is exothermic as opposed to melting peak which is endothermic. It is obtained both on heating and cooling and is associated with the change in molecular arrangement. The behavior of melting temperatures was analogous to that of the recrystallization temperatures as would be expected. The melting enthalpy of reinforced PPS was lower than that of PPS, and the higher the proportions of CNT or CNF, the greater was the reduction. This observation is in agreement with that reported [14,15] earlier for CNT-reinforced polypropylene.

The crystallinity of PPS decreased on reinforcement with CNT or CNF and the higher the proportion of these, the lower was the crystallinity. The reason for this was the propensity of CNT and CNF in hindering the orderly arrangement of PPS molecules, as indicated earlier.

6.4.2 Dynamic mechanical thermal analysis

The dynamic mechanical properties were studied because they are highly sensitive to the structure of material. The plots of storage modulus and loss tangent for all the compositions studied are shown in Fig. 6.2. The storage modulus decreases rapidly in the glass transition range and the drop in modulus for all the compositions is about the same. The storage modulus values in the glassy state are also almost equal. Thus, there is no significant effect of reinforcement with CNT or CNF on this mechanical property. This observation is agreement with the work reported by others [9,11,14]. For example, Shaffer and Windle [9] reported that there was no change in storage modulus for carbon nanotubes up to 30 wt.% in poly(vinyl alcohol). The location of the damping peak in tan δ vs. temperature plot in Fig. 6.2 shows that there is a slight reduction in the glass transition temperature of PPS when CNT and CNF were added. Since carbon nano structures position themselves between the molecules, the intermolecular attraction is reduced because of the increase in intermolecular spacing. This makes the segmental molecular motion possible at lower temperature which is necessary for glass transition. With much higher proportions of CNT and CNF in polyvinyl alcohol, reduced damping as evidenced by greater peak broadening has been reported [9].

6.4.3 Flexural behavior

The flexural properties of CNT- and CNF-reinforced PPS composites were studied by three-point flexure tests and the results are presented in Fig. 6.3. The flexural strengths of the

composites reinforced with 1-3vol.% CNT increased slightly but with larger CNT proportions there was no gain. No significant differences in the flexural moduli with CNT reinforcement existed. With CNF-reinforcement, both of the above properties worsened. Since with higher proportions of CNT and CNF the strength and modulus both were lower, the poor interfacial adhesion between the matrix and the reinforcement seems to be the reason for this behavior. This is all the more so because the tensile strengths of polystyrene [16], polyvinyl alcohol [17], PMMA [18], Epoxy [19], and polypropylene [20] have been reported to improve with CNT or CNF reinforcement. The interfacial failure is a much serious problem in flexure than in tensile loading. The problem could have also been created by the poor dispersion of the reinforcement material in the matrix. This is supported by Fig. 6.4 which shows SEM micrograph of CNF agglomerates on the fracture surface of PPS+10%CNF composite. This shows that the nanofibers are not uniformly dispersed in PPS matrix. In addition, there are voids around the agglomerates which would also cause premature failure. Figure 6.5 shows the SEM micrographs of the fracture surfaces of composites reinforced with 10 vol.% CNT and CNF. In both cases, voids on the fracture surface can be seen. Our results are in agreement with Lau *et al.* [21] who reported that the flexural strength of epoxy reinforced with 2 wt.% CNT was lower than that of neat epoxy. Similarly, Xu *et al.* [22] also showed that both flexural moduli and flexural strengths decreased with increasing nanofiber proportions in vinyl ester composites.

6.4.4 Friction and wear studies

The variation of wear and the coefficient of friction for PPS reinforced with carbon nanotubes as a function of sliding distance is shown in Fig. 6.6. As may be seen, wear of

CNT-reinforced PPS in the run-in state was considerably lower than that of PPS. Whereas PPS showed a transition to steady state wear at about 7 km, no such transition was observed for the reinforced material and so wear of this material increased linearly with sliding distance. This was the case for all CNT proportions of 1-10 vol.%. Furthermore, wear rate of the composites increased with increasing proportions of CNT. Wear rate of 1%CNT+PPS was about the same as that of PPS in the steady state but was much lower in the early part of sliding. The coefficient of friction varied from 0.44 to 0.50 for all the compositions tested. This variation was statistically insignificant.

Figure 6.7 shows the variation of wear and the coefficient of friction for PPS reinforced with CNF as a function of sliding distance. The behavior in many respects is similar to that observed for CNT-reinforced composites in respect of both the wear rate and the coefficient of friction. In other words, there was no obvious advantage of using CNF as the reinforcing material except in the early part of sliding.

In an effort to improve the wear performance, wear tests were run with three different counterfaces finished to different roughness and texture. While two surfaces with the roughness of 0.10 and 0.06 μm Ra were prepared by abrasion against emery paper, the third surface was lapped to a roughness of about 0.06 μm Ra. While the abraded and lapped surfaces had the same roughness, their textures were different. Since the lowest wear rate was obtained for 1%CNT-reinforced composite (Fig. 6.6), the same composition was used for this investigation. The wear and friction results for these surfaces are presented in Fig. 6.8. There was a slight reduction in wear rates for the smoother surfaces but the reduction was practically insignificant. Furthermore, there were no significant differences in the wear rates of abraded and lapped surfaces. The steady state coefficient of friction for the smoother

surfaces (0.06 μm Ra) was higher than for the rougher surface of 0.10 μm Ra. Since the real area of contact increases as the counterface becomes smoother, this would account for higher friction above.

6.4.5 Transfer film and worn surface studies

The transfer films formed on the steel counterfaces during sliding were examined by AFM and are shown in Fig. 6.9. It was observed that transfer film was not fully developed and some regions remained uncovered after sliding. The compositions used for this observation were the composites with 2 and 10 vol.% of CNT and CNF each. The transfer film for PPS+2vol.%CNT is thinner and smoother than that for PPS+10vol.%CNT. The transfer film for the latter composite shows lumpy formation with a very rough texture, which contributed to a very high wear rate and no changeover from transient to steady state. Similar features including the lumpy formation were also observed for PPS+CNF transfer films and the wear rates in both cases were very high.

Worn pin surfaces of the composites reinforced with 10vol.% of CNT or CNF were also examined by AFM and are shown in Fig. 6.10. A deep furrow along sliding direction is seen in Fig. 6.10(a) for PPS+10vol.%CNT composite. The depth of this groove is about 200 nm which is significantly larger than the nanotube dimension. It must have thus been caused by an asperity on exposed metal counterface. On the whole, the worn pin surface was rough with rippling features. In the case of PPS+10%CNF composite, a number of wear grooves along sliding direction are also seen and the surface exhibits some waviness. These grooves are about 50-100 nm deep. These were presumably formed by asperities on the counterface during sliding since direct pin-to-metal contact occurred in some locations due to loss of

transfer film, as stated above. Because of the plowing action, the wear rate of PPS+10%vol.CNF was fairly high.

6.5 Conclusions

The effect of carbon nanotube and carbon nanofiber reinforcements in PPS was studied in terms of thermal, mechanical, and tribological properties of PPS composites, and the following conclusions were drawn:

1. The changes in thermal transitions such as glass transition temperature, crystallization temperature, and melting point were small as a result of reinforcement.
2. There was reduction in melting enthalpy and crystallinity with higher reinforcement proportions of CNT and CNF.
3. From the dynamic mechanical thermal analysis, no significant change in storage modulus was observed with reinforcement. There was a slight decrease in glass transition temperature which was attributed to earlier molecular segmental motion because of increased intermolecular spacing from the presence of CNT and CNF.
4. With some exceptions, the flexural strength and flexural modulus were decreased from reinforcement and the effect was more pronounced with higher proportions.
5. Wear of composites increased linearly with sliding distance and no transition from run-in to steady state was observed. Similar was the case with counterfaces finished to different roughness and texture.
6. Wear rate of the composites in the early period of sliding was lower than that of PPS but for larger sliding distances it was either same or worse.

7. There were no significant variations in the coefficient of friction because of reinforcement.
8. Transfer films formed on the counterface were thick and non-uniform regardless of the CNT or CNF proportions. The coverage of wear track with transfer film was no uniform.

6.6 References

1. S. Bahadur, Mechanical and tribological behavior of polyester reinforced with short fibers of carbon and aramid, Lubrication Engineering, Vol. 47, 8, 661-667.
2. J. Theberge, B. Arkles, Wear characteristics of carbon fiber reinforced thermoplastics, Lubrication Engineering, Vol. 30, 12, 585-589.
3. S. Bahadur, Y. Zheng, Mechanical and tribological behavior of polyester reinforced with short glass fibers, Wear 137 (1990) 251-266.
4. K. Friedrich, Wear of reinforced polymers by different abrasive counterparts, Vol.1. Friction and Wear of Polymer Composites, K. Friedrich (Ed.), (1986) 233-287.
5. H. Voss, K. Friedrich, The wear behavior of short-fiber reinforced thermoplastics sliding against smooth steel surfaces, Wear of Materials, Ludema, K. C. ed., ASME, New York, 1985, 742-750.
6. B. I. Yakobson, C. J. Brabec, J. Bernholc, Nanomechanics of Carbon Tubes: Instabilities beyond Linear Response, Phys. Rev. Lett. 76, 2511–2514 (1996).
7. Eric W. Wong, Paul E. Sheehan, Charles M. Lieber, Nanobeam mechanics: elasticity, strength, and toughness of nanorods and nanotubes, Science, 1997, v277, 1971.

8. S.R. Dong, J.P. Tu, X.B. Zhang, An investigation of the sliding wear behavior of Cu-matrix composite reinforced by carbon nanotubes, Materials Science and Engineering A313 (2001) 83-87.

9. Milo S. Shaffer, Alan H. Windle, Fabrication and characterization of carbon nanotube/Poly(vinyl alcohol) composites, Adv. Mater. 1999, 11, No.11, 937-941.

10. M.Y. Chen, Z. Bai, S.C. Tan, M.R. Unroe, Friction and wear scar analysis of carbon nanofiber-reinforced polymeric composite coatings on alumina/aluminum composite, Wear 252 (2002) 624-634.

11. Jan Sandler, Philipp Werner, Milo S.P. Shaffer, Vitaly Demchuk, Volker Altstadt, Alan H. Windle, Carbon-nanofiber-reinforced poly(ether ether ketone) composites, Composites: Part A 33 (2002) 1033-1039.

12. M.H. Cho, S. Bahadur, Study of the tribological synergistic effects in nano CuO-filled and fiber-reinforced polyphenylene sulfide composites, Wear (2004) in press.

13. K. Lozano, E. V. Barrera, Nanofiber-reinforced thermoplastic composites. 1. Thermodynamical and mechanical analyses, J. of Applied Polymer Science, Vol.79, 125-133 (2001).

14. D. Puglia, L. Valentini, J. M. Kenny, Analysis of the Cure Reaction of Carbon Nanotubes/Epoxy Resin Composites Through Thermal Analysis and Raman Spectroscopy, J. of Applied Polymer Science, Vol.88, 452-458 (2003).

15. L. Valentini, J. Biagiotti, J. M. Kenny, S. Santucci, Effects of Single-Walled Carbon Nanotubes on the Crystallization Behavior of Polypropylene, J. of Applied Polymer Science, Vol.87, 708-713 (2003).

16. D. Qian, E. C. Dickey, R. Andrews, T. Rantell, Load transfer and deformation mechanisms in carbon nanotube-polystyrene composites, Applied Physics Letters, Vol. 76, Issue 20, pp. 2868-2870.

17. Milo S. Shaffer, Alan H. Windle, Fabrication and characterization of carbon nanotube/Poly(vinyl alcohol) composites, Adv. Mater. 1999, 11, No.11, 937-941.

18. R. Haggenmueller, H. H. Gommans, A. G. Rinzler, J. E. Fischer, K. I. Winey, Aligned single-wall carbon nanotubes in composites by melt processing methods, Chemical Physics Letters 330 (2000) 219-225.

19. L. S. Schadler, S. C. Giannaris, P. M. Ajayan, Load transfer in carbon nanotube epoxy composites, Applied Physics Letters, Vol. 73, No. 26, 3842-3844.

20. Satish Kumar, Harit Doshi, Mohan Srinivasarao, Jung O. Park, David A. Schiraldi, Fibers from polypropylene/nano carbon fiber composites, Polymer 43 (2002) 1701-1703.

21. Kin-Tak Lau, San-Qiang Shi, Li-Min Zhou, Hui-Ming Cheng, Micro-hardness and flexural properties of randomly-oriented carbon nanotube composites, J. of composite materials, Vol.37, No.4/2003, 365-376.

22. Jun Xu, John P. Donohoe, Charles U. Pittman Jr., Preparation, electrical and mechanical properties of vapor grown carbon fiber (VGCF)/vinyl eater composites, Composites: Part A 35 (2004) 693-701.

Table 6.1 Effect of CNT and CNF on the thermal properties from DSC analysis.

Sample	T_c, °C	T_m, °C	ΔH_m, J/g	X_c, %
PPS	118.83	280.61	37.93	27.88
PPS+2%CNT	115.82	280.28	34.35	25.28
PPS+10%CNT	117.66	275.78	24.98	22.58
PPS+2%CNF	117.00	280.11	36.01	27.49
PPS+10%CNF	116.66	278.28	28.91	25.05

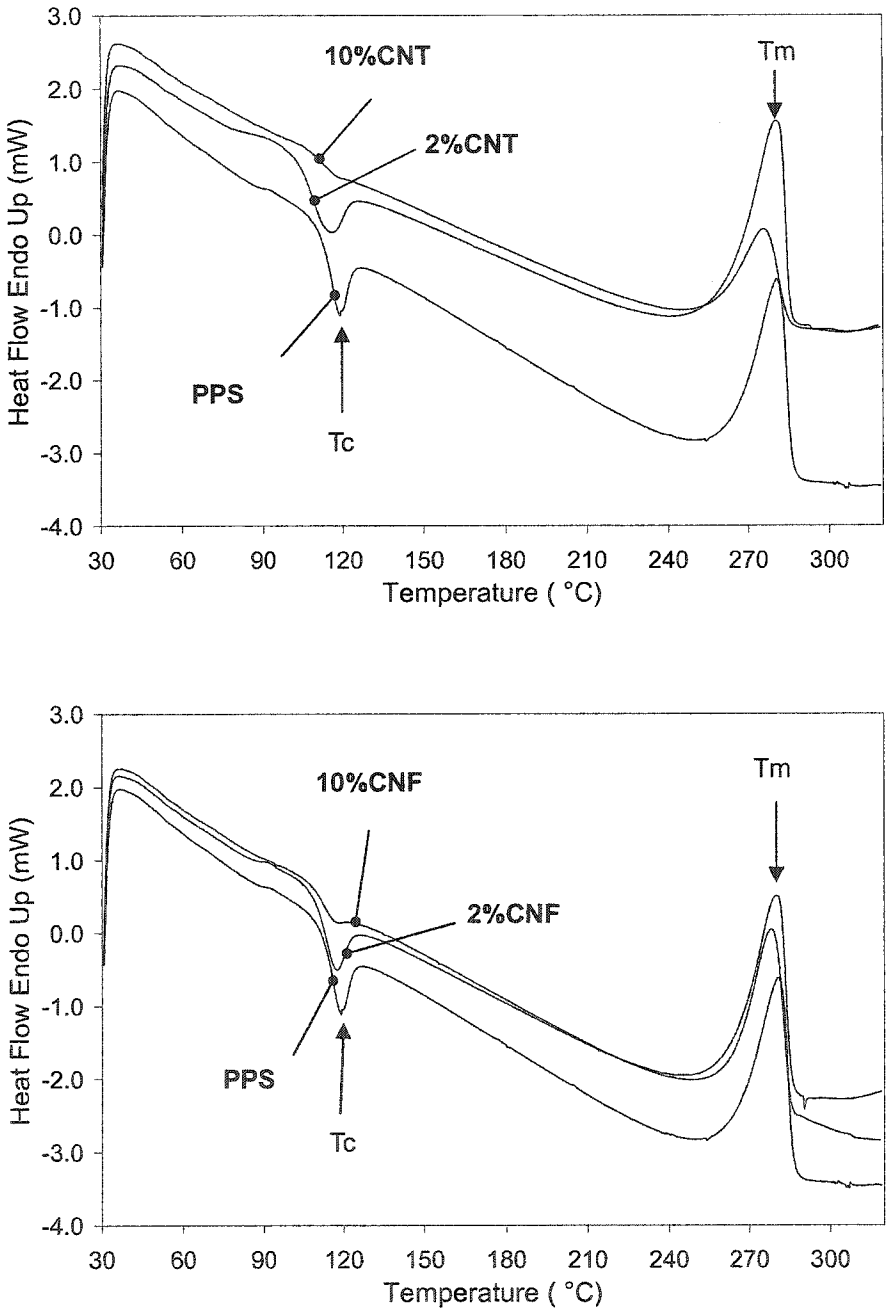

Figure 6.1 Differential scanning calorimetry analysis of PPS composites as a function of temperature. (a) PPS reinforced with CNT and (b) PPS reinforced with CNF. Heating rate 10°C/min. Temperature range 30 – 320°C. Background not subtracted.

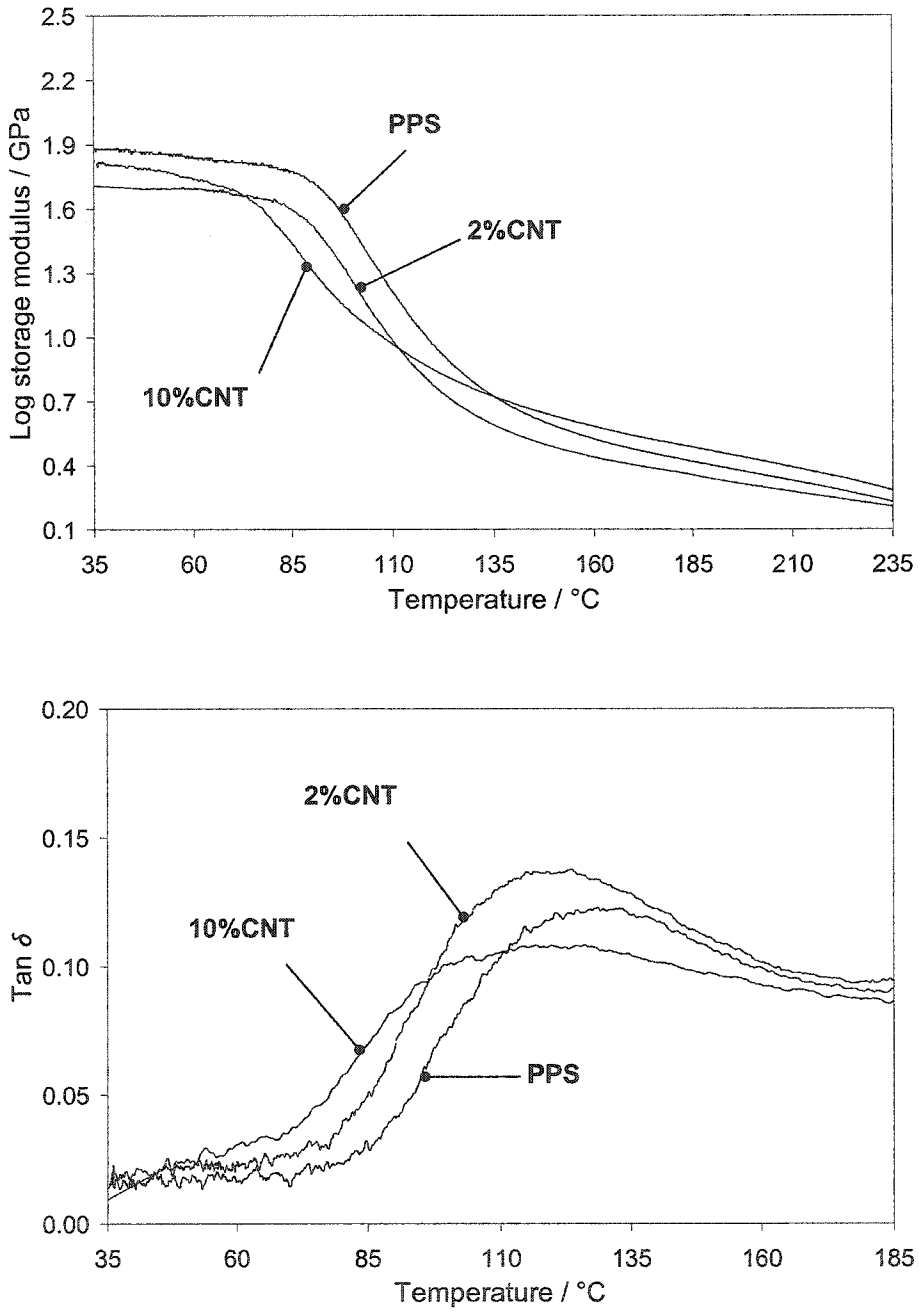

(a)

Figure 6.2 Dynamic mechanical analysis of PPS composites reinforced with CNT or CNF as a function of temperature: (a) Log storage modulus and tan δ for CNT-reinforced composites and (b) log storage modulus and tan δ for CNF-reinforced composites.

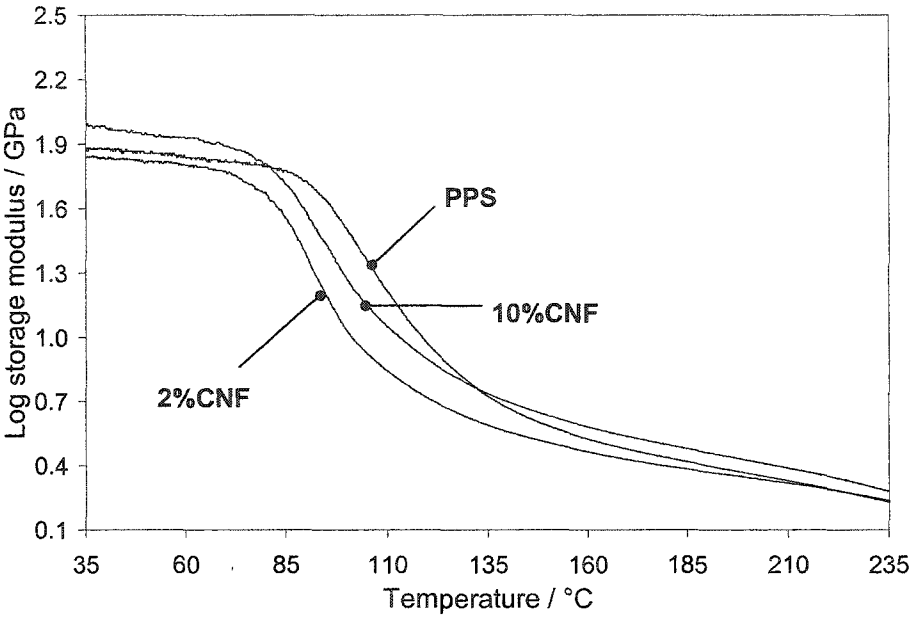

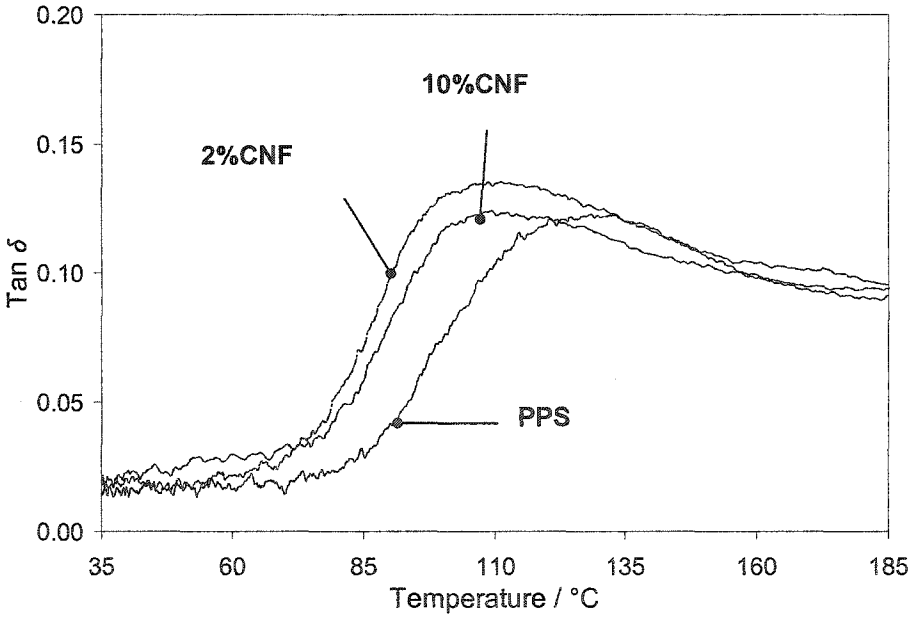

(b)

Figure 6.2 continued. Dynamic mechanical analysis of PPS composites reinforced with CNT or CNF as a function of temperature: (b) log storage modulus and tan δ for CNF-reinforced composites.

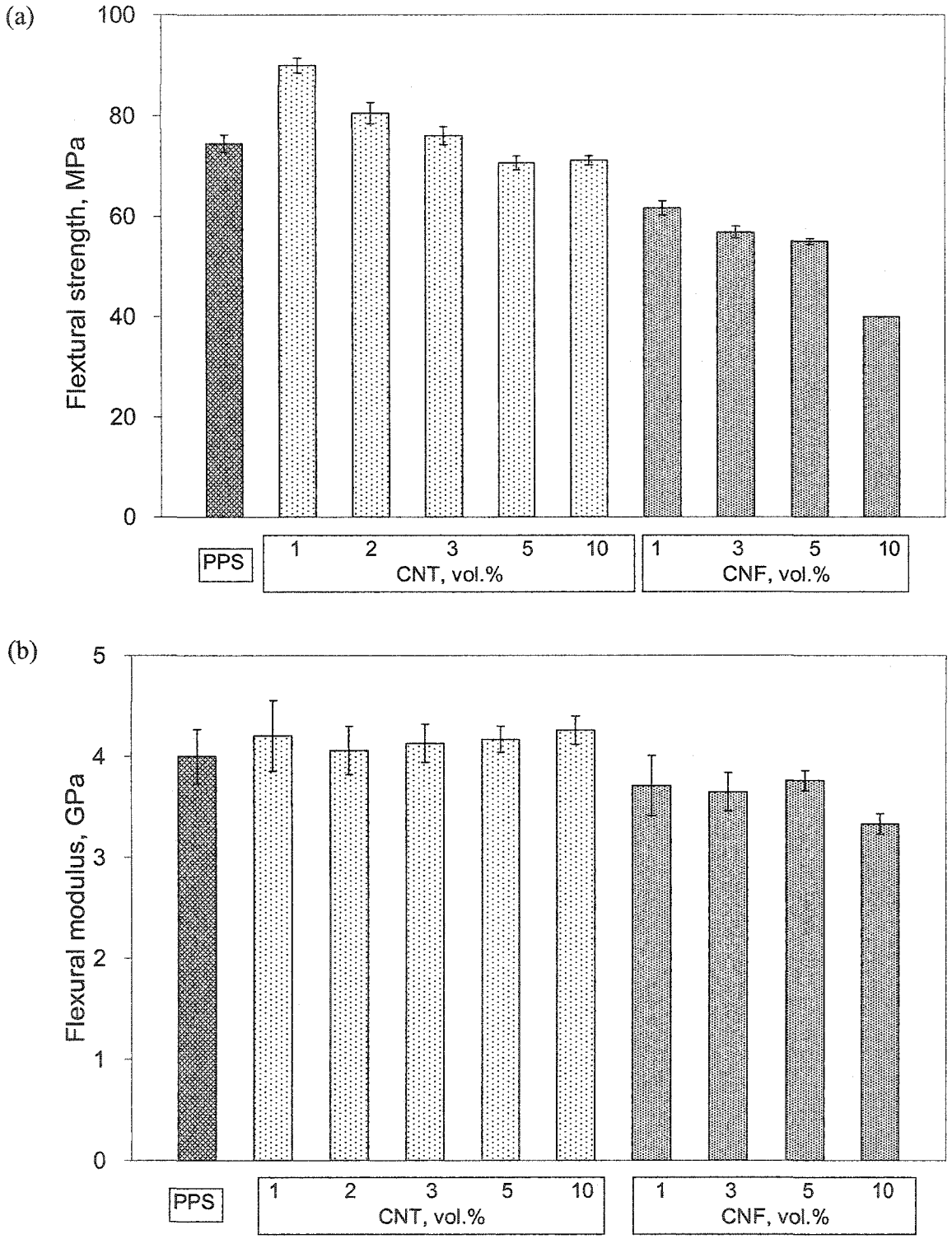

Figure 6.3 Three-point flexure test results: (a) flexural strength and (b) flexural modulus.

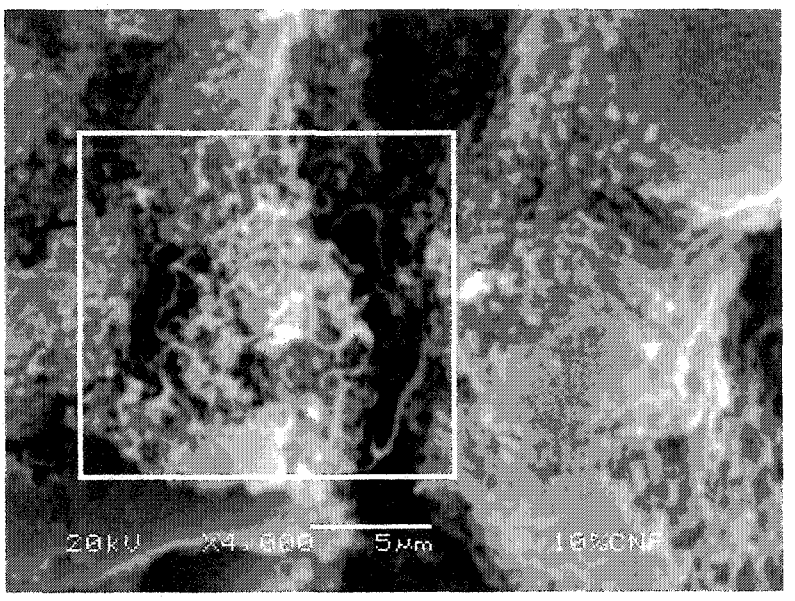

Figure 6.4 CNF agglomerates on fracture surface of PPS+10%CNF. The agglomerates are indicated by the box in this SEM micrograph.

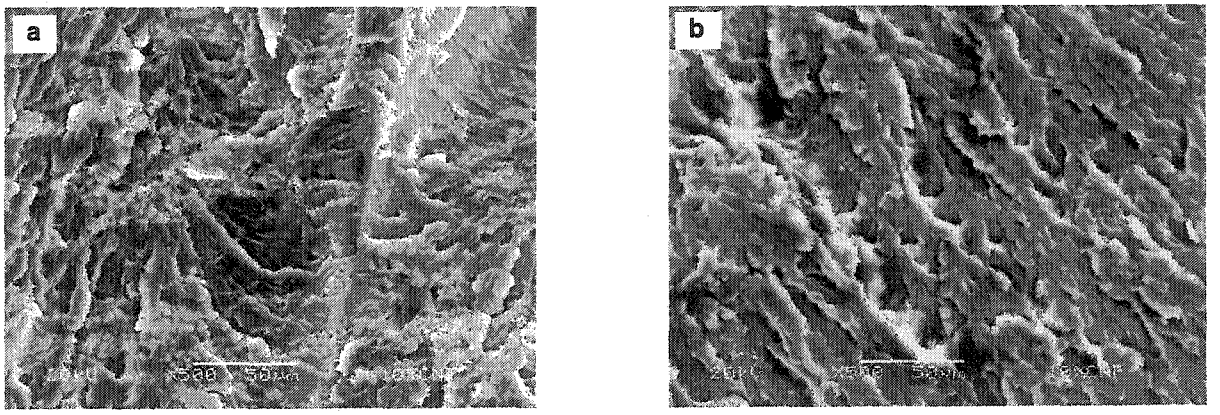

Figure 6.5 SEM flexural fracture surface: (a) PPS+10%CNT and (b) PPS+10%CNF.

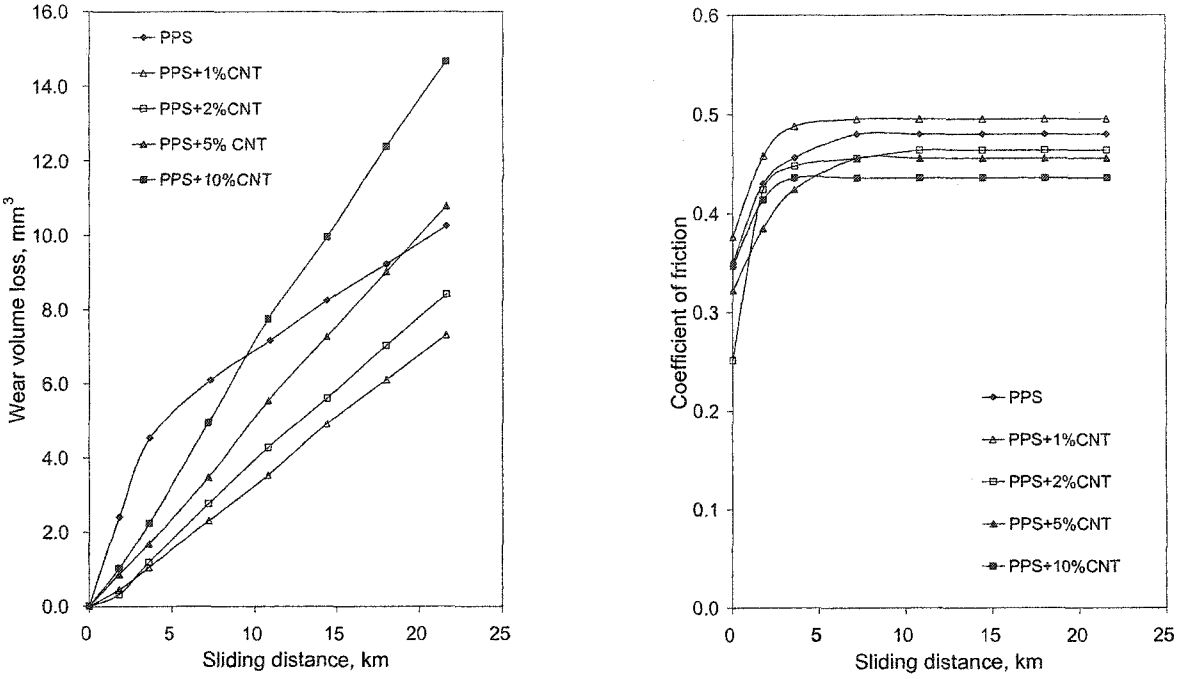

Figure 6.6 Variation of wear and coefficient of friction with sliding distance for PPS reinforced with carbon nanotubes. Test conditions: sliding speed 1.0 m/s, nominal pressure 0.65 MPa, counterface roughness 0.10 μm Ra.

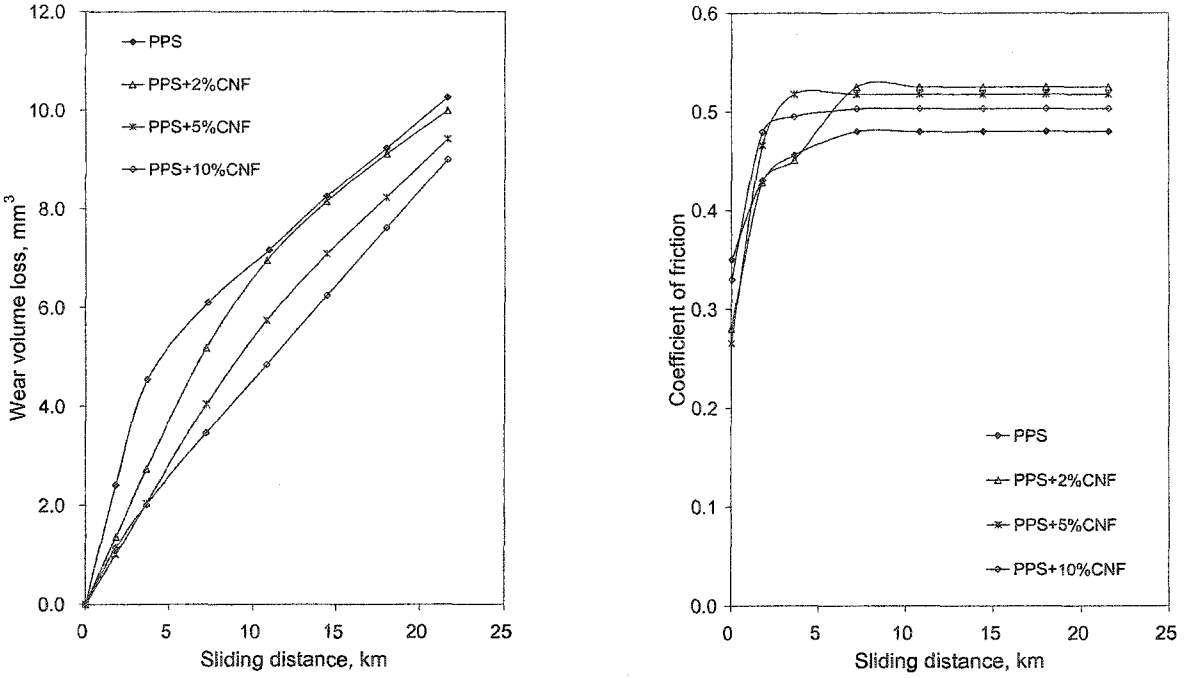

Figure 6.7 Variation of wear and coefficient of friction with sliding distance for PPS reinforced with carbon nanofibers. Test conditions same as in Fig. 6.6.

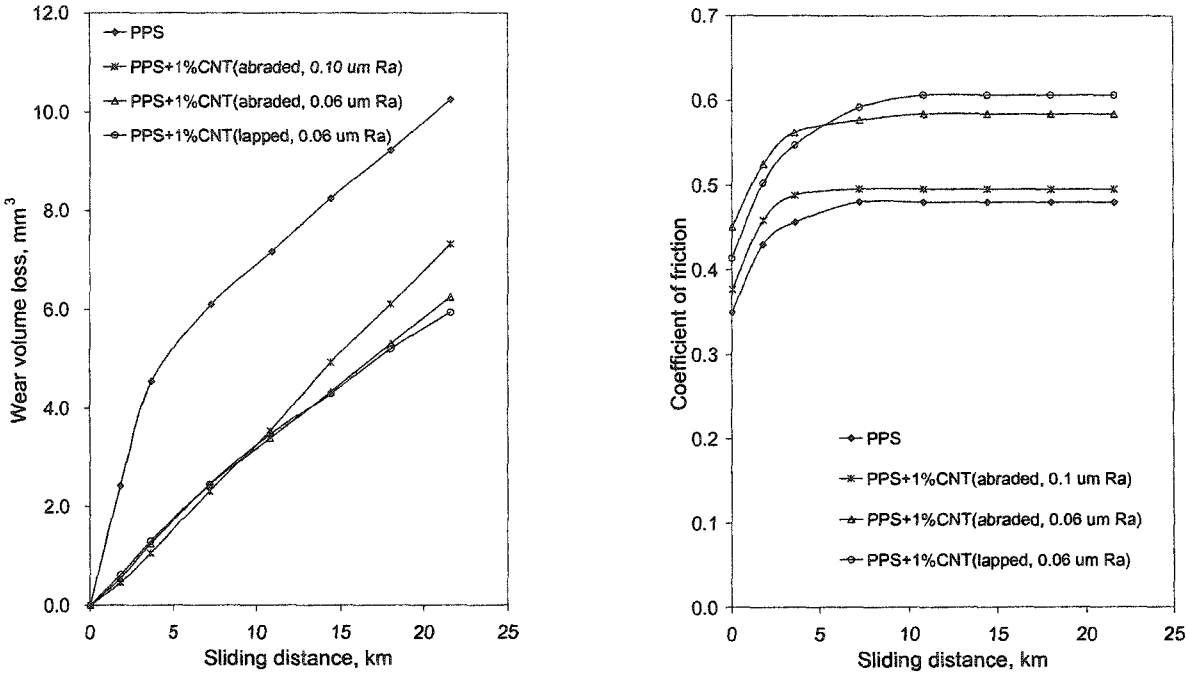

Figure 6.8 Variation of wear and coefficient of friction with sliding distance with respect to various surface roughnesses for PPS reinforced with carbon nanotubes. Sliding speed 1.0 m/s, nominal pressure 0.65 MPa.

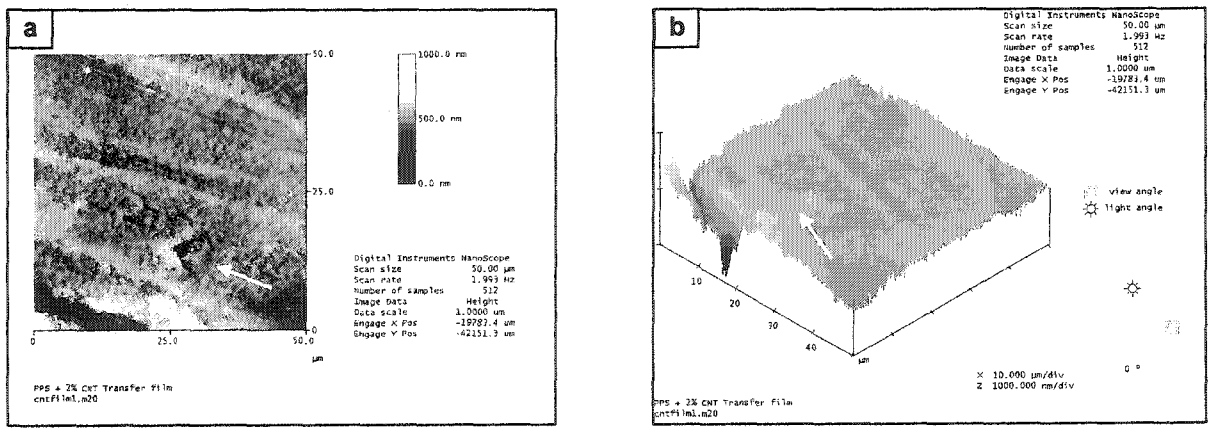

Figure 6.9 AFM micrographs of transfer film: (a-b) PPS+2%CNT, (c-d) PPS+10%CNT, (e-f) PPS+2%CNF, and (g-h) PPS+10%CNF composite. Test conditions same as in Fig. 6.6. Arrow indicates sliding direction.

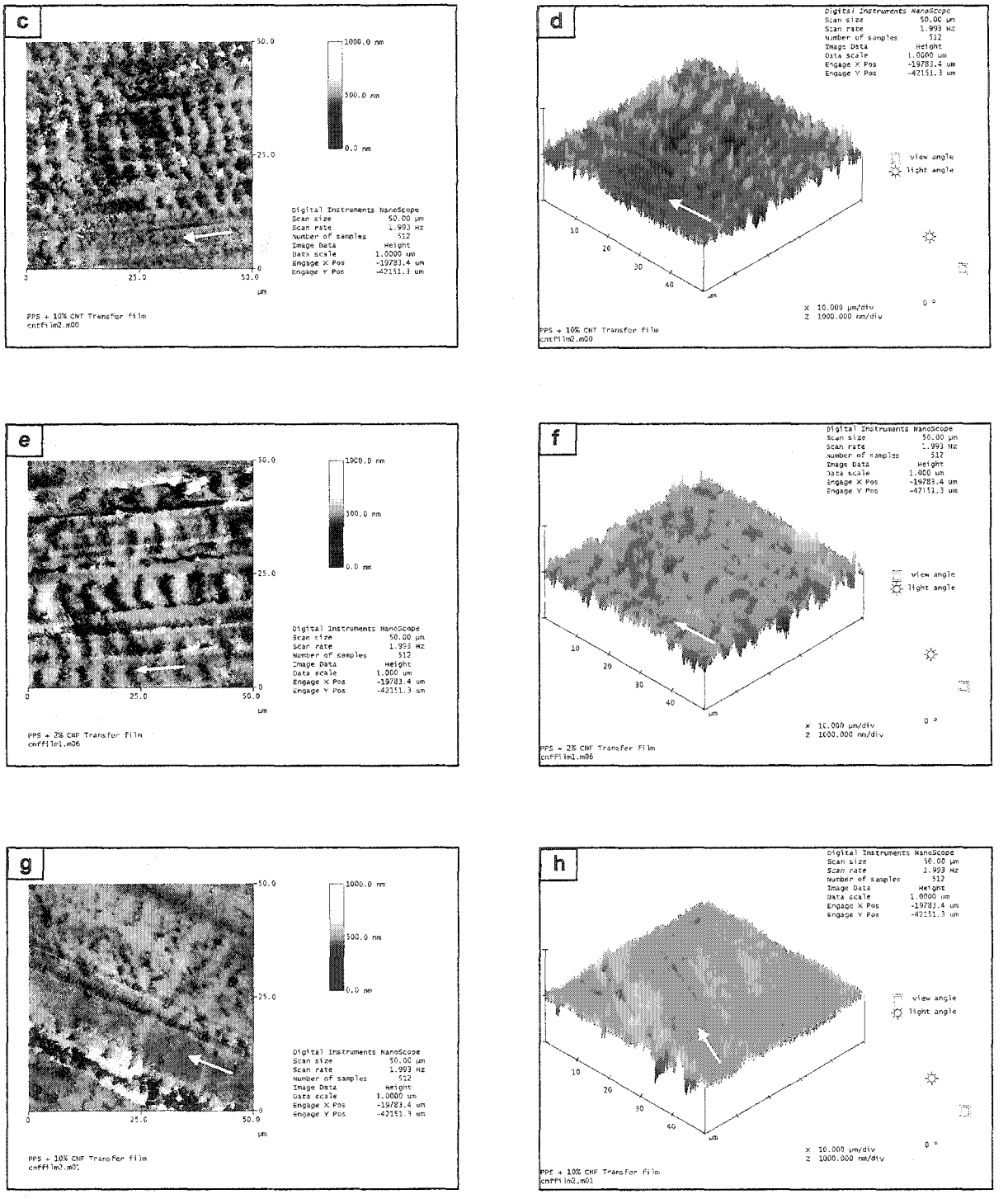

Figure 6.9 continued. AFM micrographs of transfer film: (c-d) PPS+10%CNT, (e-f) PPS+2%CNF, and (g-h) PPS+10%CNF composite. Test conditions same as in Fig. 6.6. Arrow indicates sliding direction.

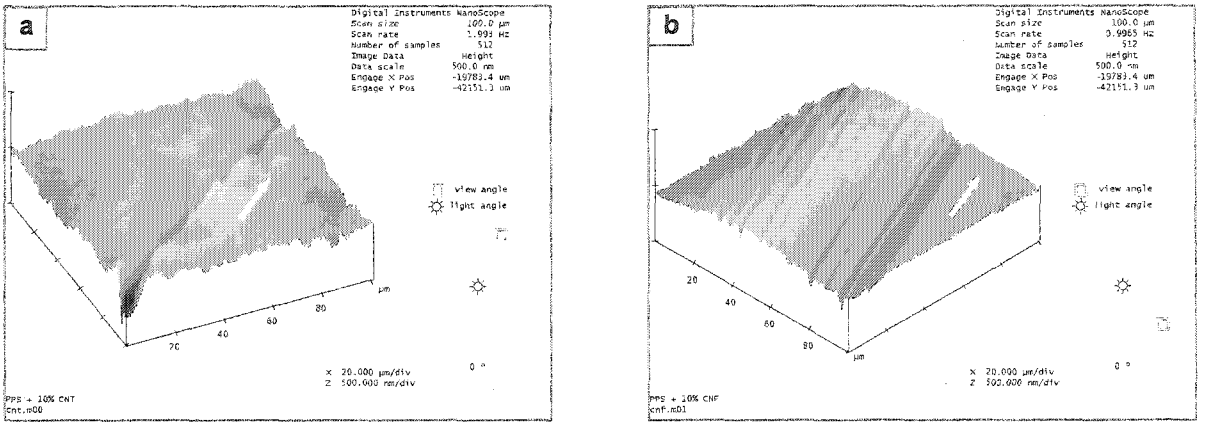

Figure 6.10 AFM micrographs of worn surface: (a) PPS+10%CNT and (b) PPS+10%CNF composite. Test conditions same as in Fig. 6.6. Arrow indicates sliding direction.

CHAPTER 7
GENERAL CONCLUSIONS

This work revealed several key factors involved in the sliding wear of PPS composites. First and foremost, the steady state wear rate of PPS is dependent to a great extent on two aspects of the sliding wear process. One aspect is the durability and resistance to material removal of the bulk composite at the wear interface, and the second aspect is the resistance to debonding of deposited transfer film from the counterface. This research has shown that both aspects can be addressed to reduce the wear rate of PPS. From this work, the following conclusions were drawn:

1. The largest reduction of wear rate which was one twentieth of that of unfilled PPS was found when both nanosize CuO particles and fiber were added to PPS. In this study, the lowest wear rate of 0.014 mm^3/km was obtained for PPS+15%Kevlar+2%CuO composite.
2. The steady state coefficient of friction was greatly lowered with 15 vol.% carbon fiber due to the lubricating action of graphite. The effect of synergism on the coefficient of friction was minute or even deleterious for other compositions.
3. The examination of transfer film of PPS+2%CuO+10%Kevlar composite by atomic force microscopy and optical microscopy revealed that smooth, compact, thin, and coherent transfer film was a prerequisite for the reduction of steady state wear rates.
4. No obvious damage on the worn pin surfaces was observed for CuO-filled PPS composites. Microcracking at fiber tips and debonding of fiber surface along with the disintegration of polymeric material were observed for fiber-reinforced PPS composites. These were the phenomena that contributed to wear.

5. Significant reduction in abrasiveness was observed with the reduction in particle size from 80 μm to 45 μm in the case of tuff, travertine, and bentonite. On the whole, surface treatments on the mineral particles and the use of smaller size of particles were not effective in reducing the wear rate of PPS. Although slight reduction in wear rate was observed for 5 vol.% 100 nm bentonite with and without 5 vol.% PTFE, it was practically insignificant.
6. Abrasion appears to be the most important factor responsible for high wear rates of the composites of PPS filled with the minerals from Armenia.
7. The coefficient of friction was lowered with larger proportions of the mineral filler in PPS due to their hygroscopic characteristic. MoO_2-filled PPS composites showed the lowest coefficient of friction owing to its lubricating ability.
8. Transfer films formed during sliding with tuff, bentonite, and travertine were considerably non-uniform and thick and became thinner and more uniform only when PTFE was added to the composite. The lowest steady state wear rate in this study was obtained with the addition of PTFE, indicating the role of PTFE as a solid lubricant.
9. Mo-concentrate (MC) lowered the wear of PPS and the reduction became larger with the addition of PTFE to PPS+MC composite. The lowest steady state wear rate of 0.024 mm^3/km was obtained for PPS+17%MC+10%PTFE composite sliding at 1 m/s, against a steel counterface roughness of 0.1 μm Ra.
10. The coefficient of friction of PPS was lowered with the addition of MC from 0.48 to 0.33 and no further reduction in the coefficient of friction was observed with the addition of PTFE.

11. Design of experiments approach by Taguchi method on MC and PTFE-filled PPS composites enabled us to analyze successfully the friction and wear behavior of composites with two fillers, sliding velocity, and counterface roughness as the variables with fewer experiments that would otherwise be needed.
12. The transfer films formed on the steel counterface during sliding in the case of PPS+MC composite with PTFE were thin and uniform. These features were responsible for very low wear rate.
13. The decomposition of MoS_2 to Mo and S was detected by XPS analysis and tribo-chemical reaction of S and Fe in the counterface produced $FeSO_4$ in transfer film. This presumably promoted adhesion of transfer film to the counterface, which contributed to the reduction in wear rate.
14. The wear reduction of PPS with 10-15% copper-concentrate (CC) was marginal. Wear resistance was considerably enhanced with the addition of PTFE to PPS+CC composite. The lowest steady state wear rate of 0.0030 mm^3/km was observed for PPS+20%CC+15%PTFE composite sliding at 1.0 m/s, against a steel counterface roughness of 0.06 μm Ra.
15. The coefficient of friction was lowered from 0.48 to 0.32 by the addition of 5% PTFE to PPS+10%CC composite.
16. The examination of transfer film by optical and scanning electron microscopy and atomic force microscopy showed abrasion marks on the transfer film of PPS+CC. With the addition of 15% PTFE, the transfer film became smoother and more uniform. Deep grooves and microcracking on the bottom of grooves were observed for PPS+20%CC+15%PTFE composite worn surface.

17. XPS analysis indicated the decomposition of CuS to Cu and S and the formation of $FeSO_4$ and FeF_2. The generation of these species provided a mechanism for stronger bonding of transfer film to the counterface.
18. Insignificant changes in thermal transitions such as glass transition temperature, crystallization temperature, and melting point were observed with the addition of CNT and CNF as reinforcement.
19. A slight decrease in glass transition was observed and this was attributed to earlier molecular segmental motion because of increased intermolecular spacing from the presence of CNT and CNF. Storage modulus was about the same in glassy state with reinforcement.
20. With some exceptions, the flexural strength and flexural modulus were decreased from reinforcement and the effect was more pronounced with higher proportions.
21. Wear of CNT- and CNF-reinforced composites increased linearly with sliding distance and no transition from run-in to steady state was observed. Similar behavior was observed with counterfaces finished to different roughness and texture. Wear rate of these composites in the earlier period of sliding was lower than that of unreinforced PPS but for longer sliding distances it was either same or worse.
22. There were no significant variations in the coefficient of friction with the addition of CNT and CNF in PPS.
23. Transfer film formed on the counterface was thick and non-uniform regardless of CNT or CNF proportions. The coverage of wear track with transfer film was non-uniform.

ACKNOWLEDGMENTS

I could not have completed my thesis without valuable helps and supports from so many people around me. Most of all, I would like to deeply thank my major adviser Dr. Shyam Bahadur for his kind guidance, encouragement, and for always making me see the brighter side of the world.

I also would like to express my appreciation to my graduate study committee, Dr. Abhijit Chandra, Dr. Scott Chumbley, Dr. Vinay Dayal, and Dr. Sundararajan Sriram for their valuable time. Special thanks to Dr. A. K. Pogosian, head of Graduate Division, State Engineering University of Armenia, for supplying research materials and providing technical guidance. The staff in the Department of Mechanical Engineering at Iowa State University also deserves special recognition for their numerous supports. Especially, I deeply thank Mr. James Dautremont and Mr. Larry Couture for their help in instrumentation and machining works, respectively.

Special thanks to Hye-young Park, Chemistry Department, Iowa State University, for her willingness to help with AFM works. Also, special thanks to Mr. James Anderegg for his help in XPS analysis.

Finally, most importantly, I would like to give my deepest appreciation, love, and thank to my family in Korea. I cannot imagine my life and study in U.S.A. without them. Their endless support and love deserve all of my appreciation from my heart.